Appendix A to D of Main Report[1]

Appendix A: Abbreviations

Appendix B: Supplemental Information

- Appendix B.1. Contextualizing Changes in Gulf Coast Temperature and Precipitation
- Appendix B.2. Selection of Relevant Environmental Variables

Appendix C: Additional Information on the Temperature, Precipitation, and Streamflow Analyses

- Appendix C.1. Data Available for Each Station and Variable
- Appendix C.2. Climate Modeling Overview
- Appendix C.3. Detailed Temperature and Precipitation Projections Methodology
- Appendix C.4. Comparing End-of-Century Temperature and Precipitation Projections by Climate Model
- Appendix C.5. Summary Tables for Projected Temperature Analysis
- Appendix C.6. Summary Tables for Projected Precipitation Analysis
- Appendix C.7. Methodology to Select Stream Gages for Historical Streamflow Analysis
- Appendix C.8. Detailed Streamflow Projections Methodology
- Appendix C.9. Summary Tables and Figures for Projected Streamflow Analysis

Appendix D: Additional Information on the Sea Level Rise and Storm Surge Analyses

- Appendix D.1. Factors Not Considered in Sea Level Rise Analysis
- Appendix D.2. Methodology to Estimate Subsidence and Uplift
- Appendix D.3. Vertical Land Surface Rates
- Appendix D.4. Supplementary Sea level Rise Exposure Statistics
- Appendix D.5. Caveats, Gaps, and Replicability of Sea Level Rise Analysis
- Appendix D.6. Detailed Case Studies
- Appendix D.7. Projected changes in U.S. and Global Storm Events
- Appendix D.8. Detailed Methodology for Scenario-based Storm Surge Analysis
- Appendix D.9. Supplementary Storm Surge Exposure Statistics
- Appendix D.10. Caveats, Gaps, and Replicability of Storm Surge Analysis

[1] Report no. FHWA-HEP-12-053

A. Abbreviations

AASHTO: American Association of State Highway and Transportation Officials

ADCIRC: ADvanced CIRCulation Model

ALDOT: Alabama Department of Transportation

ALOS: Advanced Land Observing Satellite

AOGCM: Atmosphere Ocean General Circulation Model

AREMA: American Railway Engineering and Maintenance)

ARRM: Asynchronous Regional Regression Model

ASCE: American Society of Civil Engineers

ATCF: Automated Tropical Cyclone Forecast

BCCR-BCM2.0: Bjerknes Centre for Climate Research-Bergen Climate Model, version 2.0

BM: Benchmark

Cfs: Cubic feet per second

CNRM-CM3: Centre National de Recherches Météorologiques-Coupled global climate Model, version 3

CORS: Continuously Operating Reference Stations

ENSO: El Niño-Southern Oscillation

ERS: European Remote Sensing

FEMA: Federal Emergency Management Agency

FHWA: Federal Highway Administration

FLDEP: Florida Department of Environmental Protection

GC2: Gulf Coast Project, Phase 2

GCM: Global Climate Model

GFDL-CM2.0: Geophysical Fluid Dynamics Laboratory Coupled Climate Model, version 2.0

GHCN: Global Historical Climatology Network

GHG: Greenhouse Gases

GIS: Geographic Information System

GSLR: Global Sea level Rise

HadCM3: Hadley Centre Coupled Model, version 3

HEC-HMS: Hydrologic Engineering Center-Hydrologic Modeling System

HUC: Hydrologic Unit Code

HWMs: High Water Marks

InSAR: Interferometric Synthetic Aperture Radar

IPCC AR4: IPCC Fourth Assessment Report

IPCC SRES: IPCC Special Report Emission Scenario

IPCC: Intergovernmental Panel on Climate Change

LIDAR: Light Detection and Ranging

LRFD: Load and Resistance Factor Design

LSLR: Local Sea Level Rise

LTPP: Long-Term Pavement Performance Program

MDOT: Mississippi Department of Transportation

MHHW: Mean Higher High Water

MLLW: Mean Lower Low Water

MPI ECHAM5: Max-Planck-Institut für Meteorologie ECHAM model, version 5

MPI-OM: Max-Planck-Institute Ocean Model

MSL: Mean Sea Level

NARCCAP: North American Regional Climate Change Assessment Program

NASA: National Aeronautics and Space Administration

NAVD88: North American Vertical Datum of 1988

NCAR CCM3: National Center for Atmospheric Research Community Climate Model, version 3

NCAR: National Center of Atmospheric Research

NDSEV: Number of days of severe thunderstorm environmental conditions

NGS: National Geodetic Survey

NGVD: National Geodetic Vertical Datum

NGVD29: National Geodetic Vertical Datum of 1929

NOAA CO-OP: NOAA Center for Operational Oceanographic Products and Services

NOAA NHC: NOAA National Hurricane Center

NOAA: National Oceanic Atmospheric Administration

NRC: National Research Council

NWS: National Weather Service

PALSAR: Phased Array type L-band Synthetic Aperture Radar

PCM: Parallel Climate Model

PG: Performance Grade

POP: Percent of Peak

RMS: Root Mean Square

RMS: Root Mean Square

RSLR: Relative Sea level Rise

SAP: Synthesis and Assessment Product

SARPC: South Alabama Regional Planning Commission

SD: Standard Deviation

SLOSH: Sea, Lake and Overland Surges from Hurricanes model

SLR: Sea level Rise

SS: Storm Surge

STWAVE: STeady State spectral WAVE

SWAN: Simulating Waves Nearshore model

TCP-InSAR: Temporarily Coherent Point InSAR

UKMO: UK Met Office

USACE: U.S. Army Corps of Engineers

USACE-WES: U.S. Army Corps of Engineers Waterways Experiment Station

USCCSP: U.S. Climate Change Science Program

USDOT: U.S. Department of Transportation

USGCRP: U.S. Global Change Research Program

USGS: U.S. Geological Survey

UTC: Universal Time Coordinated

WBM: Water Balance Model

WCRP CMIP3: World Climate Research Programme Coupled Model Intercomparison Project 3

WMO: World Meteorological Organization

B. Supplemental Information

B.1. Contextualizing Changes in Gulf Coast Temperature and Precipitation

This appendix characterizes changes in temperature and precipitation in Mobile over the past century within the larger context of climate changes globally, nationally, and regionally.

Drawing from an array of scientific evidence, the National Research Council supports the conclusion that "climate change is occurring, is caused largely by human activities, and poses significant risks for—and in many cases is already affecting—a broad range of human and natural systems."[2] The global average surface temperature is rising, with decades from 1970 to 2009 being progressively warmer than prior decades, with the warmest temperatures observed during 2000 to 2009.[3] Observations have also shown changes in other related environmental variables such as increases in the frequency of intense rainfall, decreases in Northern Hemisphere snow cover and Arctic sea ice, warmer and more frequent hot days and nights, reduction of cold snaps, rising sea levels, and widespread ocean acidification.[4]

Over the past 50 years, the U.S. annual average temperature has risen over 2°F (1°C) and average precipitation has increased about 5%, though there is large variability across the continental United States.[5] There is further evidence of precipitation change over the 20th century, with events such as the heaviest 1% of daily precipitation totals in the continental U.S. increasing by 20%.

Although nationally, temperatures show an increase over the 21st century, the southeastern United States has observed a cooling, termed the 'warming hole.'[6] A recent study explored the reason for this by comparing changes in monthly, bimonthly, and seasonal daily minimum temperature, daily maximum temperature, and average daily precipitation using GHCN daily station data from 1950 to 2006.[7] The study suggests the southeast has experienced less warming than the rest of the United States due to increased precipitation and cloudiness. During the day, low-level clouds block sunlight from reaching the surface, thereby keeping maximum surface temperatures cooler. Reducing maximum daily surface temperatures and/or increasing precipitation increases surface wetness. When the wetness at the surface evaporates, it does so at the expense of warming the air, furthering the cooling effect. The reason for the increased precipitation and/or cloudiness is not understood; hence, it is unclear how this relationship will affect future climate. Another recent study investigated how well climate models simulate this

[2] NRC, 2010a
[3] Arndt et al. 2010
[4] NRC, 2010a
[5] USGCRP, 2009
[6] Portmann et al., 2009
[7] Ibid.

'warming hole' in the central United States.[8] Kunkel et al. found that climate models vary in the degree of accuracy in simulating this region, suggesting hydrologic responses on the regional scale are difficult to simulate. Therefore, they recommend using a multi-model ensemble mean for future projections.

[8] Kunkel et al. 2006

B.2. Selection of Relevant Environmental Variables

To consider how climate and weather impact transportation engineering and planning decisions, a list of important environmental variables to investigate had to be identified. For example, transportation assets and operations are generally affected by short-term, extreme events (such as a 3-day period of heavy rain or a 2-hour thunderstorm) more so than overall climate characteristics (such as average annual precipitation). Therefore, it is important to understand how changing climate will affect these short-term events. This appendix summarizes the process used to select these variables, as well as the variables themselves.

First, a "wish list" of the environmental variables that currently affect transportation assets was developed. Next, the "wish list" was refined based on which of these projected variables could be developed for this study. This required a literature survey of best practices for using climate data to inform climate impact assessments. The findings of this survey were used to shape how the climate projections would be developed.

At the onset of this study, a list of all relevant environmental variables that impact transportation in Mobile, Alabama was developed collaboratively by engineers, planners, and climate scientists. This list was further refined based on the following considerations:

- *Does the environmental variable affect Mobile's transportation system?* For example, an environmental variable describing a snow/rain ratio is not of particular concern.
- *Is there a well-known model that simulates projections of this environmental variable?* For example, lightning and tornados create significant damage but projections of these variables are not available.
- *Do the benefits of using the results in a risk assessment justify the effort necessary to develop projections of the variable?* For example, the additional effort to develop projections of humidity/fog and wildfires outweighs the benefits of including these variables in a transportation impact/risk assessment.

Table 26 summarizes the "wish list" of environmental variables considered in this study. The environmental variables range in temporal scale, from monthly, seasonal, and annual averages to specific weather events/hazards. For each environmental variable, Table 26 describes additional changes in the environment that are linked to the variable as well as the part of the transportation system that may be affected. This wish list was used as a tool to assess available sets of climate data for inclusion in this study.

Table 26: Environmental Variables Identified as Useful in Transportation Assessments[9]

Variable	Changes in Environment	Transportation Sectors Affected and Uses in Impact Assessment
Temperature Projections		
Mean Annual and Seasonal Temperature	Vegetation growth, Soil moisture	■ Establishes current baseline conditions and provides context for changes in these average conditions that may impact the severity of extreme events
Mean Monthly Temperature	Vegetation growth, Soil moisture, Evapotranspiration	■ Establishes current baseline conditions and provides context for changes in these average conditions that may impact the severity of extreme events ■ Required input for monthly water balance models used to project monthly runoff and monthly evapotranspiration
Maximum Surface Air Temperature *(probability of occurrences and change in the number of events above a specific threshold temperature(s))*	Soil moisture, Evapotranspiration	■ Causes increased thermal expansion of bridge and rail joints and paved surfaces, causing possible degradation ■ Creates concerns regarding pavement integrity, traffic-related rutting and migration of liquid asphalt, greater need for maintenance of roads and pavement ■ Impairs construction activity
Minimum Surface Temperature *(probability of occurrences and change in the number of events below a specific threshold temperature(s))*	Freeze-thaw conditions.	■ Affects operational costs responding to winter weather (for cold weather climates) ■ Causes changes in pavement design (for cold weather climate)
Growing Season Duration[10]	Vegetation growth, Runoff	■ Affects maintenance and operational costs for roads and rails.

[9] Source: DOT FHWA 2010 and discussion with team of experts in various disciplines (e.g., engineers, planners, hydrologists, climatologists) across the ICF team and the DOT FHWA representatives.
[10] Average number of days per time period that fall within the prescribed "growing season" for the particular location

Variable	Changes in Environment	Transportation Sectors Affected and Uses in Impact Assessment
Precipitation Projections		
Annual and Seasonal Total Precipitation	Vegetation growth, Soil moisture	■ Establishes current baseline conditions and provides context for changes in average conditions that may impact the severity of extreme events. ■ Causes changes in wetland location and the associated natural protective services that wetlands offer to infrastructure.
Total Monthly Precipitation	Flooding, Drought, Soil moisture	■ Establishes current baseline conditions and provides context for changes in average conditions that may impact the severity of extreme events. ■ Required input for monthly water balance models projecting monthly runoff and evapotranspiration.
Daily Intensity Index[11]	Flooding, Drought, Landslides, Mudslides, Soil moisture	■ Causes flooding that affects evacuation routes, overloads drainage systems, and leads to landslides and mudslides that damage roadways and railways ■ Affects soil moisture which, if it becomes too high, will impact the structural integrity of roads and bridges; tunnels could be compromised; or if becomes too low, could cause road foundations to degrade. ■ Can impact groundwater causing degradation, failure, and replacement of road structures and pipelines
Precipitation Extremes *(probability of occurrences and change in the number of events above a specific threshold precipitation total(s))*	Flooding, Landslides, Drought, Wildfire, Erosion, Wind, Lightening	*See Daily Intensity Index*
Peak Streamflow and Monthly Runoff	Flooding, Sedimentation, Erosion	■ Increases in peak streamflow can affect scour rates and affect size requirements for bridges and culverts.
Monthly Evapotranspiration	Vegetation growth, Soil moisture	*See Peak Streamflow and Monthly Runoff*

[11] As defined in the Gulf Coast Phase 1. Total precipitation over a given time period divided by the number of days with precipitation.

Variable	Changes in Environment	Transportation Sectors Affected and Uses in Impact Assessment
Total depth of Rainfall	Flooding	*See Peak Streamflow and Monthly Runoff*
Wind Projections		
Extreme Wind Velocities *(probability of occurrences and change in the number of events above a specific threshold wind velocity)*	Wind	■ Affects bridges, signs, overhead cables, and other tall structures are ■ Affects operational clean-up costs of debris.
Tropical Cyclone Projections[12]		
Projections of Tropical Cyclone Frequency and Intensity	Flooding, Wind damage, Erosion	■ Causes flooding due to increased storm surge and waves impacting bridge structure, highways, railways, and ports ■ Causes erosion of land supporting coastal infrastructure ■ Causes reduced drainage rate of low-lying land after rainfall and flooding events ■ Causes damage to infrastructure caused by the loss of coastal wetlands and barrier islands ■ Requires operational efforts for evacuation
Wind and Precipitation of Observed storms	Storm surge	*See Projections of Tropical Cyclone Frequency and Intensity*
Storm Surge (as a function of relative sea level rise scenarios and cyclone projections, including wind velocity, fetch, wind field size, barometric pressure, etc.)	Flooding	*See Projections of Tropical Cyclone Frequency and Intensity*

[12] The ideal methodology would account for changes in tropical cyclonic development factors such as sea surface temperature, vertical moisture, temperature, and wind conditions.

Variable	Changes in Environment	Transportation Sectors Affected and Uses in Impact Assessment
Sea Level Rise		
Relative Sea Level Rise (polygon files of spatial projections of relative sea level rise)	Flooding, Salinity of freshwater rivers and estuaries, Enhancing storm surge impacts	■ Causes the expansion of locations potentially impacted by storm surge and wave action ■ Erodes road base and bridge support/scour ■ Places highway embankments at risk of subsidence/heave ■ Reduces clearance under bridges ■ Increases maintenance and replacement costs of tunnel infrastructure

Once the "wish list" was established, items on the list were identified that could be reasonably developed using available data. To refine the "wish list," publically available climate data sets were identified that would provide projections of temperature, precipitation, and wind variables. At a minimum, the data sets were required to cover the continental United States to allow for national replicability.

The review of publically available climate data sets identified which environmental variables were available and the associated modeling characteristics (e.g., emission scenario(s) and climate model(s)). Downscaled data are preferred for an impact assessment in Mobile, Alabama, because the climate of Mobile is impacted by coastal breezes that are not captured by the large climate model grid cell resolution. In addition, the IPCC AR4 illustrates that most climate models tend to underestimate observed annual temperature and precipitation in this area of the Gulf Coast, suggesting that downscaled data may be more reflective of local climate. These data sets generally downscale the projections produced by the IPCC AR4 climate models and the results can be processed and tailored for assessment purposes.

Each data set provides unique benefits for use in an impact assessment. For example, the North American Regional Climate Change Assessment Program's (NARCCAP) international program provides dynamically downscaled data of temperature, precipitation, and wind projections along with a number of other variables such as specific humidity. This data set uniquely provides daily maximum wind at the 10-meter height, which is important for many transportation assessments. However, this data set was not selected, because it only provides projections at mid-century for the moderately-high (A2) emission scenario. If suitable for other impact assessments, this data set should be used carefully as it has not been bias-corrected.

After assessing each of the available or soon-to-be available data sets, it was determined that the statistically downscaled USGS climate data was best suited for this study. This data set will provide downscaled mean daily maximum and minimum temperature and total daily precipitation across 10 climate models for lower (B1) and moderately-high (A2) emission

scenarios from 1960 to 2100 at 1/8 degree spatial resolution. Though the climate data was not publically available at the start of this work, it was understood it would become available shortly. As this data was not publically available in time for use in this study, the USGS provided downscaled daily temperature and precipitation simulations specific to five observation stations in Mobile and Baldwin counties. The simulations for the lower (B1) and moderately-high (A2) emission scenarios were downscaled for 10 climate models, and simulations for the high (A1FI) emission scenario was downscaled for 4 climate models. Once the climate data set was chosen, the wish list was refined by removing the wind variable.

Note that this study does not rely on IPCC AR4 climate model projections for sea level rise because those models conservatively simulate the physical processes of ice melt, thereby underestimating potential sea level rise. Instead, sea level rise projections were estimated using a literature review of studies published after the IPCC AR4 and scenario-based modeling. As climate models cannot adequately resolve tropical storms and hurricanes, storm event projections were also characterized by a literature review and scenario-based modeling of storm surge (see Section 2.8.2 for the methodology).

Table 27: Modeling Characteristics of Publicly Available National Downscaled Data Based on the Selection Criteria

Data set	Spatial Resolution	Temporal Resolution	Climate Models	Emission Scenarios	Time Horizon	Downscaling	Variables
North American Regional Climate Change Assessment Program (NARCCAP)*	50 kilometers (30 miles)	From every three hours to daily	4 atmosphere ocean general circulation models (AOGCMs)*	IPCC A2	2041-2070 relative to 1971-2000	Dynamic : 6 regional climate models (RCM)*****	Over 80 Variables
NCAR GIS Climate Change Scenarios**	Approximately 4.5 kilometers (2.7 miles)	Monthly	NCAR's Community Climate Model	IPCC A1B, A2, B1	20 year periods from 2000 to 2099	Statistical	Mean Temperature, Total Precipitation
Bias Corrected and Downscaled WCRP CMIP3 climate projections (supports the Climate Wizard website)***	Approximately 12 kilometers (7 miles)	Monthly	16 CMIP3 models	IPCC A1B, A2, B1	1950 to 2099	Statistical	Surface Air Mean Temperature and Precipitation Rate
USGS climate data******	1/8 degree	Daily	13 GCMs	IPCC A1b, A1Fi, A2, B1	1960 to 2099	Statistical	Minimum Temperature, Maximum Temperature, Total Precipitation

*http://www.narccap.ucar.edu/

**https://gisclimatechange.ucar.edu/

***This website (http://gdo-dcp.ucllnl.org/downscaled_cmip3_projections/dcpInterface.html) also provides daily downscaled data for the Western states and monthly WCRP CMIP3 bias-corrected data (i.e., monthly projections provided by a number of climate models for the three emission scenarios that has not been downscaled but have been uniformly gridded and bias-corrected).

****USGS Downscaled Climate Projections by Katharine Hayhoe (Provisional). Available at http://cida.usgs.gov/climate/hayhoe_projections.jsp

*****Regional models include: OURANOS/UQAM's Canadian Regional Climate Model (CRCM), UC San Diego/Scripps' Experimental Climate Prediction Center Regional Spectral Model (ECPC), Hadley Centre's Hadley Regional Model 3/Providing Regional Climates for Impact Studies (HRM3), Iowa State University's PSU/National Center for Atmospheric Research (NCAR) Mesoscale Model (MM5), UC Santa Cruz's Regional Climate Model version 3 (RCM3), and Pacific Northwest National Laboratories' Weather Research & Forecasting model (WFRP). The drivers of the regional models include: NCAR's Community Climate System Model (CCSM), Third Generation Coupled Global Climate Model (CGCM3), Hadley Centre Coupled Model, version 3 (HadCM3), and NCEP/DOE AMIP-II Reanalysis.

C. Additional Information on the Temperature, Precipitation, and Streamflow Analyses

C.1. Data Available for Each Station and Variable

Historical data from five National Oceanic and Atmospheric Administration (NOAA) Global Historical Climatology Network (GHCN) stations in the Mobile region were analyzed to investigate existing climatic trends and baseline conditions. Two of the stations (Coden and Mobile Airport) are located in Mobile County and three of the stations are located in neighboring Baldwin County. Each station records daily minimum and maximum temperature and total daily precipitation. The Baldwin County stations have the longest record of temperature measurements dating back to 1915, while the Mobile County stations' temperature observations began in 1948. Precipitation measurements in Baldwin County began between 1912 and 1918, while precipitation measurements for the two Mobile County stations began in 1948 and 1956, respectively. The data availability for each station is plotted in a timeline in Figure 87.

Figure 87: Data Available for Each Station and Variable

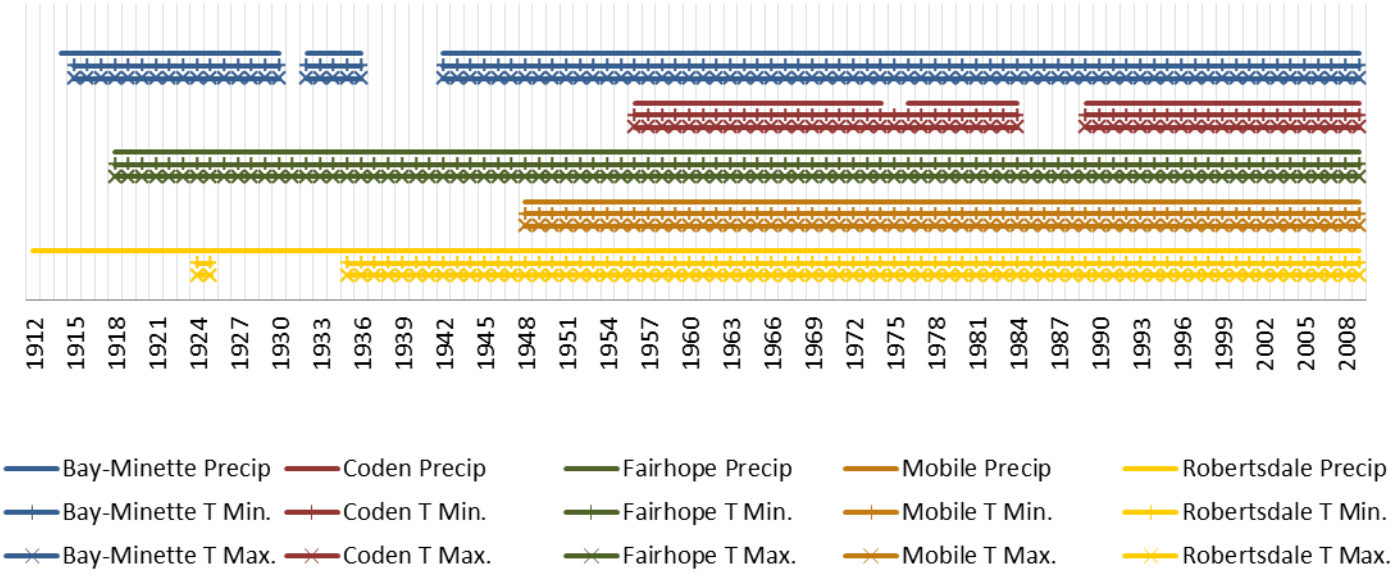

C.2. Climate Modeling Overview

Projections of environmental variables can be developed using a number of different tools, ranging from a simple relationship trend analysis to sophisticated climate models. Deciding what tool to use depends on factors such as the nature of the variable, the costs, and the use of the variable in the climate impact assessment.

Climate models can be used when a study requires projections of temperature, precipitation, wind, or relative humidity, as well as other environmental variables. Projections of sea level rise and specific localized storm events are not included in this discussion. In this study, these two sets of projections were produced through a qualitative review of the literature and scenario-based modeling, as discussed in Section 2.7 and Section 2.8.

This appendix first provides some important background information on climate models, including a discussion of the uncertainty inherent in climate models, and then describes the approach used in this study to identify optimum modeling parameters (e.g., future time horizons of interest) to inform transportation vulnerability assessments.

C.2.1. Introduction to Climate Models

Climate models simulate how climate may change in the future (see textbox titled, "What is a Climate Model?"). Climate model projections indicate how the climate may respond to future variations in greenhouse gas emissions. Climate models can project temperature, precipitation, specific humidity, winds, and a number of other physical parameters. Climate models are not intended to provide a projection of future *weather* (e.g., the temperature and precipitation on May 12, 2050), but are intended to provide an *average of twenty to thirty years of simulated weather*. Hence, climate projections are generally averaged over a twenty to thirty year period.

There are a number of different climate models developed and currently maintained by research groups around the world. Using the same inputs and initialization schemes, different climate models may project different degrees of warming and changes in precipitation. Climate sensitivity is a metric climate scientists can use to compare and evaluate models. Climate sensitivity describes projected global temperature change in response to a doubling of carbon dioxide emission.

The IPCC Fourth Assessment Report (AR4) (2007a) determined the climate sensitivity projected by 23 well-known climate models from 14 modeling groups. The climate sensitivity of these models ranges from 3.8°F (2.1°C) to 7.9°F (4.4°C), with a climate model ensemble average of approximately 5.9°F (3.3°C). Some climate models (e.g., the Hadley Center for Climate Predictions and Research HadCM3 model) simulate a warmer future than others (e.g., the National Center of Atmospheric Research (NCAR) Parallel Climate Model (PCM)).

Some climate models may "perform" better than others at representing observations for particular regions of the globe. However, the standard best practice is to average across climate models that represent the span of climate sensitivity.[13] This is why an ensemble average, which averages the projections across a large number of climate models, is generally preferred. These climate projections can be accessed from the publically available WCRP CMIP3 database.

What is a Climate Model?

A climate model is a mathematical representation of the climate system: "…climate models are used to simulate how… changes in GHG [greenhouse gas] emissions and other climate forcing agents will translate into changes in the climate system. Climate models are computer-based representations of the atmosphere, oceans, cryosphere [ice and snow], land surface, and other components of the climate system. All climate models are fundamentally based on the laws of physics and chemistry that govern the motion and composition of the atmosphere and oceans."

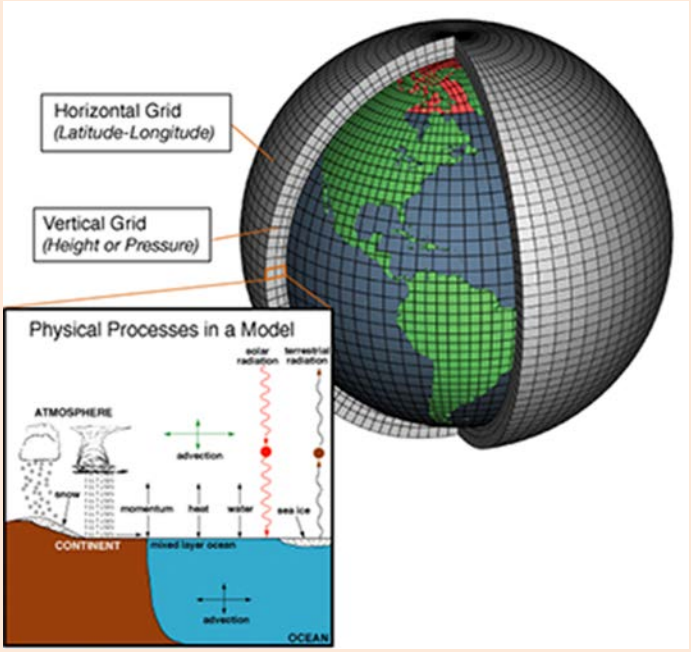

Sources: NRC, 2010a; NOAA, 2012

C.2.2. Introduction to Emission Scenarios[14]

An emission scenario is a plausible representation of future greenhouse gas (GHG) emissions based on a set of assumptions about driving forces (such as demographic, socioeconomic, and technological change), and their key relationships. Emission scenarios describe how greenhouse gas emissions may change over time. In 2000, the IPCC published multiple emission scenarios accounting for variations in demographics, socioeconomics, and technology that are used as inputs into climate models. Emission scenarios vary from low to high levels of greenhouse gases

[13] Knutti et al., 2011; Mote et al. 2011
[14] IPCC, 2000; IPCC, 2007a; IPCC, 2007b; Knutti et al., 2011

emissions over time. Scenarios that have similar demographic, socioeconomic, and technological-change storylines are grouped into scenario families. The four scenario families that comprise the IPCC Special Report: Emissions Scenarios (SRES) set are A1, A2, B1 and B2. These scenarios do not include additional climate policies that differ from current practices (i.e., no new mitigation efforts are considered).

Figure 88 illustrates the differences in carbon dioxide emissions across several IPCC SRES emission scenarios. The differences between scenarios become increasingly noticeable from the near-term projections (e.g., 2020) to the end-of-century projections.

Figure 88: Simulated Carbon Dioxide Emissions from 1990 to 2100 by Emission Scenario (IPCC 2007a)

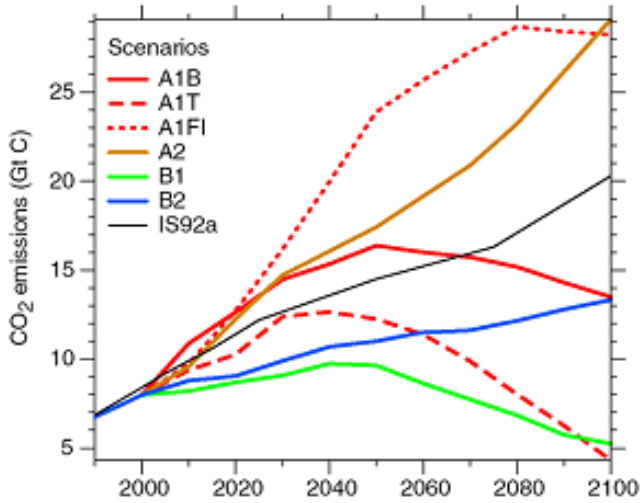

Climate models are "run" under an emission scenario. As illustrated by Figure 89, the climate model ensemble run under the high (A1FI) emission scenario[15] projects the greatest amount of global surface warming, at approximately 7.2°F (4.0°C) by the end of the century. Meanwhile, the low (B1) emission scenario[16] projects the lowest amount of warming at about (3.2°F (1.8°C). The moderately-high (A2) emission scenario[17] is considered a moderately-high emission scenario projecting a global surface warming of 6.1°F (3.4°C) by the end of the century.

[15] The A1FI scenario group describes a convergent world of low population growth, very rapid economic growth, and rapid introduction of new and more efficient technologies. However, the A1FI world is one of less concern for environmental sustainability compared to the B1 storyline, and the direction of technological change in A1FI is fossil intensive.

[16] The B1 scenario family describes a convergent world in which regional per capita income gap substantially decreases. The scenario is characterized by low population growth, rapid changes in economic structures toward a service and information economy, with reductions in material intensity, and the introduction of clean and resource-efficient technologies.

[17] The A2 scenario family describes a heterogeneous world in which economic growth is uneven and the income gap between now-industrialized and developing parts of the world does not narrow. The scenario is characterized by high population growth, slow economic development, and slow technological change.

Figure 89. Multimodal Simulated Change in Global Surface Temperatures, as a Function of Emission Scenario, Relative to 1980 to 1999

Source: IPCC 207a. The bars on the right of the figure provide the climate model ensemble mean and the shading provides likely ranges across the models

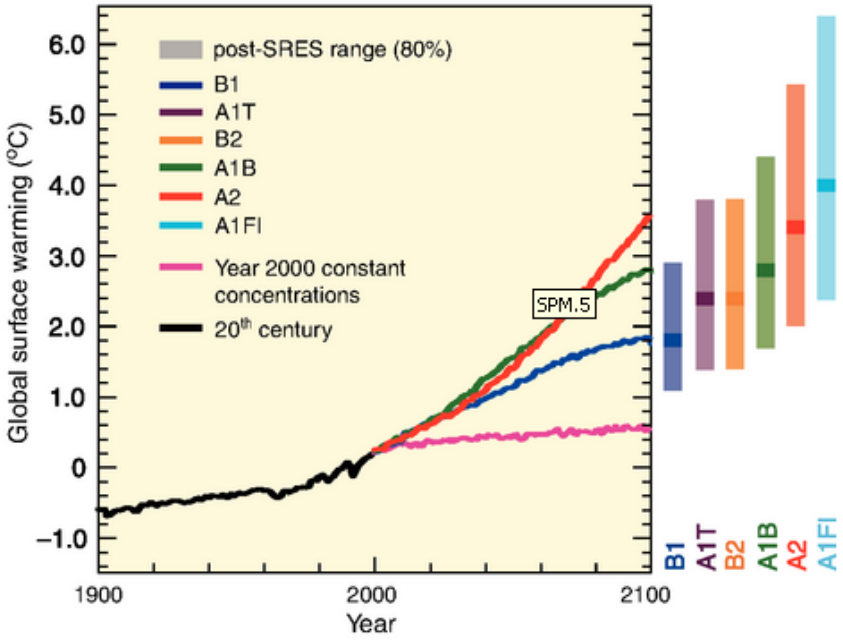

The scientific community has not assigned probabilities to the emission scenarios suggesting which is more or less likely to occur; hence, each emission scenario should be considered with equal probability.

The IPCC Fifth Assessment Report (AR5), scheduled for release in 2013-2014, will present climate projections run with a set of new integrated socioeconomic, emissions, and climate scenarios. Past scenario development was conducted in a mainly sequential form, with socioeconomic and emission scenarios developed first and climate change projections developed based on those scenarios. The new and integrated scenarios will allow the modeling of climate system responses to human activities in parallel with emission scenario development. As a result, the AR5 will include scenarios that explore approaches to climate change mitigation in addition to the traditional "no climate policy" scenarios used in previous assessments.

C.2.3. Dealing with Uncertainty in Climate Projections

There is considerable confidence in the capability of climate models to simulate temperature projections,[18] particularly at the continental scale, but less confidence in climate models ability to project precipitation.[19] This difference in confidence should be qualitatively considered when incorporating risk and vulnerability assessment results into future planning.

[18] Climate models utilize well-understood physical principles and have been demonstrated to reproduce observed features of recent and past climate changes. (IPCC, 2007a)
[19] IPCC, 2008; USGCRP, 2009

There are three main sources of uncertainty in climate model simulations:[20]

1. **Natural variability** (the unpredictable nature of the climate system)
2. **Model uncertainty** (the ability to accurately model the Earth's many complex processes)
3. **Scenario uncertainty** (the ability to project future societal choices such as energy use)

The relative contribution of each uncertainty component to the climate model simulation's overall uncertainty varies with time. Hawkins and Sutton (2009) investigated how these relative contributions change over time when considering the global decadal mean surface air temperature (the approximate values provided here are for qualitative discussion purposes only).[21] Most notably, scenario uncertainty is relatively minimal in the near-term but is the greatest contribution to total uncertainty by end-of-century. The model uncertainty represents a large portion of the total uncertainty throughout the time period, and is a dominant contributor by near-term and mid-century. Meanwhile, natural variability is a significant contributor to total uncertainty in the near-term, but becomes much less significant by end-of-century.

Near-term: A large portion (21%) of near-term uncertainty is from natural variability. Most (70%) uncertainty is from model uncertainty. Scenario uncertainty contributes minimally (9%) to total uncertainty.

Mid-century: Most uncertainty by mid-century is from model and scenario uncertainty, which contribute 54% and 39% of total uncertainty, respectively. Natural variability is a much smaller contributor to total uncertainty, contributing only 7%.

End-of-century: Most uncertainty at end-of-century (70%) is a result of scenario uncertainty. Model uncertainty contributes 27% of total uncertainty and natural variability contributes less than 3%.

These uncertainties also change relative to each other for projections on different spatial scales. Natural variability becomes a greater source of uncertainty at finer scales.[22] This is one reason why incorporating downscaled projections expands the potential uncertainty in climate projections.

As climate science progresses, the degree of uncertainty will likely be reduced—particularly for regional-scale projections. Hawkins and Sutton (2009) suggest that the uncertainty associated with regional projections in the near-term, dominated by model uncertainty and natural variability, could be significantly reduced through scientific progress.

The uncertainty around each of these components should be considered when conducting vulnerability assessments, making decisions, and implementing risk-averse policies. Various techniques can be used to address uncertainty, including probabilistic approaches to quantify uncertainty, modeling various emission scenarios to produce a wide range of future possibilities,

[20] IPCC, 2007a
[21] For each time period, the approximate percent-contribution are estimated as an average of each percent-contribution noted for the end-points. These values presented here are only intended for qualitative and illustrative purposes.
[22] Hawkins and Sutton, 2009

comparing present-day model results with observations, and engaging expert judgment to express uncertainty based on level of agreement and amount of evidence.[23]

Incorporating Climate Projections into Transportation Planning

Transportation planners and engineers consider a wealth of potential impacts when designing, maintaining, and operating the transportation system. These impacts include hazards and extreme events including earthquakes, flooding, mudslides, and landslides, unexpected events such as failures and incidents, and even terrorist attacks. Many of these hazards are low-probability, but high-risk events, requiring careful consideration by planners and designers. (NCHRP, 2009)

Typically, the frequency and severity of natural events are determined by inspecting past observations. This study presents a range of potential changes in the frequency and severity of future events that represent a collection of sound state-of-the-science data. These defensible projections can be used to more adequately address the risk of climate change, along with the other threats and hazards already being considered when making budgetary decisions.

In this study, a number of uncertainties are qualitatively addressed:

- Scenario uncertainty is intrinsically incorporated in the study design by providing projections driven by three different emissions scenarios: 'low' (B1), 'moderately-high' (A2), and 'high' (A1FI). Using these emission scenarios is a way to bound the projections, though it is quite possible that actual emissions in the 21st century will be above this range.
- Model uncertainty is captured, to some extent, by comparing projections across a number of climate models.

In addition to the common uncertainties inherent in climate modeling, this study incorporates an additional layer of uncertainty by using statistically downscaled temperature and precipitation projections. Downscaling climate model projections allows scientists to incorporate local conditions, such as the effect of local topography or prevailing sea breezes, by tailoring larger-scale climate model results to a finer-scale analysis. However, using downscaled data introduces an additional degree of model uncertainty and natural variability into the projections that is not quantified here. Downscaling further assumes that the relationship between today's observed data and modeled data remains stationary over time.

[23] IPCC, 2007a

Likelihood and Confidence in Climate Projections

The IPCC assessments and the U.S. Climate Change Science Program (CCSP) Synthesis and Assessment Product (SAP) reports provide some guidance regarding likelihood and confidence and how this information can be used to filter and understand projected climate changes. Likelihood represents how likely the outcome will occur, and confidence characterizes the consensus across modeling groups or experts that the projections are correct.

Table A-1 outlines the likelihood and confidence for changes in climate variables most relevant to the transportation system: temperature rise, changes in precipitation, changes in frequency and intensity of storm events, and sea-level rise. These likely and very likely indicators provide measures of a portion of the uncertainty and can act as a general guide in assessing overall findings. However, they do not account for uncertainty associated with future emissions, downscaling techniques, or the uptake of greenhouse gases, nor do they account for any systematic errors in the climate models. As shown, there is greater confidence in temperature projections than precipitation projections. This is because precipitation is heavily influenced by small-scale phenomena and natural variability.

Likelihood and Confidence for Climate Variables Identified to Affect the Highway System

Climate Variable		Likelihood	Confidence
Temperature Rise	Annual mean	Very likely[a]	High confidence[a]
	Seasonal mean	Very likely [a]	High confidence [a]
	Extreme Heat Events	Very likely [a]	High confidence[b]
Changes in Precipitation	Annual mean	Very likely[a,b]	Not found
	Seasonal mean	Very likely [b]	Medium confidence[c]
	Change in frequency and intensity	Very likely[b]	Not found
Intensification of storm events		Likely[b]	High confidence (extratropical)[a]
Sea-level rise		Cannot assess likelihood[b]	Not confident in upper bound of SLR[b]

[a]USCCSP, 2007; [b]IPCC, 2007a
Very Likely refers to a greater than 90% probability; Likely refers to a greater than 66% probability
High confidence represents an 8 out of 10 chance; Medium confidence represents a 5 out of 10 chance
Not found means there was no information about confidence in the projections of this variable in the reports cited.

Sources: IPCC 2007a; DOT FHWA 2010

C.2.4. Approach to Identify Optimum Climate Modeling Parameters

Two steps were taken to determine the best climate model projections to use in this study:

1. Optimum climate modeling parameters were determined
2. Available climate projection data sets were evaluated against these parameters.

This process determined what time periods of projections would be useful, the number of climate models to use, which emission scenarios to use, and whether and how to downscale the data. These determinations are summarized below.

Time Periods

Climate projections are generally provided for twenty to thirty year periods. The shorter, twenty year periods are more likely to be affected by natural variability, particularly in the near-term. However, the shorter time period reduces the impact from climate simulations that continue to evolve with time (i.e., climate model simulations used in this study will not project a stationary future but one that is constantly evolving with time). The longer, thirty year periods are preferred for extreme event analyses as it provides a longer data record.

Because they are preferred for extreme event analyses, thirty year periods were selected for this study. This study provides climate projections in three time periods: near-term (2010-2039), mid-century (2040-2069) and end-of-century (2070-2099).

A reference baseline period of 1980 to 2009 was chosen. This period replicates the weather and climate that transportation planners currently plan for. However, it may underestimate the magnitude of projected change, which might have been larger if an earlier baseline period was chosen. In addition, this choice in time period may not reflect the design values (such as 24-hour precipitation return periods) that were used to build current infrastructure, as most infrastructure was built decades ago.

Number of Climate Models

The scientific climate community recommends averaging across as many climate models as possible when developing projections for impact/risk assessments.[24] The models selected had to provide continuous daily output, robust results, and ideally capture the breadth of climate model sensitivity.[25] As a result, ten climate models were selected to generate an ensemble average for the A2 and B1 emission scenarios and four climate models were selected for the A1FI emission scenario ensemble average.

Emission Scenarios

To capture a range of possible futures, three emission scenarios were used for a scenario-based analysis: a low emission scenario, B1; a moderately-high emission scenario, A2; and a high emission scenario, A1FI.

If resources do not allow multiple scenarios to be used, a high or moderately-high emission scenario (such as A1FI or A2) might be used so that the impact assessment captures the highest degree of risk to temperature change, or a more moderate emission scenario (such as A1B) might be used if planners prefer a more conservative set of estimates. As noted in the findings of this report, changes in baseline and extreme precipitation events may not change in proportion to the rate of increasing greenhouse gas emissions. As a result, it is useful to understand how available

[24] Mote et al, 2011; Knutti et al., 2011
[25] Climate sensitivity is defined as the temperature change resulting from a doubling of atmospheric carbon dioxide concentrations relative to pre-industrial times (IPCC, 2007a).

climate model simulations for the study area change as a function of emission scenario, before committing to one or more scenarios to inform the impact assessment.

C.2.5. Downscaling Techniques

Over the past two decades, climate models have provided results at increasingly finer spatial resolution. As the spatial resolution increases, the details in the topography of the land, such as mountainous regions and coastlines, become more obvious. However, higher spatial resolutions require increased computational resources and continued evaluation of the physics represented in the model. For example, at finer spatial scales, some of the terms that are not relevant at large scales may need to be reconsidered for inclusion.

For many transportation impact assessments, even these finer-scaled climate models produce projections at spatial resolutions that are too coarse to be informative. For example, the current spatial resolution of climate models (i.e., the size of the model grid cell) ranges from a surface area of about 180 miles by 180 miles (288 kilometers by 288 kilometers, or about 2.8 degrees by 2.8 degrees, varying by latitude) down to about 60 miles by 60 miles (96 kilometers by 96 kilometers, or about 1 degree by 1 degree, varying by latitude). This spatial resolution may be acceptable for some assessments and not for others.

To determine the optimum spatial resolution for a given study, the temporal resolution required for the assessment should also be considered. The types of questions poised in this study to determine downscaling technique included:

- Will daily, monthly, or annual averages need to be provided for the variable?
- Does the study area tend to be affected by coastal sea breezes?
- Is Mobile's weather significantly affected by changes in small-scale topography?

These questions were prompted by the current state-of-the-literature describing when downscaling techniques were preferred for specific locations. A number of methods have been developed to further reduce or "downscale" the spatial resolution of climate projections from climate models. These methods can be divided into two distinct techniques: statistical downscaling and dynamic downscaling.

Statistical downscaling

Statistical downscaling determines a statistical relationship between locally observed data and large-scale modeled data over a historical time period. This relationship is then applied to climate model data for future time periods. A number of locations may be used to determine the best algorithm for statistical downscaling. This technique assumes the relationship between the larger-scale modeled variable and the local observations will not change over time.

The performance of statistical downscaling is largely constrained by the accuracy of the climate model to simulate regional temperature, humidity, and circulation patterns.[26] In addition, accuracy is affected by whether the observation set used to train the algorithms captures the range of local weather conditions.[27]

Statistical downscaling is relatively affordable, which allows this method to be applied at a number of observation locations, for various emission scenarios, and for a number of climate models. Impact assessments informed by statistically downscaled data can include a number of climate models run with a multitude of emission scenarios.

Dynamic downscaling

Dynamic downscaling uses a global climate model to drive a regional climate model (RCM). Regional climate models are fine resolution models that incorporate enhanced algorithms and topography and can be nested within the climate model. Though not always done, this allows the regional climate model output to be incorporated into the climate model simulation.

Dynamic downscaling is appropriate when the global climate model does not adequately represent a region's climate.[28] Because the technique is very computationally intensive and regional climate models require a significant development effort, dynamic downscaling is quite costly. Generally, studies of impact assessments informed by dynamic downscaling rely on one climate model and a few emission scenarios.

Selecting a technique

Deciding whether and how to downscale climate projections depends on a number of factors, such as whether the data will be used to inform additional modeling (such as hydrologic modeling), the scale of the variables that are needed to inform the assessment, the availability of data from public sites, and the study's budget and timeline.

This study uses downscaled data, because the data will inform transportation asset-specific (i.e., fine spatial scale) assessments at a coastal location (affected by factors such as coastal sea breezes). Statistical downscaling was selected because of its ability to simulate future changes in temperature and precipitation for a continuous time period and its capacity to affordably produce a number of climate projections by climate model and emission scenario. The Asynchronous Regional Regression Model (ARRM) method of statistical downscaling, in particular, was applied because it is capable of downscaling at daily timescales.[29]

[26] USCCSP, 2008c
[27] Hayhoe and Stoner, 2012
[28] USCCSP, 2008c
[29] Hayhoe and Stoner, 2012

C.3. Detailed Temperature and Precipitation Projections Methodology

This Appendix describes the methodology that was used to develop projections of future temperature and precipitation in the Mobile region. Projections of temperature and precipitation were produced using up to ten climate models, run under three emission scenarios, for three future time periods. To account for local influences, the large-scale climate data was statistically downscaled using the Asynchronous Regional Regression Model (ARRM) method to the locations of the five GHCN observation stations.

Under this method, historical statistical relationships between weather and climate were derived by comparing the local temperature and precipitation observations to the modeled climate data.[30] After deriving and testing them, the relationships were used to translate future modeled climate projections of temperature and precipitation to the individual station level. This technique assumes the relationship between weather and climate does not change over time.

The statistical downscaling methodology was cross-validated and bias-corrected for each of the five station locations. The results of this cross-validation process showed:

- The downscaling method had a very low bias of +/- 0.2°F (0.1°C) modeling minimum and maximum temperature for a majority of the days from 1980 to 2009. However, for the few days that were observed to have extreme temperature values (i.e., either very cold or very hot), the biases were as high as +/- 1.0°F (0.6°C); biases were slightly higher for modeling the minimum temperature than for modeling the maximum temperature.[31]
- The downscaling method was not as accurate at simulating precipitation, due to the higher spatial and temporal variability associated with precipitation. Nevertheless, for the days from 1980 to 2009 with low observed amounts of precipitation, the modeled precipitation amounts tended to be 5 to 15% lower than the observational data. For the days with the highest observed amounts of precipitation (i.e., for the 99th percentile of precipitation), the models tended to overestimate observational data by 20 to 30%.[32]

The remainder of this appendix is presented in three sections, corresponding to the steps taken to identify and present relevant projections:

- Identification of relevant climate projections
- Identification of statistically significant climate projections
- Determination of reporting format

[30] See Hayhoe and Stoner (2012) for description of methodology of statistically downscaling the daily data.
[31] Hayhoe and Stoner, 2012
[32] Hayhoe and Stoner, 2012

C.3.1. Identification of Relevant Climate Projections

The climate "wish list" described in Appendix B.2 provided a starting point for the type of climate projections useful for impact assessments. The "wish list" does not define the thresholds or probability of occurrence best suited for assessing impacts on local transportation in Mobile, Alabama. Relevant thresholds and probabilities were defined based on three strategies:

- Discussions among local transportation engineers and planners about how local transportation infrastructure, maintenance, and operations in Mobile are impacted by today's weather hazards
- An extensive literature review, summarized in the *Assessing Sensitivity* report
- Meetings of transportation infrastructure engineers, federal transportation planners, and climate scientists

Table 28 provides a list of the temperature and precipitation weather hazards and climatic averages that were deemed useful for this study. These variables can be directly estimated using the daily downscaled precipitation and temperature data.

Terminology

Threshold—A critical value that may create difficulties for an asset when exceeded.

Probability of Occurrence—The chance an event will occur in a given time period.

Exceedance Probability—The probability that a threshold will be met or exceeded within a given time period.

Return Period-- Average length of time between events of similar magnitude and direction.

Percentile—The percentage of the observations that fall below a given threshold.

The modeled results for all variables were provided for each emission scenario, for each of the five station locations, and for the baseline and projected time frames (i.e., 1980-2009, 2010-2039, 2040-2069, 2070-2099). The results were then averaged across the statistically downscaled climate models.[33]

[33] Since there are ten GCMs providing results for the A2 and B1 emission scenarios, the uncertainty estimates include ranges of one standard deviation from the mean based on the set of all relevant climate model simulations. Since only four GCMs provide results for the A1FI emission scenario, the uncertainty estimates are a coarser range of model results described by the minimum and maximum GCM values.

Table 28: Temperature and Precipitation Variables Developed for this Study

An asterisk denotes a variable or percentile that does not provide robust quantitative results (per communication with Dr. Katharine Hayhoe) and its use should be limited to qualitatively informing the impact assessment.

Variable	Transportation Mode	Methodology	Related Figures and Tables
Temperature			
Annual, seasonal, and monthly average minimum, maximum, and mean temperature for each 30-year time period (9 components)	Airports (runway design)	For each 30-year period, the daily minimum, maximum, and mean temperature corresponding to each month, season, or year were averaged for each station location, climate model, and emission scenario. Then, the 30-year average was determined for each station location, climate model, and emission scenario. Averages and standard deviations were then calculated across climate models for each station location and emission scenario. For purposes of discussion, the results were averaged across station locations to produce an average for the Mobile region.	Main Body – Figures 10, 11, 12, 13, 14, 15, 16, 17 Appendix C – Tables 30, 31, 32 Appendix E – Tables 56, 57, 58, 59, 60, 61, 62, 63, 64
Mean, 50th and 95th*percentile of high daily maximum temperature and the warmest day of the year for each 30-year time period (4 components)	Rail (AREMA rail design, buildings)	For each 30-year period, the daily maximum temperature for each year was identified. This resulted in a total of 30 data points in each time period for each climate model, station location, and emission scenario. The mean, 50th, and 95th percentile levels were estimated from this set of 30 data points using a quantile distribution and then averaged across climate models for each station location and emission scenario. The warmest day in summer for the 30-year period was estimated in the same way. For purposes of discussion, the results were averaged across station locations to produce an average for the Mobile region.	Main Body – Figures 22, 23 Appendix C – Table 33 Appendix E – Tables 65, 66, 67, 68

Variable	Transportation Mode	Methodology	Related Figures and Tables
Seasonal and annual number of days and maximum consecutive days of maximum temperatures at or above 95°F (35°C), 100°F (38°C), 105°F (41°C), and 110°F (43°C) during each 30-year time period (16 components)	Civil, Geotech, Pavement	For each 30-year period, the number of days where the maximum temperature was at or above 95°F, 100°F, 105°F, and 110°F was counted for each year. This resulted in 30 data points in each time period (one for each year), for each climate model, station location, and emission scenario. The 30 data points were averaged to estimate the annual number of days at or above each high temperature threshold for each climate model, station location, and emission scenario. The mean and standard deviation was then determined across the climate models for each station location and emission scenario. The process was repeated to obtain seasonal projections. The maximum consecutive days of high temperature for each threshold was likewise calculated. For purposes of discussion, the results were averaged across station locations to produce an average for the Mobile region.	Main Body – Figures 18, 19, 20, 21 Appendix C – Tables 33, 34 Appendix E – Tables 69, 70, 71, 72, 73, 74, 75, 76, 77, 78, 79, 80, 81, 82, 83, 84
Mean; 5th*, 25th, 50th, 75th, and 95th* percentile; and minimum value for the average minimum air temperature over four consecutive days in winter and the average maximum temperature over four consecutive days in summer for each 30-year time period (14 components)	Bridge, Rail	For each winter in the 30-year period, the average of the minimum air temperature for any four consecutive days for each year was estimated for each climate model projection, emission scenario, and location. The 5th, 25th, 50th, 75th, and 95th percentile; mean; and coldest period across the 30 data points was estimated using a quantile distribution for each climate model, emission scenario, and location. For each summer in the 30-year period, the average of the maximum air temperature for any four consecutive days was estimated for each year, ultimately providing the 5th, 25th, 50th, 75th, 95th percentile; mean; and hottest period across the 30 data points for each climate model, emission scenario, and location. The average across climate models for each location was determined, and then averaged across station locations to provide an average for the Mobile region.	Main Body – Figures 24, 27 Appendix C – Tables 35, 36 Appendix E – Tables 85, 86, 87, 88, 89, 90, 91, 92, 93, 94, 95, 96, 97, 98

Variable	Transportation Mode	Methodology	Related Figures and Tables
The mean, 1st*, 5th *, 10th, and 50th percentile of the coldest day of the year during each 30-yr time period (5 components)	Multi (pavement design)	Using the daily minimum temperatures, the coldest minimum temperature for each year was identified for each climate model, emission scenario, and station location. Across the 30 data points for each time period, the mean, 1st, 5th, 10th, and 50th percentile was calculated using the quantile distribution for each climate model, emission scenario, and station location. The average across climate models for each location was determined, and then averaged across station locations to provide an average for the Mobile region.	Main Body – Figures 25, 26 Appendix C – Table 36 Appendix E – Tables 99, 100, 101, 102, 103
Maximum 7-day average air temperature per year with the % probability of occurrence during each 30-yr period (mean, 50th, 90th, 95th*, 99th*percentile) for each 30-yr time period (5 components)	Multi (pavement design - asphalt)	Using the daily maximum temperature, the maximum 7-day average temperature for each year was determined. This produced a total of 30 data points in each time period, for each climate model, emission scenario, and station location. Across the 30 data points, the mean, 50th, 90th, 95th, and 99th percentile was estimated using the quantile distribution for each climate model, emission scenario, and station location. The average across climate models for each location was determined, and then averaged across station locations to provide an average for the Mobile region.	Appendix C – Table 35 Appendix E – Tables 104, 105, 106, 107, 108
Precipitation			
Annual, seasonal, and monthly total precipitation for each 30-year time period (3 components)	Multi (pavement design)	Daily precipitation corresponding to each month, season, or year was summed for each year, station location, climate model, and emission scenario. Then the 30-year average of each sum was determined. Averages and standard deviations were calculated across climate models for each station location and emission scenario. For purposes of discussion, the results were averaged across station locations to produce an average for the Mobile region.	Main Body – Figures 32, 33 Appendix C – Table 37, Table 38 Appendix E – Tables 109, 110, 111

Variable	Transportation Mode	Methodology	Related Figures and Tables
Precipitation for 24-hour period with a 0.2%*, 1%*, 2%, 5%, 10%, 20%, and 50% probability of occurrence (7 components)	Multi (drainage, liquid storage)	The day with the maximum total daily precipitation for each year was found for each emission scenario, climate model, and station location. This produced a total of 30 data points for each time period. Across the 30 data points, the daily precipitation representing each probability of occurrence was estimated by fitting the 30 data points to the Gumbel extreme value distribution for each emission scenario, climate model, and station location. Averages and standard deviations were calculated across climate models for each station location and emission scenario. For purposes of discussion, the results were averaged across station locations to produce an average for the Mobile region.	Main Body – Figures 36, 37 Appendix C – Table 40 Appendix E – Tables 112, 113, 114, 115, 116, 117, 118

Variable	Transportation Mode	Methodology	Related Figures and Tables
Occurrence of precipitation for 24-hour period based on today's 0.2%*, 1%*, 2%, 5%, 10%, 20%, and 50% occurrence probabilities (7 components)	Multi (drainage)	For the 1980 to 2009 time period, the value of the occurrence probabilities using the maximum total daily precipitation was identified using the results of the variable above for each climate model, emission scenario, and station location. For each of the future time periods, the day with the maximum total daily precipitation for each year was found for each emission scenario, climate model, and station location. This produced a total of 30 data points Across these 30 data points, the occurrence probabilities were determined by applying a Gumbel extreme value distribution. These fitted distributions provided the new probabilities associated with the historical value of each baseline occurrence probabilities . Averages and standard deviations were calculated across climate models for each station location and emission scenario. For purposes of discussion, the results were averaged across station locations to produce an average for the Mobile region.	Appendix C – Table 41 Appendix E – Tables 119, 120, 121, 122, 123, 124, 125

Variable	Transportation Mode	Methodology	Related Figures and Tables
Exceedance probability of precipitation across four consecutive days: 0.2%, 1%, 2%, 5%, 10%, 20%, 50%; Exceedance probability of precipitation across two consecutive days: 0.2%, 1%, 2%, 5%, 10%, 20%, 50% (14 components)	Pipeline	For each time period, a sum of daily precipitation was calculated for every four consecutive days. This produced a total of 10,950 data points. The data was ranked from high to low, and the exceedance probabilities of 0.2%, 1%, 2%, 5%, 10%, 20%, and 50% were then determined for each climate model, emission scenario, and station location. Averages and standard deviations were calculated across climate models for each station location and emission scenario. For purposes of discussion, the results were averaged across station locations to produce an average for the Mobile region. This was repeated for the two-day exceedance probabilities.	Main Body – Figures 38, 39 Appendix C – Table 42 Appendix E – Tables 126, 127, 128, 129, 130, 131, 132, 133, 134, 135, 136, 137, 138, 139
Largest three-day total precipitation each season (1 component)	Multi	The maximum three-day total precipitation for each season was identified for each year. This produced 30 data points for each of the four seasons. The 30 data points were averaged to produce the average maximum three-day total for each season. For purposes of discussion, the results were averaged across station locations to produce an average for the Mobile region	Main Body – Figures 34, 35 Appendix C – Table 39 Appendix E – Table 140

The occurrence probabilities of the 24-hour precipitation variable were estimated by fitting the Gumbel Extreme Value (GEV) distribution to the maximum daily precipitation projected for each year in the 30 year period for each climate model, emission scenario, and station location.[34] As the extreme events are not based on 100 years or more of data, there is a large amount of uncertainty associated with these extreme event projections.[35] Precipitation events at a finer temporal scale (e.g., 3-hour events) are not investigated in this study as the downscaling approach applied is only appropriate to the daily time scale.

The two-day, three-day, and four-day precipitation events were provided by Dr. Katharine Hayhoe. The two-day and four-day precipitation events were developed by applying a quantile distribution[36] to the running sum for each 30 year period (e.g., this method does not fit the data to a theoretical distribution but, in essence, "bins" the modeled data into percentiles). The seasonal three-day events are simply the climate model ensemble average of the heaviest three-day event for each season.

C.3.2. Identification of Statistically Significant Climate Projections

To focus the study on climate projections that represent a robust projected change from baseline conditions, a statistical test (a paired t-test) was used to identify significant ($p<0.05$) changes, i.e., climate projections that are statistically different from simulations of today's climate. The statistical test compared the projected climate model mean for each climate variable, emission scenario, station location, and future time period to the corresponding climate model baseline of 1980 to 2009. Other statistical tests are available which require additional analyses. The paired t-test was chosen for the following reasons:

- It is simple to apply (i.e., replicable) and explain.
- It is accepted by the statistical community and reasonable.
- It requires no additional data processing to complete.
- It is applicable for the limited sample size used in this study (i.e., 4 to 10 climate models).

The climate variables demonstrating the most robust trends were identified using the following two-step process:

> **Step 1**. A paired t-test was applied to all projections for each station location. The climate variables that show a statistically significant change from the baseline at the 95% confidence level ($p<0.05$) were identified.[37]

[34] The daily precipitation data was used as a substitute for 24-hour precipitation. This study does not apply a conversion factor of 1.143 for converting 1-day to 24-hr rainfall (see Durrans and Brown).
[35] Goodness of fit tests (i.e., how well the theoretical distribution fits the data) were applied for each station, scenario, climate model, and 30 year period. The model was reasonable at the 5% level for about 60% of the cases and was reasonable at the 1% level for all of the cases.
[36] Hyndam and Fan, 1996
[37] Variations of statistical significance were considered for this study (e.g., 90%, 95%, and 99% confidence). It was decided that, though interesting, this level of effort and detail was likely more than what was needed for the Task 3 assessment (e.g., how would a statistical difference at the 99% level be treated differently than a 95% level). Therefore, a streamlined description of what is significant at the 95% level was agreed as adequate for purposes of this study.

Step 2. The climate variables that demonstrate a statistically significant change (as determined in Step 1) at *all five* station locations were identified. For purposes of this study, all other climate variables were not considered to demonstrate robust statistically significant differences.

This test helps identify which of the climate projections show a significant amount of change. The paired t-test identifies whether the projected case is significantly different from the baseline case. This statistical test assumes that the distribution of differences between climate model averages of projected simulations and baseline simulations is a Gaussian distribution (this is not saying the temperature or precipitation variable itself follows a Gaussian distribution, but is saying the distribution of climate model mean differences of a temperature or precipitation variable is Gaussian). The hypothesis is that the true mean difference between the baseline case and projected case for a given climate variable is zero (this is rejected if the difference between the baseline case and projected case for a given climate variable is significant, thereby suggesting this variable should be considered in the climate change vulnerability/risk assessments). This test assumes the climate models represent a sample or subset of the entire population of climate model simulations (e.g., changes in initialization, small physical variations within models, etc.).

The algorithm for the paired t-test is:

$$t = \frac{(\overline{x_A} - \overline{x_B})}{\sqrt{(\frac{S_d}{n})^2}}$$

where $\overline{x_A}$ is the mean of the baseline case (e.g., A1 emission scenario, 1980-2009), $\overline{x_B}$ is the mean of the projected case (e.g., A1 emission scenario, 2040-2069 time period), S_d is the sample standard deviation of the differences between the baseline and projected cases, and n is the total number of climate models (i.e., 10 climate models for A1 and B2 emission scenario, and 4 climate models for the A1Fi emission scenario).

The hypothesis can be rejected with 95% confidence if:

$$|(\overline{x_A} - \overline{x_B})| > K * \sqrt{\frac{S_d}{n}^2}$$

where K is the 97.5th percentile of a t distribution with n – 1 degrees of freedom, i.e. 2.262 for 10 climate models and 3.182 for 4 climate models. This is a two-tailed test because temperature variables get warmer for all emission scenarios, but precipitation may be projected to get drier or wetter**.**

For an example, the table below shows the application of the paired t-test of the annual total precipitation for the B1 emission scenario for the Mobile station location. The baseline case is

the average total annual precipitation across 1980 to 2009, and the projected case is the average total annual precipitation across 2010 to 2039.

Table 29: Application of the Paired T-Test of the Annual Total Precipitation for the B1 Emission Scenario for the Mobile Station Location

Total Annual Precipitation	B1			
Climate Model	1980-2009	2010-2039	Diff	Sqr Diff
BCM2	67.93	59.47	-8.46	71.57
CCSM3	64.7	71.02	6.32	39.94
CGCM3-T47	62.78	74.55	11.77	138.5
CGCM3-T63	63.13	63.9	0.77	0.593
CNRM	64.32	68.28	3.96	15.68
ECHAM5	66.53	78.56	12.03	144.7
GFDL-CM2.0	64.91	70.2	5.29	27.98
GFDL-CM2.1	62.04	68.6	6.56	43.03
HadCM3	61.97	60.45	-1.52	2.31
PCM	65.87	70.3	4.43	19.62
Mean of the climate ensemble	64.42	68.53	4.12	
Std dev of the climate ensemble	1.98	5.94	6.10	
Numerator of t test				4.12
Std dev of the t test				7.48
Reject?				**No**

The steps in applying the paired t-test are as follows (note that some rounding errors may be evident in the numbers):

(1) Calculate the climate model ensemble mean for the baseline case and for the projected case. In this example, the values are 64.42 inches and 68.53 inches. The absolute value of the difference, 4.12 inches, between these ensemble means provides the left hand side of equation above (second equation).
(2) Calculate the differences between the projected case and baseline case for each climate

model. In this example, the difference between the projected and baseline case for the HadCM3 is a reduction in precipitation of 1.52 inches.

(3) Calculate the standard deviation of the differences across all climate models.

(4) Square the standard deviation of the differences and divide by the number of climate models. In this example, there are 10 climate models.

(5) Take the square root of the value calculated in (4) and multiply by 2.262 as 10 climate models were used (or 3.182 if 4 climate models were used). In this example, the value is 4.36 inches. This step provides the value of the right hand side of equation.

(6) Check if the value of (1) is greater than the value of (5). If so, then the projected case is statistically significant from the baseline case and this variable should be considered in assessments.

The paired t-test is applied to all temperature and precipitation variables across all five station locations, three emission scenarios, and three projected time periods. This test accounts for not only the amount of change projected by the mean averaged across all the climate models but also the variability across the climate models.

C.3.3. Determination of Reporting Format

As this study produced voluminous amounts of projected data, it was important to present the findings in a way that will be useful for the vulnerability assessment to be conducted in later stages of the Gulf Coast Study. Though projections are available for the five station locations from the downscaling process, the vulnerability assessment can initially draw from regional climate projections that are averaged across all five locations. Appendices 5.7 and 5.8 provide a complete database of the climate projections by emission scenario, location, and time period.

Comparing results that have been averaged for each emission scenario at each future time period illustrates some of the uncertainty that is associated with future development pathways and resulting greenhouse gas emissions. As discussed in Appendix C.2, the climate model ensemble average is considered the most robust design by the scientific modeling community for informing assessments. As a result, the climate projections for each emission scenario are provided as an average across all downscaled climate models. The range across the climate models is also provided, describing an important component of the model uncertainty. During the vulnerability assessment, changes will be assessed to determine which have a magnitude large enough to impact the asset.

Due to the large number of climate variables and projections, only those variables with a significant change projected (based on the paired t-test described above) were illustrated and discussed. This helped to focus the illustrations and discussion on variables that should be considered in the climate change impact assessment of Task 3.

The paired t-test was applied to all provided USGS climate projections. The results of the paired t-test along with the magnitude and direction of the projected change are presented in tables in Appendix C.5 and Appendix C.6.

- Shaded cells with the letter "Y" indicate projections that exhibit a significant change.
- Cells with grayed-out font and the letter "N" indicate projections that do not exhibit a significant change. These projections are not considered different from baseline conditions.

The projected changes in environmental variables are also illustrated by box plots. Each box on the plot shows the mean (represented by the line between the two colors) and variability (represented by the height of the box) of climate projections for each time period and emission scenario, averaged across all five stations and climate model ensemble. The variability of projections under the low (B1) and moderately-high (A2) emission scenarios is estimated as one standard deviation from the mean. The variability of projections under the high (A1FI) emission scenario is estimated as the full range across all climate models at all five stations. The "model baseline" is the average daily temperature from 1980 to 2009, as modeled by all climate models and averaged across emission scenarios. There is negligible difference between the baseline projections across emission scenarios, and this line is functionally equivalent to the observed average temperature over that time period. The simulated baseline is used to determine projected changes, as this helps correct for any preexisting biases in the climate models.

C.4. Comparing End-of-Century Temperature and Precipitation Projections by Climate Model

As discussed in Appendix C.2, climate models project varying levels of temperature and precipitation change. This appendix provides a high-level investigation of how the end-of-century projections vary by climate model and emission scenario. The findings are helpful in loosely guiding the interpretation of the temperature and precipitation projections in this report.

The scatterplot shown in Figure 90 explores the relationship between the change in total annual precipitation and the change in mean annual temperature at end-of-century, relative to baseline conditions. The projections are provided by climate model and emission scenario, averaged across all five station locations.

Figure 90: Projected Changes in Temperature and Precipitation by Climate Model and Emission Scenario, Changes by End-of-Century (2070-2099) Relative to Baseline (1980-2009)

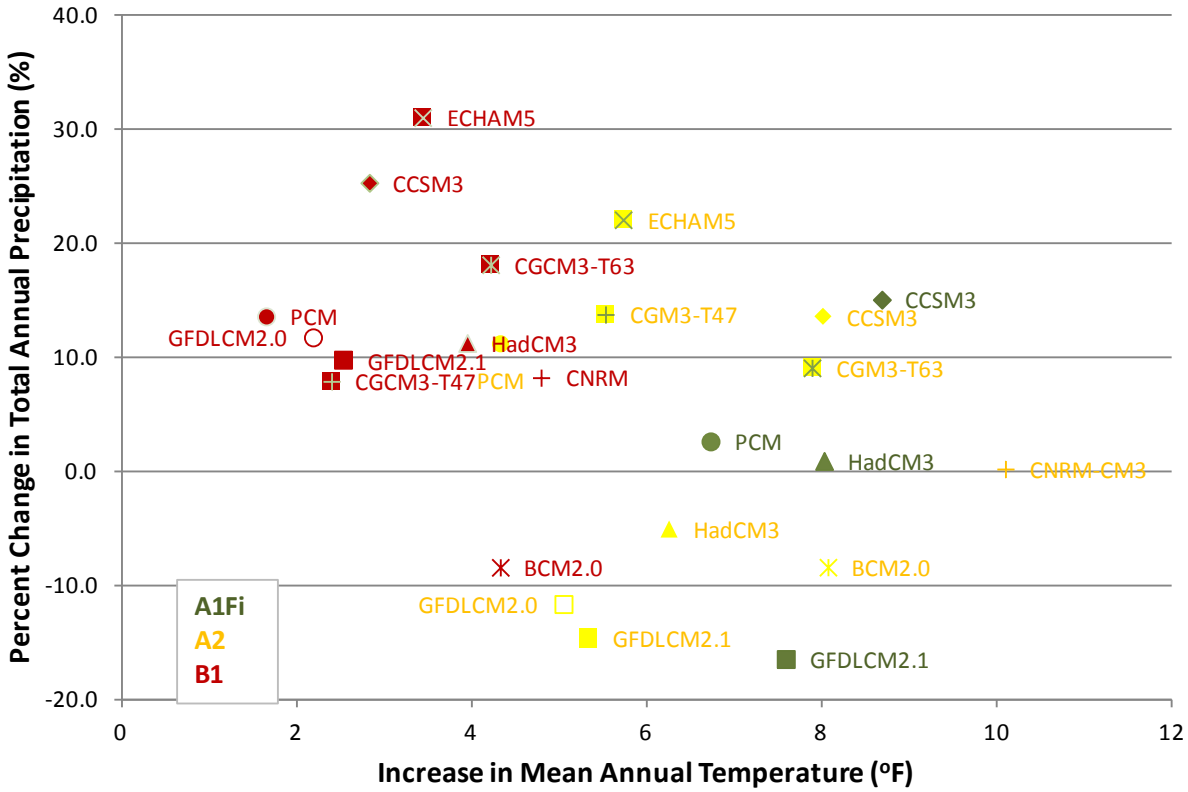

Figure 90 suggests that the models show an inverse relationship, where increasing temperatures are associated with decreasing precipitation. Drawing upon this qualitative observation, the Pearson's correlation coefficient and the Spearman rank correlation coefficient were computed where a result of -1 would indicate a one-to-one relationship between increasing temperature and decreasing precipitation. These computations indicate that the relationship is not particularly strong, with a Pearson's correlation coefficient of -0.4 and a Spearman rank correlation

coefficient of -0.3. However, both coefficients suggest a tendency towards an inverse relationship, supporting the qualitative observation. Additional analysis with 'finer-tuned' temperature and precipitation variables (e.g., with extreme outliers removed) could reveal a stronger relationship.

Figure 90 also illustrates some interesting patterns by emission scenario. Climate model simulations driven by the low (B1) emission scenario project the smallest increase in annual mean temperature but the greatest increase in total annual precipitation. As described in Section 2.5.2, the simulations driven by the low (B1) emission scenario uniquely project a statistically significant change in precipitation compared to the baseline. Climate model simulations driven by the moderately-high (A2) emission scenario project a warmer world, but do not project any statically significant change in precipitation. In fact, almost as many climate models project an increase in precipitation as a decrease in precipitation. Climate model simulations driven by the high (A1FI) emission scenario suggest the greatest increase in temperature, but also do not project a statistically significant change in precipitation. Note that comparing the projections associated with the high (A1FI) emission scenario to the climate projections associated with the moderately-high (A2) and low (B1) emission scenarios may be misleading, as the high (A1FI) simulations are only informed by four climate models.

Some climate models exhibit a tendency towards wetter or warmer projections. For example, the CCSM3 model consistently projects a warmer and wetter climate than the climate model ensemble mean. The climate projections in this report are provided using the climate model ensemble mean with the variability across climate models provided for each emission scenario and averaged across all five station locations.

C.5. Summary Tables for Projected Temperature Analysis

This appendix contains summary tables corresponding to the projected temperature analysis described in Section 2.4.2. Please note that shaded cells with the letter "Y" indicate statistically significant changes. Cells with grayed-out font and the letter "N" indicate projections that do not exhibit a statistically significant change. These projections are not considered different from baseline conditions. Though this test accounts for both the amount of change projected by the mean averaged across all the climate models and the variability across the climate models, the table only provides the change in ensemble mean and does not describe the change in variability (see associated figures for an illustrative description of the change in mean and variability). The following tables are included in this appendix:

- Table 30: Projected Change in the Average Annual Temperatures (°F) from the Model Baseline (1980-2009), Averaged Across All Five Stations
- Table 31: Projected Change in the Average Seasonal Temperatures (°F) Relative to the Model Baseline (1980-2009), Averaged Across All Five Stations
- Table 32: Projected Change in Average Monthly Temperatures (°F) Relative to Model Baseline (1980-2009), Averaged Across All Five Stations
- Table 33: Increase in Projected Heat Events Relative to Model Baseline (1980-2009), Averaged Across All Five Stations
- Table 34: Projected Change in Seasonal Heat Events Relative to Model Baseline (1980-2009), Averaged Across All Five Stations
- Table 35: Projected Change in Extreme Heat Events Relative to Model Baseline (1980-2009), Averaged Across All Five Stations
- Table 36: Projected Change in Extreme Cold Events Compared to Model Baseline (1980-2009), Averaged Across All Five Stations

Table 30: Projected Change in the Average Annual Temperatures (°F) from the Model Baseline (1980-2009), Averaged Across All Five Stations.

Projections representing a significant change are highlighted and marked with a "Y".

	1980-2009 (°F)	2010-2039 (Δ°F)			2040-2069 (Δ°F)			2070-2099 (Δ°F)		
Variable	Observed	B1	A2	A1FI	B1	A2	A1FI	B1	A2	A1FI
Average Annual Mean Temperature	66.6	1.4 (Y)	1.4 (Y)	1.7 (Y)	2.4 (Y)	3.5 (Y)	4.6 (Y)	3.2 (Y)	6.6 (Y)	7.7 (Y)
Average Annual Minimum Temperature	56.2	1.5 (Y)	1.6 (Y)	2.0 (Y)	2.6 (Y)	3.9 (Y)	5.5 (Y)	3.5 (Y)	7.5 (Y)	9.2 (Y)

	1980-2009 (°F)	2010-2039 (Δ°F)			2040-2069 (Δ°F)			2070-2099 (Δ°F)		
Variable	Observed	B1	A2	A1FI	B1	A2	A1FI	B1	A2	A1FI
Average Annual Maximum Temperature	77.0	1.3 (Y)	1.3 (Y)	1.3 (Y)	2.2 (Y)	3.1 (Y)	3.8 (Y)	2.9 (Y)	5.8 (Y)	6.3 (Y)

Table 31: Projected Change in the Average Seasonal Temperatures (°F) Relative to the Model Baseline (1980-2009), Averaged Across All Five Stations

Projections representing a significant change are highlighted and marked with a "Y".

	1980-2009 (°F)	2010-2039 (Δ°F)			2040-2069 (Δ°F)			2070-2099 (Δ°F)		
Variable	Observed	B1	A2	A1FI	B1	A2	A1FI	B1	A2	A1FI
Average Seasonal Mean Temperature										
Winter	52.0	1.0 (Y)	1.3 (Y)	1.2 (Y)	2.2 (Y)	3.0 (Y)	3.3 (Y)	2.9 (Y)	5.7 (Y)	5.7 (Y)
Spring	66.3	1.3 (Y)	1.0 (Y)	1.7 (Y)	2.1 (Y)	3.0 (Y)	4.7 (Y)	2.8 (Y)	6.0 (Y)	7.8 (Y)
Summer	80.4	1.5 (Y)	1.5 (Y)	1.8 (Y)	2.4 (Y)	3.8 (Y)	5.5 (Y)	3.0 (Y)	6.9 (Y)	9.0 (Y)
Fall	68.0	1.8 (Y)	1.9 (Y)	1.9 (Y)	2.9 (Y)	4.2 (Y)	5.1 (Y)	4.2 (Y)	7.9 (Y)	8.5 (Y)
Average Seasonal Maximum Temperature										
Winter	62.7	1.0 (Y)	1.3 (Y)	1.1 (Y)	2.2 (Y)	3.0 (Y)	3.2 (Y)	3.0 (Y)	5.7 (Y)	5.6 (Y)
Spring	77.2	1.1 (Y)	0.9 (Y)	1.5 (Y)	1.8 (Y)	2.6 (Y)	4.2 (Y)	2.5 (Y)	5.3 (Y)	6.6 (Y)
Summer	89.7	1.3 (Y)	1.3 (Y)	1.3 (Y)	2.0 (Y)	3.2 (Y)	4.2 (Y)	2.5 (Y)	5.7 (Y)	6.7 (Y)
Fall	78.7	1.7 (Y)	1.6 (Y)	1.4 (Y)	2.6 (Y)	3.5 (Y)	3.8 (Y)	3.7 (Y)	6.5 (Y)	6.4 (Y)
Average Seasonal Minimum Temperature										
Winter	41.3	0.9 (Y)	1.3 (Y)	1.4 (Y)	2.2 (Y)	3.2 (Y)	3.3 (Y)	2.8 (Y)	5.8 (Y)	5.7 (Y)
Spring	55.4	1.5 (Y)	1.2 (Y)	1.9 (Y)	2.4 (Y)	3.3 (Y)	5.3 (Y)	3.2 (Y)	6.6 (Y)	8.9 (Y)
Summer	71.2	1.7 (Y)	1.7 (Y)	2.3 (Y)	2.7 (Y)	4.3 (Y)	6.9 (Y)	3.5 (Y)	8.1 (Y)	11.4 (Y)
Fall	57.3	1.9 (Y)	2.2 (Y)	2.5 (Y)	3.2 (Y)	4.9 (Y)	6.4 (Y)	4.7 (Y)	9.3 (Y)	10.5 (Y)

Table 32: Projected Change in Average Monthly Temperatures (°F) Relative to Model Baseline (1980-2009), Averaged Across All Five Stations

Projections representing a significant change are highlighted and marked with a "Y"

	1980-2009 (°F)	2010-2039 (Δ°F)			2040-2069 (Δ°F)			2070-2099 (Δ°F)		
Variable	Observed	B1	A2	A1FI	B1	A2	A1FI	B1	A2	A1FI
Average Monthly Mean Temperature										
Jan	50.4	1.0 (Y)	1.6 (Y)	1.3 (N)	2.0 (Y)	3.7 (Y)	3.0 (Y)	2.8 (Y)	6.5 (Y)	5.5 (Y)
Feb	53.5	0.6 (N)	0.8 (N)	0.8 (Y)	1.8 (Y)	2.1 (Y)	3.3 (Y)	2.0 (Y)	4.9 (Y)	5.2 (Y)
Mar	59.7	1.6 (Y)	1.0 (Y)	1.6 (N)	2.0 (Y)	2.6 (Y)	4.2 (Y)	2.7 (Y)	5.5 (Y)	6.8 (Y)
Apr	65.7	1.1 (Y)	1.1 (Y)	1.5 (Y)	2.1 (Y)	2.9 (Y)	4.6 (Y)	2.8 (Y)	6.0 (Y)	7.6 (Y)
May	73.4	1.3 (Y)	1.1 (Y)	2.0 (Y)	2.2 (Y)	3.4 (Y)	5.3 (Y)	3.0 (Y)	6.8 (Y)	8.9 (Y)
Jun	79.1	1.4 (Y)	1.3 (Y)	1.7 (Y)	2.2 (Y)	3.5 (Y)	5.3 (Y)	2.7 (Y)	6.6 (Y)	8.7 (Y)
Jul	81.3	1.5 (Y)	1.5 (Y)	1.9 (Y)	2.3 (Y)	3.9 (Y)	5.7 (Y)	3.0 (Y)	7.1 (Y)	9.1 (Y)
Aug	81.0	1.6 (Y)	1.8 (Y)	2.0 (Y)	2.6 (Y)	4.0 (Y)	5.6 (Y)	3.3 (Y)	7.3 (Y)	9.3 (Y)
Sept	77.1	1.8 (Y)	1.8 (Y)	2.1 (Y)	2.7 (Y)	4.3 (Y)	5.3 (Y)	4.0 (Y)	7.6 (Y)	9.1 (Y)
Oct	67.9	1.8 (Y)	2.3 (Y)	2.2 (Y)	2.8 (Y)	4.7 (Y)	5.8 (Y)	4.3 (Y)	8.9 (Y)	9.4 (Y)
Nov	59.2	1.7 (Y)	1.5 (Y)	1.5 (Y)	3.3 (Y)	3.6 (Y)	4.1 (Y)	4.2 (Y)	7.3 (Y)	6.8 (Y)
Dec	52.3	1.3 (Y)	1.6 (Y)	1.6 (Y)	2.7 (Y)	3.5 (Y)	3.5 (Y)	3.8 (Y)	6.3 (Y)	6.3 (Y)
Average Monthly Maximum Temperature										
Jan	61.0	0.9 (Y)	1.5 (Y)	1.0 (N)	2.0 (Y)	3.4 (Y)	3.0 (Y)	2.8 (Y)	6.1 (Y)	5.5 (Y)
Feb	64.5	0.6 (N)	0.8 (N)	0.8 (Y)	1.7 (Y)	2.0 (Y)	3.3 (Y)	2.2 (Y)	4.9 (Y)	5.3 (Y)
Mar	70.9	1.3 (Y)	1.0 (Y)	1.5 (N)	1.8 (Y)	2.5 (Y)	3.9 (Y)	2.5 (Y)	5.2 (Y)	6.2 (Y)
Apr	76.9	1.0 (Y)	0.9 (Y)	1.5 (N)	1.7 (Y)	2.5 (Y)	4.1 (Y)	2.5 (Y)	5.1 (Y)	6.6 (Y)
May	83.8	1.0 (Y)	0.8 (Y)	1.4 (Y)	1.8 (Y)	2.8 (Y)	4.4 (Y)	2.4 (Y)	5.6 (Y)	7.1 (Y)
Jun	88.5	1.1 (Y)	1.0 (Y)	1.3 (N)	1.8 (Y)	2.8 (Y)	4.2 (Y)	2.1 (Y)	5.1 (Y)	6.7 (Y)
Jul	90.3	1.3 (Y)	1.3 (Y)	1.4 (Y)	2.0 (Y)	3.3 (Y)	4.2 (Y)	2.6 (Y)	5.8 (Y)	6.6 (Y)
Aug	90.1	1.4 (Y)	1.6 (Y)	1.3 (N)	2.1 (Y)	3.3 (Y)	4.0 (Y)	2.8 (Y)	6.0 (Y)	6.7 (Y)
Sept	86.8	1.6 (Y)	1.4 (Y)	1.3 (Y)	2.2 (Y)	3.4 (Y)	3.5 (Y)	3.3 (Y)	6.0 (Y)	6.4 (Y)
Oct	78.9	1.7 (Y)	1.8 (Y)	1.6 (Y)	2.6 (Y)	3.8 (Y)	4.2 (Y)	3.7 (Y)	7.1 (Y)	6.8 (Y)
Nov	70.4	1.7 (Y)	1.5 (Y)	1.3 (Y)	3.1 (Y)	3.3 (Y)	3.6 (Y)	4.0 (Y)	6.5 (Y)	6.1 (Y)
Dec	62.9	1.4 (Y)	1.7 (Y)	1.4 (Y)	2.7 (Y)	3.5 (Y)	3.4 (Y)	4.0 (Y)	6.0 (Y)	6.0 (Y)

	1980-2009 (°F)	2010-2039 (Δ°F)			2040-2069 (Δ°F)			2070-2099 (Δ°F)		
Variable	Observed	B1	A2	A1FI	B1	A2	A1FI	B1	A2	A1FI
Average Monthly Minimum Temperature										
Jan	39.8	1.0 (Y)	1.6 (Y)	1.5 (N)	2.0 (Y)	3.7 (Y)	3.1 (Y)	2.7 (Y)	6.3 (Y)	5.5 (Y)
Feb	42.6	0.5 (N)	0.6 (N)	0.8 (Y)	1.8 (Y)	2.2 (Y)	3.2 (Y)	1.9 (Y)	4.7 (Y)	5.2 (Y)
Mar	48.5	1.8 (Y)	1.1 (Y)	1.7 (N)	2.2 (Y)	2.8 (Y)	4.5 (Y)	2.9 (Y)	5.6 (Y)	7.3 (Y)
Apr	54.6	1.2 (Y)	1.2 (Y)	1.6 (Y)	2.4 (Y)	3.2 (Y)	5.1 (Y)	3.1 (Y)	6.6 (Y)	8.7 (Y)
May	63.0	1.6 (Y)	1.3 (Y)	2.5 (Y)	2.6 (Y)	3.9 (Y)	6.2 (Y)	3.7 (Y)	7.7 (Y)	10.8 (Y)
Jun	69.7	1.6 (Y)	1.5 (Y)	2.0 (Y)	2.6 (Y)	3.9 (Y)	6.4 (Y)	3.2 (Y)	7.5 (Y)	10.7 (Y)
Jul	72.2	1.7 (Y)	1.6 (Y)	2.4 (Y)	2.6 (Y)	4.5 (Y)	7.1 (Y)	3.5 (Y)	8.3 (Y)	11.6 (Y)
Aug	71.8	1.8 (Y)	1.9 (Y)	2.6 (Y)	3.0 (Y)	4.7 (Y)	7.2 (Y)	3.8 (Y)	8.6 (Y)	11.9 (Y)
Sept	67.4	2.1 (Y)	2.2 (Y)	2.9 (Y)	3.3 (Y)	5.1 (Y)	7.0 (Y)	4.7 (Y)	9.3 (Y)	11.8 (Y)
Oct	57.0	1.9 (Y)	2.8 (Y)	2.7 (Y)	3.0 (Y)	5.7 (Y)	7.3 (Y)	4.9 (Y)	10.6 (Y)	12.0 (Y)
Nov	47.9	1.8 (N)	1.6 (Y)	1.8 (Y)	3.4 (Y)	3.9 (Y)	4.7 (Y)	4.4 (Y)	7.9 (Y)	7.6 (Y)
Dec	41.8	1.2 (Y)	1.6 (Y)	1.7 (Y)	2.7 (Y)	3.5 (Y)	3.5 (Y)	3.6 (Y)	6.2 (Y)	6.5 (Y)

Table 33: Increase in Projected Heat Events Relative to Model Baseline (1980-2009), Averaged Across All Five Stations.

Projections representing a significant change are highlighted and marked with a "Y"

	1980-2009 (days/°F)	2010-2039 (Δ/Δ°F)			2040-2069 (Δ/Δ°F)			2070-2099 (Δ/Δ°F)		
Variable	Observed	B1	A2	A1FI	B1	A2	A1FI	B1	A2	A1FI
# days per year above 95°F	9.6	8 (Y)	8 (Y)	9 (Y)	14 (Y)	28 (Y)	38 (Y)	21 (Y)	64 (Y)	76 (Y)
# days per year above 100°F	0.6	1 (N)	0 (N)	0 (N)	1 (N)	4 (Y)	6 (Y)	3 (N)	18 (Y)	20 (Y)
# days per year above 105°F	0.0	0 (N)	0 (N)	0 (N)	0 (N)	0 (N)	0 (N)	0 (N)	2 (N)	1 (N)
# days per year above 110°F	0.0	0 (N)	0 (N)	0 (N)	0 (N)	0 (N)	0 (N)	0 (N)	0 (N)	0 (N)

	1980-2009 (days/°F)	2010-2039 (Δ/Δ°F)			2040-2069 (Δ/Δ°F)			2070-2099 (Δ/Δ°F)		
Variable	Observed	B1	A2	A1FI	B1	A2	A1FI	B1	A2	A1FI
Longest # of consecutive days above 95°F	3.9	3 (Y)	3 (Y)	2 (N)	6 (Y)	12 (Y)	15 (N)	9 (Y)	30 (Y)	34 (N)
Longest # of consecutive days above 100°F	0.4	0 (Y)	0 (N)	0 (N)	1 (N)	2 (Y)	3 (Y)	2 (N)	8 (Y)	8 (Y)
Longest # of consecutive days above 105°F	0.0	0 (N)	0 (N)	0 (N)	0 (N)	0 (N)	0 (N)	0 (N)	2 (N)	1 (Y)
Longest # of consecutive days above 110°F	0.0	0 (N)	0 (N)	0 (N)	0 (N)	0 (N)	0 (N)	0 (N)	0 (N)	0 (N)
Hottest Day of the Year (°F)										
Mean	97.0	1.4 (Y)	1.4 (Y)	1.4 (Y)	2.2 (Y)	3.8 (Y)	4.4 (Y)	3.0 (Y)	6.9 (Y)	7.0 (Y)
50th Percentile	96.8	1.4 (Y)	1.6 (Y)	1.5 (Y)	2.3 (Y)	4.0 (Y)	4.3 (Y)	3.1 (Y)	7.1 (Y)	6.8 (Y)
95th Percentile	101.3	1.5 (Y)	1.1 (N)	0.8 (N)	1.6 (Y)	3.9 (Y)	4.3 (Y)	2.7 (Y)	7.2 (Y)	7.0 (Y)
Maximum	102.8	2.2 (Y)	0.8 (N)	0.6 (N)	1.7 (Y)	3.9 (Y)	4.5 (Y)	2.9 (Y)	7.2 (Y)	7.9 (Y)

Table 34: Projected Change in Seasonal Heat Events Relative to Model Baseline (1980-2009), Averaged Across All Five Stations

Projections representing a significant change are highlighted and marked with a "Y"

	1980-2009 (days)	2010-2039 (Δ)			2040-2069 (Δ)			2070-2099 (Δ)		
Variable	Observed	B1	A2	A1FI	B1	A2	A1FI	B1	A2	A1FI
Number of Days Above 95°F										
Winter	0.0	0.0 (N)	0.0 (N)	0.0 (N)	0.0 (N)	0.0 (N)	0.0 (N)	0.0 (N)	0.1 (N)	0.0 (N)

	1980-2009 (days)	2010-2039 (Δ)			2040-2069 (Δ)			2070-2099 (Δ)		
Variable	Observed	B1	A2	A1FI	B1	A2	A1FI	B1	A2	A1FI
Spring	0.0	0.3 (N)	0.2 (N)	0.5 (N)	0.5 (N)	1.4 (N)	2.7 (N)	0.6 (N)	5.3 (Y)	6.9 (N)
Summer	9.0	6.7 (Y)	6.2 (Y)	8.2 (Y)	11.9 (Y)	22.8 (Y)	31.5 (Y)	16.5 (Y)	45.0 (Y)	56.3 (Y)
Fall	0.8	1.2 (N)	1.2 (Y)	0.7 (N)	2.2 (N)	4.2 (Y)	3.6 (N)	4.5 (N)	13.4 (Y)	13.0 (Y)
Number of Days Above 100°F										
Winter	0.0	0.0 (N)	0.0 (N)	0.0 (N)	0.0 (N)	0.0 (N)	0.0 (N)	0.0 (N)	0.0 (N)	0.0 (N)
Spring	0.0	0.0 (N)	0.0 (N)	0.0 (N)	0.0 (N)	0.1 (N)	0.3 (N)	0.0 (N)	0.6 (N)	0.9 (N)
Summer	0.6	0.7 (N)	0.4 (N)	0.4 (N)	1.2 (N)	3.5 (Y)	4.9 (N)	2.0 (N)	13.9 (Y)	17.0 (Y)
Fall	0.0	0.1 (N)	0.1 (N)	0.0 (N)	0.2 (N)	0.2 (N)	0.4 (N)	0.8 (N)	2.8 (N)	2.3 (Y)
Longest Number of Consecutive Days Above 95°F										
Winter	0.0	0.0 (N)	0.0 (N)	0.0 (N)	0.0 (N)	0.0 (N)	0.0 (N)	0.0 (N)	0.1 (N)	0.0 (N)
Spring	0.1	0.2 (N)	0.1 (N)	0.3 (N)	0.3 (N)	0.9 (Y)	1.9 (N)	0.4 (Y)	3.6 (Y)	4.9 (N)
Summer	3.8	3.0 (Y)	2.6 (Y)	2.5 (Y)	5.2 (Y)	10.8 (Y)	14.7 (Y)	7.4 (Y)	25.7 (Y)	31.2 (Y)
Fall	0.5	0.8 (N)	0.8 (Y)	0.5 (N)	1.3 (N)	2.6 (Y)	2.4 (N)	2.9 (N)	8.4 (Y)	8.2 (Y)
Longest Number of Consecutive Days Above 100°F										
Winter	0.0	0.0 (N)	0.0 (N)	0.0 (N)	0.0 (N)	0.0 (N)	0.0 (N)	0.0 (N)	0.0 (N)	0.0 (N)
Spring	0.0	0.0 (N)	0.0 (N)	0.0 (N)	0.0 (N)	0.1 (N)	0.2 (N)	0.0 (N)	0.6 (N)	0.6 (N)
Summer	0.4	0.4 (Y)	0.3 (N)	0.3 (N)	0.7 (N)	2.0 (Y)	2.7 (Y)	1.2 (Y)	7.6 (Y)	8.1 (Y)
Fall	0.0	0.1 (N)	0.1 (N)	0.1 (N)	0.2 (N)	0.2 (N)	0.4 (N)	0.7 (N)	1.8 (N)	1.6 (Y)

Table 35: Projected Change in Extreme Heat Events Relative to Model Baseline (1980-2009), Averaged Across All Five Stations

Projections representing a significant change are highlighted and marked with a "Y"

	1980-2009 (°F)	2010-2039 (Δ°F)			2040-2069 (Δ°F)			2070-2099 (Δ°F)		
Variable	Observed	B1	A2	A1FI	B1	A2	A1FI	B1	A2	A1FI
Hottest Week of the Year										

	1980-2009 (°F)	2010-2039 (Δ°F)			2040-2069 (Δ°F)			2070-2099 (Δ°F)		
Variable	Observed	B1	A2	A1FI	B1	A2	A1FI	B1	A2	A1FI
Mean	94.4	1.4 (Y)	1.3 (Y)	1.3 (Y)	2.1 (Y)	3.6 (Y)	4.3 (Y)	3.0 (Y)	6.7 (Y)	6.8 (Y)
50th Percentile	94.2	1.3 (Y)	1.4 (Y)	1.4 (Y)	2.2 (Y)	3.8 (Y)	4.2 (Y)	3.0 (Y)	6.6 (Y)	6.7 (Y)
90th percentile	97.2	1.4 (Y)	1.1 (Y)	1.2 (N)	1.6 (Y)	3.7 (Y)	4.4 (Y)	2.4 (Y)	6.9 (Y)	6.9 (Y)
95th Percentile	98.5	1.5 (Y)	1.2 (Y)	0.8 (N)	1.7 (Y)	3.7 (Y)	4.4 (Y)	2.8 (Y)	7.0 (Y)	7.1 (Y)
99th percentile	99.7	1.8 (Y)	1.2 (Y)	0.7 (N)	1.6 (Y)	3.7 (Y)	4.4 (Y)	3.0 (Y)	7.1 (Y)	7.8 (Y)
Warmest Four Days in Summer										
Mean	84.1	1.3 (Y)	1.3 (Y)	1.3 (Y)	2.0 (Y)	3.2 (Y)	4.1 (Y)	2.5 (Y)	5.6 (Y)	6.6 (Y)
5th percentile	87.6	1.3 (Y)	1.5 (Y)	1.4 (N)	2.3 (Y)	3.1 (Y)	4.6 (Y)	2.9 (Y)	5.5 (Y)	7.0 (Y)
25th percentile	89.7	1.3 (Y)	1.4 (Y)	1.4 (Y)	1.9 (Y)	2.9 (Y)	4.0 (Y)	2.4 (Y)	5.2 (Y)	6.4 (Y)
50th percentile	91.7	1.2 (Y)	1.3 (Y)	1.4 (Y)	1.9 (Y)	3.0 (Y)	3.9 (Y)	2.4 (Y)	5.4 (Y)	6.5 (Y)
75th percentile	95.0	1.2 (Y)	1.3 (Y)	1.6 (Y)	2.0 (Y)	3.4 (Y)	4.3 (Y)	2.5 (Y)	5.9 (Y)	6.7 (Y)
95th percentile	89.7	1.2 (Y)	1.1 (Y)	1.4 (Y)	1.9 (Y)	3.5 (Y)	4.2 (Y)	2.5 (Y)	6.5 (Y)	6.7 (Y)
Warmest summer in 30 years	100.8	1.8 (Y)	0.9 (N)	0.2 (N)	1.5 (Y)	3.5 (Y)	3.7 (Y)	2.7 (Y)	7.0 (Y)	7.6 (Y)

Table 36: Projected Change in Extreme Cold Events Compared to Model Baseline (1980-2009), Averaged Across All Five Stations

Projections representing a significant change are highlighted and marked with a "Y"

	1980-2009 (°F)	2010-2039 (Δ°F)			2040-2069 (Δ°F)			2070-2099 (Δ°F)		
Variable	Observed	B1	A2	A1FI	B1	A2	A1FI	B1	A2	A1FI
Coldest Day of the Year										
Mean	18.9	1.2 (N)	1.6 (Y)	2.7 (Y)	2.8 (Y)	3.3 (Y)	4.7 (Y)	2.7 (Y)	6.1 (Y)	6.8 (Y)
1st percentile	4.2	1.2 (N)	3.9 (N)	5.7 (Y)	4.0 (N)	4.1 (N)	8.2 (N)	2.9 (N)	8.6 (Y)	9.2 (Y)
5th percentile	7.9	2.4 (Y)	3.0 (N)	5.6 (Y)	4.0 (Y)	5.2 (Y)	8.5 (Y)	3.1 (Y)	9.0 (Y)	11.0 (Y)
10th percentile	8.9	3.4 (Y)	2.2 (Y)	5.6 (Y)	4.9 (Y)	4.9 (Y)	8.0 (N)	4.4 (Y)	7.7 (Y)	11.0 (Y)
50th percentile	20.3	0.7 (N)	1.0 (N)	1.9 (N)	2.3 (Y)	2.7 (Y)	3.8 (Y)	2.2 (Y)	5.6 (Y)	6.0 (Y)
Coldest Four Days in Winter										
5th percentile	28.1	1.0 (Y)	0.9 (Y)	1.3 (N)	1.9 (Y)	2.7 (Y)	3.1 (Y)	2.3 (Y)	5.0 (Y)	5.3 (Y)
25th percentile	35.1	0.9 (Y)	1.2 (Y)	1.1 (Y)	2.0 (Y)	2.9 (Y)	2.9 (Y)	2.6 (Y)	5.4 (Y)	5.2 (Y)
50th percentile	40.9	0.8 (Y)	1.4 (Y)	1.3 (Y)	2.2 (Y)	3.2 (Y)	3.3 (Y)	2.8 (Y)	5.8 (Y)	5.9 (Y)
75th percentile	47.4	0.8 (N)	1.4 (Y)	1.2 (Y)	2.3 (Y)	3.3 (Y)	3.2 (Y)	3.0 (Y)	6.2 (Y)	6.0 (Y)
95th percentile	56.2	1.0 (N)	1.5 (Y)	1.8 (N)	2.5 (Y)	3.5 (Y)	3.4 (Y)	3.0 (Y)	6.3 (Y)	6.6 (Y)
Mean	41.3	0.9 (Y)	1.3 (Y)	1.4 (Y)	2.2 (Y)	3.2 (Y)	3.2 (Y)	2.8 (Y)	5.8 (Y)	5.8 (Y)
Coldest winter in 30 years	12.6	1.0 (N)	2.3 (N)	2.7 (N)	4.2 (Y)	3.6 (N)	6.7 (N)	2.5 (N)	8.9 (Y)	7.8 (N)

C.6. Summary Tables for Projected Precipitation Analysis

This appendix contains summary tables corresponding to the projected precipitation analysis described in Section 2.5.2. Please note that shaded cells with the letter "Y" indicate statistically significant changes. Cells with grayed-out font and the letter "N" indicate projections that do not exhibit a statistically significant change. These projections are not considered different from baseline conditions. The following tables are included in this appendix:

- Table 37: Projected Change in Total Annual Precipitation (inches) Relative to Model Baseline (1980-2009), Averaged Across All Five Stations
- Table 38: Projected Change in Total Seasonal and Monthly Precipitation (inches)
- Table 39: Projected Change in Maximum Three-Day Precipitation Totals (inches)
- Table 40: Projected Change in the Magnitude of 24-Hour Storm Events (inches)
- Table 41: Change in the Probability of Current Storms (1980-2009) Occurring in the Future
- Table 42: Projected Change in Precipitation Events (inches) by Exceedance Probability

Table 37: Projected Change in Total Annual Precipitation (inches) Relative to Model Baseline (1980-2009), Averaged Across All Five Stations

Projections representing a significant change are highlighted and marked with a "Y"

	1980-2009 (in.)	2010-2039 (Δ in.)			2040-2069 (Δ in.)			2070-2099 (Δ in.)		
Variable	**Observed**	**B1**	**A2**	**A1FI**	**B1**	**A2**	**A1FI**	**B1**	**A2**	**A1FI**
Total Annual Precipitation	65.4	3.4 (N)	3.5 (N)	4.4 (N)	6.9 (Y)	3.3 (N)	3.5 (N)	8.4 (Y)	2.0 (N)	0.6 (N)

Table 38: Projected Change in Total Seasonal and Monthly Precipitation (inches) Relative to Model Baseline (1980-2009), Averaged Across All Five Stations

Projections representing a significant change are highlighted and marked with a "Y"

	1980-2009 (in.)	2010-2039 (Δ in.)			2040-2069 (Δ in.)			2070-2099 (Δ in.)		
Variable	**Observed**	**B1**	**A2**	**A1FI**	**B1**	**A2**	**A1FI**	**B1**	**A2**	**A1FI**
Total Seasonal Precipitation										
Winter	15.3	1.6 (Y)	0.9 (N)	1.7 (N)	1.7 (Y)	1.3 (N)	0.6 (N)	2.0 (N)	1.8 (N)	-0.7 (N)
Spring	15.7	-0.1 (N)	0.6 (N)	0.7 (N)	-0.2 (N)	-0.3 (N)	-0.4 (N)	1.1 (N)	-0.8 (N)	-0.7 (N)
Summer	20.2	0.9 (N)	0.8 (N)	0.0 (N)	3.2 (N)	0.8 (N)	-0.5 (N)	2.7 (N)	-1.0 (N)	-1.9 (N)

	1980-2009 (in.)	2010-2039 (Δ in.)			2040-2069 (Δ in.)			2070-2099 (Δ in.)		
Variable	Observed	B1	A2	A1FI	B1	A2	A1FI	B1	A2	A1FI
Fall	14.2	1.0 (N)	1.2 (N)	2.0 (N)	2.2 (Y)	1.6 (N)	3.8 (N)	2.6 (N)	2.0 (N)	3.9 (N)
Total Monthly Precipitation										
Jan	5.5	0.7 (N)	0.3 (N)	0.0 (N)	0.6 (N)	0.4 (N)	0.1 (N)	0.8 (N)	0.9 (N)	-0.5 (N)
Feb	5.1	0.3 (N)	0.2 (N)	0.5 (N)	0.4 (N)	-0.1 (N)	0.1 (N)	0.4 (N)	0.2 (N)	0.0 (N)
Mar	5.9	0.0 (N)	-0.1 (N)	0.4 (N)	-0.1 (N)	0.0 (N)	0.2 (N)	0.4 (N)	0.0 (N)	-0.1 (N)
Apr	4.8	0.2 (N)	0.5 (N)	-0.1 (N)	0.0 (N)	-0.4 (N)	0.0 (N)	0.2 (N)	-0.4 (N)	-0.4 (N)
May	5.0	-0.3 (N)	0.2 (N)	0.4 (N)	0.0 (N)	0.0 (N)	-0.6 (N)	0.4 (N)	-0.4 (N)	-0.1 (N)
Jun	6.1	0.2 (N)	0.3 (N)	-0.7 (N)	0.6 (N)	-0.3 (N)	-0.8 (N)	0.6 (N)	-1.0 (N)	-0.4 (N)
Jul	7.7	0.5 (N)	-0.4 (N)	-1.2 (N)	1.5 (N)	0.6 (N)	-1.7 (N)	1.3 (N)	-0.3 (N)	-2.4 (N)
Aug	6.4	0.3 (N)	0.9 (N)	1.8 (N)	1.1 (N)	0.4 (N)	2.0 (N)	0.8 (N)	0.4 (N)	0.9 (N)
Sept	5.5	0.2 (N)	0.8 (N)	1.3 (Y)	1.2 (N)	0.7 (N)	2.0 (N)	1.0 (N)	1.5 (N)	2.4 (N)
Oct	3.9	0.5 (N)	0.2 (N)	0.3 (N)	0.6 (Y)	0.5 (N)	1.8 (N)	0.9 (N)	0.0 (N)	1.8 (N)
Nov	4.8	0.2 (N)	0.3 (N)	0.4 (N)	0.4 (N)	0.4 (N)	0.0 (N)	0.7 (N)	0.4 (N)	-0.3 (N)
Dec	4.7	0.6 (N)	0.5 (N)	1.2 (N)	0.7 (N)	0.9 (N)	0.4 (N)	0.8 (N)	0.7 (N)	-0.2 (N)

Table 39: Projected Change in Maximum Three-Day Precipitation Totals (inches) Relative to Model Baseline (1980-2009), Averaged Across All Five Stations

	1980-2009 (in.)	2010-2039 (Δ in.)			2040-2069 (Δ in.)			2070-2099 (Δ in.)		
Variable	Observed	B1	A2	A1FI	B1	A2	A1FI	B1	A2	A1FI
Maximum Three-Day Precipitation										
Winter	3.7	0.9 (Y)	0.4 (N)	0.6 (N)	0.9 (Y)	0.7 (N)	0.8 (N)	1.1 (Y)	1.3 (Y)	0.5 (N)
Spring	4.8	0.4 (N)	0.5 (N)	0.3 (N)	0.4 (N)	0.5 (N)	0.4 (N)	0.7 (N)	0.6 (N)	0.4 (N)
Summer	4.9	0.6 (N)	0.6 (N)	0.6 (N)	1.2 (Y)	0.8 (N)	0.6 (N)	1.0 (N)	0.2 (N)	0.1 (N)
Fall	4.7	0.4 (N)	0.5 (N)	1.1 (N)	0.9 (Y)	0.7 (N)	1.2 (N)	1.2 (Y)	0.6 (N)	1.2 (N)

Table 40: Projected Change in the Magnitude of 24-Hour Storm Events (inches) Relative to Model Baseline (1980-2009), Averaged Across All Five Stations

	1980-2009 (in)	2010-2039 (Δ in.)			2040-2069 (Δ in.)			2070-2099 (Δ in.)		
Variable	Observed	B1	A2	A1FI	B1	A2	A1FI	B1	A2	A1FI
24-Hour Precipitation Events										
500-year storm	13.5	6.1 (Y)	5.2 (Y)	5.4 (N)	6.3 (Y)	6.4 (Y)	4.2 (N)	8.0 (N)	7.8 (Y)	4.3 (N)
100-year storm	13.5	4.7 (Y)	4.0 (Y)	4.2 (N)	4.9 (Y)	4.9 (Y)	3.3 (N)	6.2 (N)	6.0 (Y)	3.3 (N)
50-year storm	12.5	4.1 (Y)	3.5 (Y)	3.7 (N)	4.3 (Y)	4.3 (N)	2.9 (N)	5.4 (N)	5.2 (Y)	2.9 (N)
20-year storm	9.5	3.3 (N)	2.8 (Y)	3.0 (N)	3.5 (N)	3.5 (Y)	2.3 (N)	4.4 (N)	4.2 (Y)	2.4 (N)
10-year storm	8.5	2.7 (Y)	2.3 (Y)	2.5 (N)	2.9 (Y)	2.9 (Y)	1.9 (N)	3.6 (Y)	3.4 (Y)	1.9 (N)
5-year storm	7.1	2.0 (N)	1.8 (Y)	1.9 (N)	2.3 (Y)	2.2 (N)	1.5 (N)	2.7 (Y)	2.6 (Y)	1.5 (N)
2-year storm	4.8	1.1 (N)	0.9 (Y)	1.1 (N)	1.3 (N)	1.2 (Y)	0.8 (N)	1.5 (Y)	1.4 (Y)	0.8 (N)

Table 41: Change in the Probability of Current Storms (1980-2009) Occurring in the Future

	1980-2009 (%)	2010-2039 (Δ%)			2040-2069 (Δ%)			2070-2099 (Δ%)		
Variable	Observed	B1	A2	A1FI	B1	A2	A1FI	B1	A2	A1FI
24-Hour Precipitation Events – Change in Probability of Occurrence of Baseline Storm Event										
500-year storm	0.2%	3.6% (Y)	2.6% (Y)	3.1% (N)	3.7% (Y)	3.0% (Y)	1.4% (N)	5.0% (Y)	4.5% (Y)	1.8% (N)
100-year storm	1.0%	6.7% (Y)	5.7% (Y)	5.8% (N)	7.4% (Y)	6.8% (Y)	3.7% (N)	9.5% (Y)	9.0% (Y)	4.1% (N)
50-year storm	2.0%	8.8% (Y)	7.9% (Y)	7.5% (N)	9.8% (Y)	9.5% (Y)	5.4% (N)	12.2% (N)	12.0% (Y)	5.8% (N)
20-year storm	5.0%	12.2% (Y)	11.7% (Y)	10.3% (N)	14.0% (Y)	14.0% (Y)	8.7% (N)	16.7% (Y)	16.9% (Y)	8.8% (N)
10-year storm	10.0%	14.8% (Y)	15.0% (Y)	12.7% (N)	17.4% (Y)	17.9% (Y)	11.9% (N)	20.0% (Y)	20.7% (Y)	11.4% (N)
5-year storm	20.0%	16.4% (Y)	17.4% (Y)	14.7% (N)	20.0% (Y)	20.7% (Y)	14.6% (N)	21.9% (Y)	23.0% (Y)	13.3% (N)
2-year storm	50.0%	11.9% (N)	13.6% (Y)	12.7% (N)	16.1% (Y)	16.3% (Y)	12.6% (N)	16.2% (Y)	16.8% (Y)	10.5% (N)

Table 42: Projected Change in Precipitation Events (inches) by Exceedance Probability Relative to Model Baseline (1980-2009), Averaged Across All Five Stations

	1980-2009 (in)	2010-2039 (Δ in.)			2040-2069 (Δ in.)			2070-2099 (Δ in.)		
Variable	**Observed**	**B1**	**A2**	**A1FI**	**B1**	**A2**	**A1FI**	**B1**	**A2**	**A1FI**
Maximum Four-Day Precipitation										
0.2%	11.3	3.7 (N)	3.9 (Y)	2.4 (N)	4.8 (Y)	4.6 (N)	3.7 (N)	4.8 (Y)	5.1 (Y)	3.0 (N)
1%	6.9	1.2 (N)	0.9 (N)	1.1 (N)	1.5 (Y)	1.3 (Y)	1.4 (Y)	2.0 (Y)	1.7 (Y)	1.2 (Y)
2%	5.3	0.5 (N)	0.5 (N)	0.7 (N)	1.0 (Y)	0.8 (Y)	1.0 (Y)	1.2 (Y)	1.0 (Y)	0.9 (Y)
5%	3.7	0.2 (N)	0.3 (Y)	0.3 (N)	0.5 (Y)	0.4 (Y)	0.4 (N)	0.6 (Y)	0.5 (Y)	0.4 (Y)
10%	2.7	0.1 (N)	0.2 (N)	0.1 (N)	0.3 (Y)	0.2 (Y)	0.2 (N)	0.3 (Y)	0.2 (N)	0.2 (N)
20%	1.7	0.1 (N)	0.1 (N)	0.1 (N)	0.1 (N)	0.1 (N)	0.1 (N)	0.2 (Y)	0.1 (N)	0.1 (N)
50%	0.7	0.0 (N)	0.0 (N)	0.0 (N)	0.0 (N)	0.0 (N)	0.0 (N)	0.1 (N)	0.0 (N)	0.0 (N)
Maximum Two-Day Precipitation										
0.2%	9.3	3.6 (N)	3.3 (Y)	3.0 (N)	3.9 (Y)	4.2 (N)	3.8 (N)	4.6 (Y)	4.8 (Y)	2.4 (N)
1%	5.5	0.7 (N)	0.6 (N)	0.9 (N)	1.1 (Y)	1.0 (Y)	1.0 (Y)	1.4 (Y)	1.3 (Y)	0.8 (N)
2%	4.1	0.3 (N)	0.3 (N)	0.6 (N)	0.7 (Y)	0.6 (Y)	0.6 (Y)	0.8 (Y)	0.7 (Y)	0.5 (Y)
5%	2.8	0.1 (N)	0.1 (N)	0.1 (N)	0.3 (N)	0.2 (Y)	0.3 (N)	0.3 (Y)	0.2 (N)	0.3 (N)
10%	2.0	0.1 (N)	0.1 (N)	0.1 (N)	0.2 (Y)	0.1 (Y)	0.1 (N)	0.2 (Y)	0.1 (N)	0.1 (N)
20%	1.3	0.0 (N)	0.1 (N)	0.0 (N)	0.1 (N)	0.1 (Y)	0.0 (N)	0.1 (Y)	0.0 (N)	0.1 (N)
50%	0.4	0.0 (N)	0.0 (N)	0.0 (N)	0.0 (N)	0.0 (N)	0.0 (N)	0.0 (N)	0.0 (N)	0.0 (N)

C.7. Methodology to Select Stream Gages for Historical Streamflow Analysis

This appendix discusses how five stream gages were selected for this analysis of historical streamflow, runoff, and flooding in Mobile.

Initially, the following three USGS networks of streamflow and runoff data were considered.

- USGS Water Watch program of historical and current runoff data[38]
- USGS Hydro-Climatic Data Network
- USGS Surface-Water database of stream gage data

The USGS Water Watch program data are aggregated values across the stream gage sites located within each basin or hydrologic unit. Unlike individual stream gage data, this hydrologic unit runoff data set tends to provide long-term historical records. However, this runoff data set was not ideal for the analysis because the stream gage sites used to inform the basin values are not uniform across the period of record, thereby artificially affecting the long-term trend.

The USGS Hydro-Climatic Data Network is a subset of the USGS Surface-Water database of stream gages that have been identified to be largely unaffected by human disturbance. As such, these stream gages can be used to inform climatic analysis. This database, however, does not provide stream gages in Mobile County.

Ultimately, the USGS Surface-Water database of stream gage data was used to provide streamflow data for this analysis.

Criteria were developed to select stream gages from this database that provide a representative range of basin characteristics and stream sizes. This allows the analysis of this smaller sample set to be representative of the various streams in the study region. The selection criteria include the following requirements:

- Located in Mobile County
- USGS regional flood-frequency analysis[39] available
- Description of the explanatory basin characteristics of greatest relevance to predict peak flows available
- Data sets of streamflow properties (peak streamflow, annual mean discharge, monthly mean discharge) available
- Full period of record (≥20 years) available

[38] Historical runoff data for hydrologic units provided by the USGS Water Watch program (http://waterwatch.usgs.gov/new/index.php?id=romap3). A hydrologic unit is, in theory, equivalent to a basin.
[39] The U.S. Geological Survey (USGS), in cooperation with Alabama Department of Transportation (ALDOT) updated flood-frequency estimates for a number of steam gages. The purpose of updating these estimates was to accurately inform the design drainage structures for highways in Alabama (USGS, 2004; USGS, 2010a).

USGS has conducted analyses determining the explanatory basin characteristics for stream gages in Alabama and summarized these findings in a series of reports.[40] The basin characteristics initially considered are provided in the textbox titled, "Basin Characteristics." The USGS analysis for urban streams in Alabama found that the key characteristics needed to inform estimates of peak flow include the contributing drainage area and the percentage of development in the drainage area.[41] A similar analysis conducted for small rural streams in Alabama found the key characteristics needed to inform estimates of peak flow include the contributing drainage area, the main channel slope, and the percentage of forest cover in the drainage area.[42]

Basin Characteristics

- Contributing drainage area upstream from the streamflow gaging station
- Length of the main channel between the streamflow gaging station to the basin divide
- Main channel slope
- Basin lag-time factor (main channel length / main channel slope)
- Percent of forest cover in drainage area
- Percent of impervious area in drainage area
- Percent of development in drainage area
- Ratio of the average basin width to basin length

Sources: USGS, 2004; USGS, 2010a

The application of the selection criteria outlined above began with over 390 stream gage sites in Alabama, of which approximately 14 were operating in Mobile County.[43] Figure 91 outlines the stream gage selection process.

The selection criteria identified three stream gage sites for the analysis: Chickasaw Creek (site 02471001), Crooked Creek (site 02479980), and Hamilton Creek (site 02480002). Two sites did not meet the criteria but were included due to their unique location, size, and basin characteristics: Mobile River (site 02470630) and Fowl River (site 02471078). The Mobile River site provides only peak streamflow data while the Fowl River site period of record does not begin until 1995.

An additional check was conducted to ensure that the five sites are near high-density areas of transportation assets. Detailed information on the data available at each of these stream gage sites is shown in Table 43.

[40] USGS, 2004; USGS, 2007; USGS, 2010a
[41] USGS, 2010a
[42] USGS, 2004
[43] These numbers are an estimate as the number of stream gage stations change as new gages become operational and operational gages are retired. The USGS website provides the most up-to-date information (http://waterdata.usgs.gov/nwis/annual/?referred_module=sw).

Figure 91: Flowchart Describing the Stream Gage Selection Process

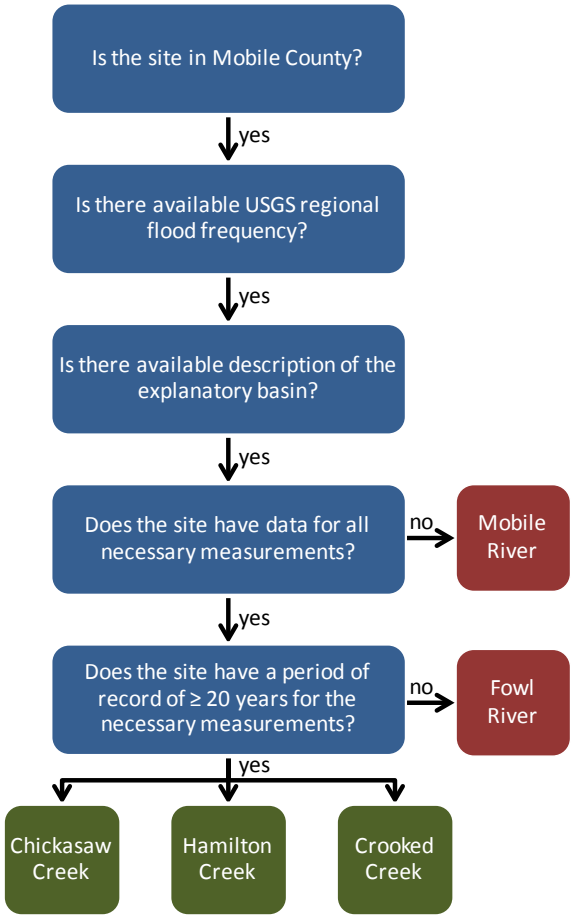

Table 43: Streamflow and Discharge Data Available for Selected Mobile County Stream Gage Stations

Site	Site Number	Characteristics	Annual Peak Streamflow		Monthly Mean Discharge		Annual Mean Discharge	
			Start	End	Start	End	Monthly	Annual
Chickasaw Creek[44]	02471001	Large stream; 125 mi^2 (325 km^2) drainage area	5/1952	5/2010	10/1951	9/2010	1952	2010
Mobile River[45]	02470630	Large river; 44,000 mi^2 (114,400 km^2) drainage area	4/1951	2/2004	X	X	X	X
Fowl River[46]	02471078	Urban stream; 16.5 mi^2 (42.9 km^2) drainage area	4/1995	1/2010	3/1995	9/2010	1995	2010

[44] USGS, 2011a
[45] USGS, 2011d
[46] USGS, 2011b

Site	Site Number	Characteristics	Annual Peak Streamflow		Monthly Mean Discharge		Annual Mean Discharge	
			Start	End	Start	End	Monthly	Annual
Crooked Creek[47]	02479980	Small rural stream; 8 mi^2 (21 km^2) drainage area	1/1991	1/2010	6/1990	9/2010	1990	2010
Hamilton Creek[48]	02480002	Small urban stream; 8 mi^2 (21 km^2) drainage area	5/1991	1/2010	6/1990	9/2010	1990	2010

Figure 93 shows a map of Mobile County, the individual stream gage stations used in this study (defined by green diamonds), and key highways in the region. Major rivers in the area are shown in Figure 92. Three of the four basins in Mobile County are represented by the selected stream gage stations (there are no stream gage sites selected in the southern coastal basin (number 03170009)).

Figure 92: Map of the Mobile-Alabama-Coosa River

Source: Evans

[47] USGS, 2011c
[48] USGS, 2011e

Figure 93: Selected Stream Gage Sites in the Mobile Region

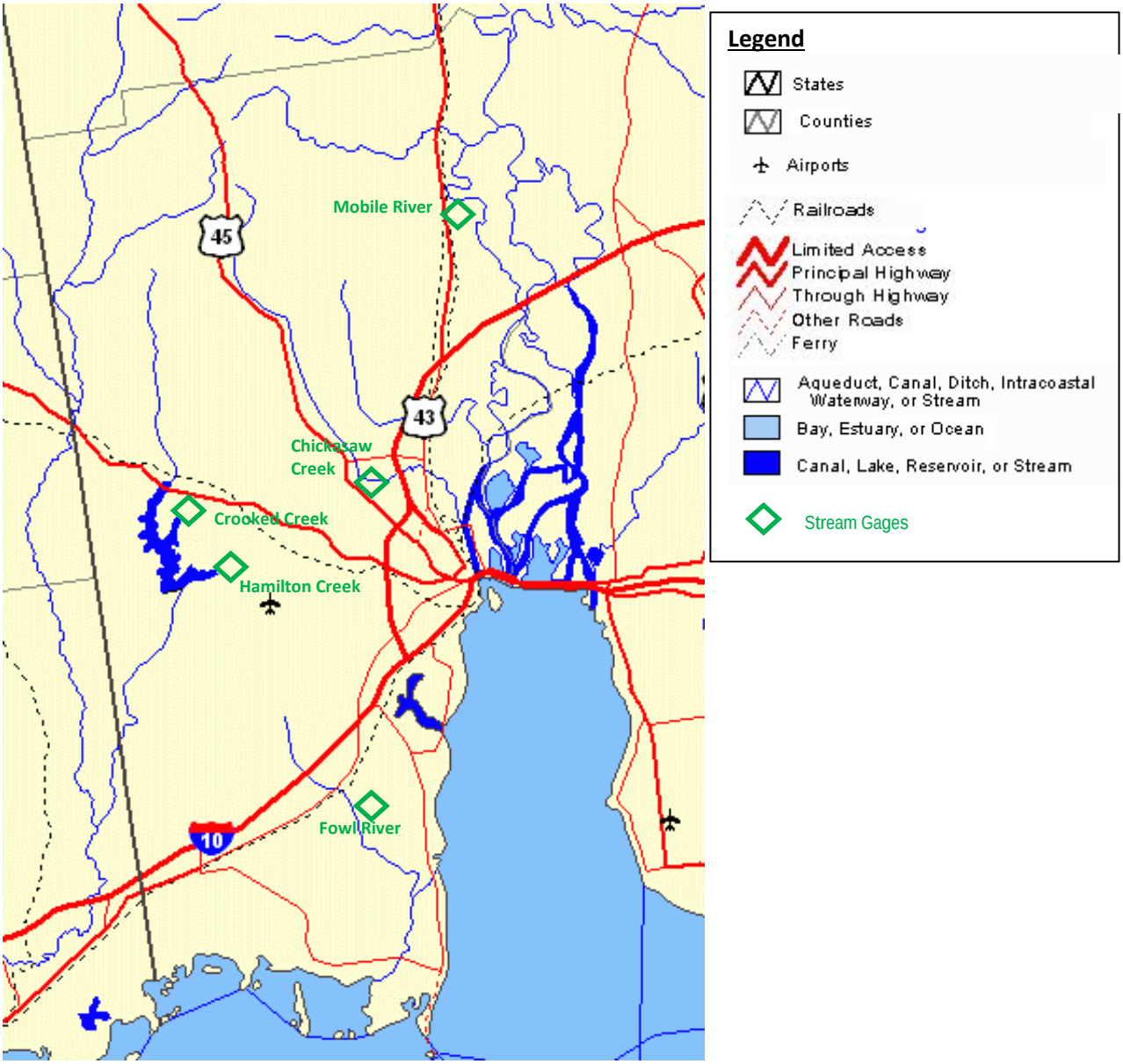

C.8. Detailed Streamflow Projections Methodology

This Appendix describes the methodology that was used to develop projections of future streamflow in the Mobile region. Monthly discharge projections were developed for an artificial basin using the USGS's modified Thornwaite monthly water balance model (WBM) driven by Mobile-specific information.[49] This model estimates monthly runoff which can be converted to stream-specific discharge, evapotranspiration, and soil moisture within a basin or sub-basin using user-provided monthly precipitation and temperature data.

C.8.1. Model Assumptions

The model assumes:

- A portion of precipitation immediately becomes runoff (termed the "direct runoff factor"). This portion is determined by the model user.
- A portion of precipitation infiltrates into the soil and is stored (termed the "soil moisture"). This portion is determined by the model user.
- A portion of precipitation that evaporates back into the atmosphere from land surface, water surface, or plants (termed "evapotranspiration"). This portion is a function of temperature.
- Any remaining precipitation is multiplied by a user-defined runoff factor which determines how much of the remaining precipitation becomes additional runoff and how much is considered surplus that gets carried over to the next month. The monthly runoff (mm) results from WBM can be converted to monthly discharge (cubic feet per second) using the basin area.

Hay and McCabe (2002) tested the performance of a monthly water balance model at a set of diverse physiographic and climatic basins across the United States and concluded that "WB models can be used reliably to estimate monthly runoff in the eastern U.S., mountainous areas of the western U.S., and the Pacific Northwest." This study suggests it is acceptable to use a WBM for the Mobile region for modeling monthly runoff.

Optimum values for the user-defined parameters were determined for Mobile using runoff data from three stream gage sites and meteorological data averaged across the observation station data from Coden and Mobile (Coden and Mobile were chosen because they are located in Mobile County).[50] Stream gage sites were selected that provided monthly stream gage discharge for 1990 to 2010. The discharge was first converted to monthly runoff (millimeters) and then compared against the WBM results. The optimum user-defined parameters were the same as those described in the Hay and McCabe (2002) study.

Once calibrated, the WBM was run with the climate model baseline simulations and compared against the stream gage runoff values. Then the WBM was run with projected temperature and

[49] http://wi.water.usgs.gov/Soil_Water_Balance/index.html
[50] A sensitivity analysis was conducted in which additional station location data were included. This analysis revealed Mobile and Coden provided the best data.

precipitation simulations to provide projected runoff and evapotranspiration for each emission scenario and time period.

Soil parameters tend to vary seasonally and interannually (by year). The WBM, however, assumes a steady-state value across each thirty-year climate period. An important question is whether these values can be assumed to remain constant in the future.

To answer this question, a literature review was conducted and available historical data sets were reviewed. One study investigated how soil moisture changes with temperature using records from over 600 global stations that provided a minimum of 6 years of information (most with more than 15 years). The study found: "in contrast to predictions of summer desiccation with increasing temperatures, for the stations with the longest records summer soil moisture in the top 1 meter has increased while temperatures have risen. The increased trend in precipitation more than compensated for the enhanced evaporation."[51] This suggests soil moisture may increase with projected increasing temperatures; however, a quantitative relationship was not provided. A sensitivity analysis could be conducted to see how sensitive estimated monthly runoff may be to changes in soil moisture.

C.8.2. Model Calibration

To calibrate the model, modeled runoff data was calibrated using observed stream gage data. More specifically, monthly runoff data for 1990 to 2009 produced by the WBM and driven by monthly temperature and precipitation data observed at Mobile and Coden stations were calibrated against the stream gage data.

Figure 94 illustrates that the WBM time series of monthly runoff appears to be similar to the monthly runoff measured at the stream gage sites. The WBM does not capture the extreme peaks in runoff, underestimating periods of low precipitation such as the fall of 1990, 1993, and 1996 and overestimating periods of high precipitation such as the fall of 2002 and summer of 2003. Overall, the model has the most difficulty accurately portraying fall monthly runoff. It is unclear what environmental reason can explain this seasonal signal.

[51] Robock et al., 1999

Figure 94: Monthly Runoff by Stream Gage Station (mm), 1990-2009

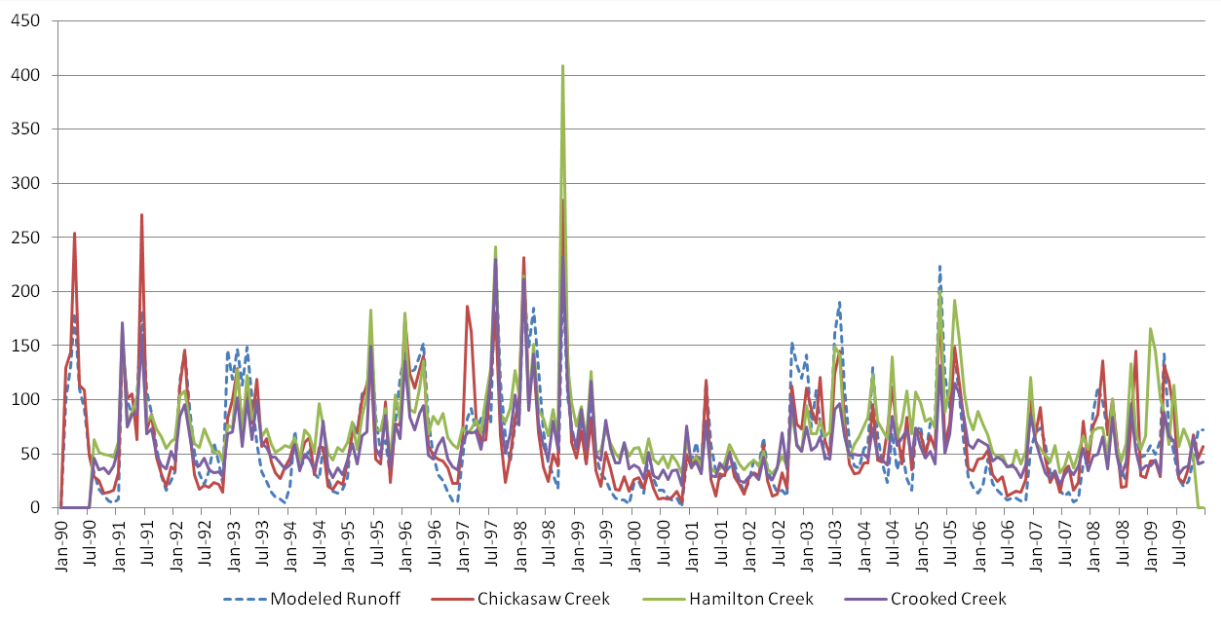

Table 44 shows how well the WBM represents monthly runoff for each stream gage site. For the 1990 to 2009 time period, the WBM captures much of the variability at the Chickasaw Creek stream gage with a coefficient of determination (R^2) of 0.74 (where an R^2 of 1.0 would suggest the WBM explains all variability observed at the stream gage site). The WBM underestimates the period's average monthly runoff by only 1%. The WBM does a less accurate job replicating runoff for Hamilton and Crooked Creeks.

Table 44: The WBM and Goodness-of-fit Parameters for Each Stream Gage Site

Stream Gage site	Observation Stations for Meteorological Data	WBM Parameters	Average Monthly Runoff (mm) (% diff compared to WBM)	Standard error	R^2
Chickasaw Creek	Coden, Mobile	Runoff Factor of 44%; Direct Runoff of 5%; Soil Moisture at 145 mm	63 (-1%)	5	0.74
Hamilton Creek			76 (-18%)	16	0.53
Crooked Creek			59 (+6%)	15	0.62

As the WBM will be used to project monthly runoff based on projections of temperature and precipitation, the WBM was run with baseline modeled conditions and compared against the stream gage sites. These runs show that the monthly runoff for baseline conditions driven by climate model data underestimates the observed stream gage monthly runoff data. The WBM does a reasonable job across baselines from all emission scenarios, with an R^2 of approximately

0.8, for Chickasaw Creek. However, Hamilton and Crooked Creeks are below an R^2 of 0.5. This suggests the projected runoff may be most able to represent changes at Chickasaw Creek.

C.9. Summary Tables and Figures for Projected Streamflow Analysis

This appendix contains summary tables and figures corresponding to the projected streamflow analysis described in Section 9.2 of the main report. The following tables and figures are included in this appendix:

- Figure 95: Modeled Baseline and Projected Monthly Streamflow Discharge (ft^3/sec) for Chickasaw Creek and Actual Evapotranspiration (mm) by Time Period and Emission Scenario
- Table 45: Monthly Streamflow Discharge (ft^3/sec) for Chickasaw Creek and Evapotranspiration (mm), Change from Baseline (1980-2009)
- Figure 96: Modeled Baseline and Projected Monthly Streamflow Discharge (ft^3/sec) by Time Period and Emission Scenario for Crooked Creek and Hamilton Creek

Figure 95: Modeled Baseline and Projected Monthly Streamflow Discharge (ft³/sec) for Chickasaw Creek and Actual Evapotranspiration (mm) by Time Period and Emission Scenario

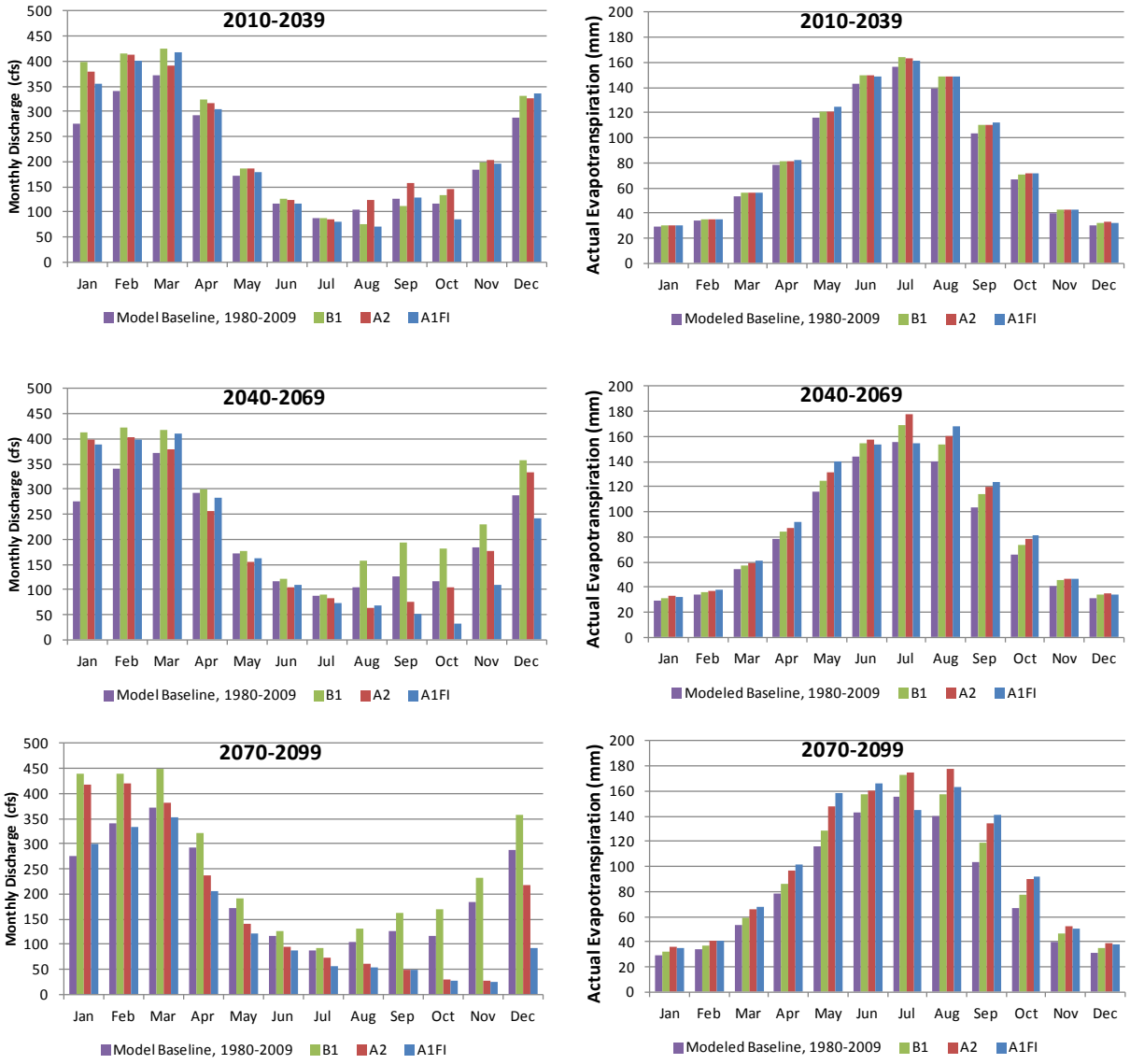

Table 45: Monthly Streamflow Discharge (ft^3/sec) for Chickasaw Creek and Evapotranspiration (mm), Change from Baseline (1980-2009)

	1980-2009	2010-2039 (Δ)			2040-2069 (Δ)			2070-2099 (Δ)		
Variable	**Observed**	**B1**	**A2**	**A1FI**	**B1**	**A2**	**A1FI**	**B1**	**A2**	**A1FI**
Monthly Streamflow Discharge (ft^3/sec)										
Jan	390.4	121.7	103.7	77.7	135.3	123.8	111.4	160.5	141.7	23.9
Feb	337.5	76.8	62.7	69.2	83.7	52.9	65.7	101.6	70.9	0.9
Mar	386.8	42.3	25.2	49.5	35.0	12.8	43.1	66.2	14.9	-15.4
Apr	301.5	25.2	32.4	8.5	2.6	-26.0	-13.7	24.8	-47.0	-90.5
May	271.0	12.0	18.4	7.3	2.6	-12.8	-10.7	17.1	-26.0	-49.5
Jun	214.6	8.5	11.1	-0.9	3.4	-9.0	-8.5	10.2	-19.6	-30.7
Jul	243.2	6.4	-3.0	-13.7	8.1	-6.4	-20.9	11.1	-15.4	-37.6
Aug	189.1	-26.5	3.4	-21.3	56.3	-56.8	-23.5	30.7	-58.9	-37.6
Sept	237.0	-14.5	24.8	9.4	65.7	-57.2	-65.3	35.9	-82.8	-67.9
Oct	172.7	6.8	8.5	1.7	53.8	-32.4	-52.9	42.3	-107.6	-56.3
Nov	204.1	16.2	14.1	19.6	46.1	-12.4	-66.2	49.9	-163.1	-150.7
Dec	297.7	36.3	26.9	65.7	63.2	32.9	-28.2	63.2	-82.0	-175.4
Monthly Evapotranspiration (mm)										
Jan	-	1.0	1.7	1.4	2.1	4.0	3.3	3.0	7.3	6.2
Feb	-	0.7	1.0	0.9	2.2	2.6	4.0	2.5	6.3	6.6
Mar	-	3.0	2.0	3.0	3.9	5.3	8.3	5.4	11.5	14.1
Apr	-	3.0	3.1	4.3	5.9	8.3	13.7	8.1	18.3	23.6
May	-	5.4	4.4	8.5	9.3	14.5	23.8	13.0	31.2	42.3
Jun	-	6.2	6.5	6.0	11.3	14.4	10.7	13.8	16.5	23.1
Jul	-	8.4	7.8	5.4	13.0	22.1	-1.6	17.0	19.5	-11.2
Aug	-	7.9	8.7	9.7	12.9	20.4	29.1	16.7	37.1	24.0
Sept	-	6.9	6.8	8.0	10.6	16.6	20.3	15.4	30.9	36.9
Oct	-	4.4	5.7	5.2	7.0	11.9	14.9	10.9	23.9	25.4
Nov	-	2.6	2.3	2.1	4.9	5.5	6.1	6.4	11.9	10.7
Dec	-	1.4	1.8	1.6	3.0	4.0	3.8	4.4	7.5	7.2

Figure 96: Modeled Baseline and Projected Monthly Streamflow Discharge (ft³/sec) by Time Period and Emission Scenario for Crooked Creek and Hamilton Creek

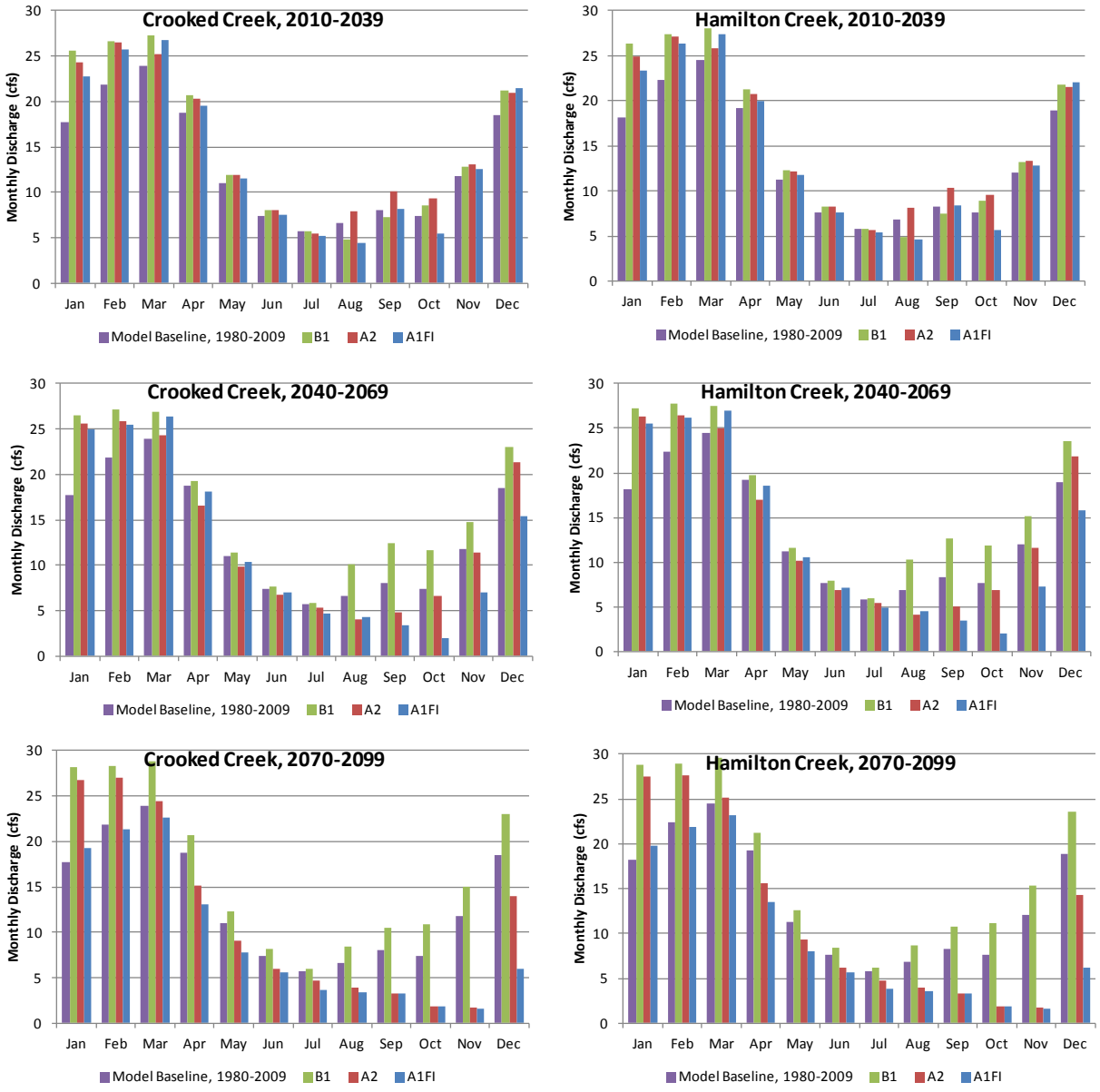

D. Additional Information on the Sea Level Rise and Storm Surge Analyses

D.1. Factors Not Considered in Sea Level Rise Analysis

Several factors that can affect local sea level rise were not considered in this study because they were not considered to likely significantly impact the results, or due to resources constraints. These factors are described in this appendix and include:

- Sedimentation and erosion
- Gravitational changes
- Changes in circulation patterns and ocean density

Modeling coastal sedimentation and erosion is quite complex and outside the scope of this study, but might be considered in future studies. Sedimentation and erosion are not major factors for parts of the coastline that are naturally rocky or artificially hardened, such as the port and downtown areas of Mobile. However, sedimentation and erosion may be important for parts of the coastline that are composed of soft sediments, such as sandy beaches and marshes. These vulnerable conditions do exist in large parts of the study area. In some places, vertical accretion of marshes is able to keep pace with the rate of sea level rise. However, it is unclear whether marshes will be able to keep pace with the scenarios of 0.75 and 2.0 meters GSLR explored in this study. In addition, sedimentation and erosion, particularly following major storms, could lead to changes in the coastal landscape in some parts of the Mobile region. For example, barrier islands such as Dauphin Island are particularly vulnerable to storm damage and storm-induced erosional and depositional processes, which may dramatically change their topography.

Gravitational changes from ice sheet loss could affect sea level rise in Mobile, however, they were not considered in this study. A large reduction in the mass of the Greenland and Antarctic ice sheets would affect regional sea level around the world. Regions close to where the ice sheets have shrunk will experience a reduction in sea level due to a reduction in the gravitational attraction from the mass of the ice sheet. In contrast, the regions farthest away from the shrinking ice sheets will tend to experience an increase in regional sea level. Mitrovica et al. estimate that if the West Antarctic Ice Sheet were to collapse, local sea level rise along the U.S. coast would be roughly 20 to 25% greater than global sea level rise due to gravitational changes. However, gravitational changes from ice sheet loss were not considered in this study because they are considered a second-order and smaller effect compared to global sea level rise from ice sheet melting. Furthermore, the understanding of the interplay between gravitational effects from the Antarctic and Greenland ice sheets is highly uncertain.

Changes in circulation patterns and ocean density were also not considered. These factors could potentially affect sea level. A decrease in ocean density due to warming or an increase in salinity

will tend to reduce regional sea level. Changes in wind-patterns can lead to local and regional differences in sea level. However, the long-term influence of ocean circulation and density changes is likely to be near zero in the central Gulf region. Therefore, these factors were not examined in this study.

D.2. Methodology to Estimate Subsidence and Uplift

This appendix details the methodology used to estimate subsidence (downward land surface motion) and uplift (upward land surface motion) as part of the projected sea level rise analysis. USGS estimated subsidence and uplift rates using Interferometric Synthetic Aperture Radar (InSAR) data together with a series of stable survey benchmarks and tide gages. In summary, the InSAR data provided vertical movement data for most of the study area, while the benchmark data helped to augment the InSAR data outside the spatial domain of the InSAR data.[52] InSAR data were used where possible, because they are spatially continuous and possess relatively high accuracy. A spatially complete data set of vertical motion from these two datasets was arithmetically added to a high resolution Digital Elevation Model based on LIDAR data[53] to estimate the vertical position of the land surface out to 2050 and 2100.

D.2.1. Interferometric Synthetic Aperture Radar Data

InSAR data provided vertical movement data for most of the study area. Land surface deformation maps, showing rates of uplift and subsidence, were developed for the Mobile region using analysis of satellite-derived multi-temporal Interferometric Synthetic Aperture Radar (InSAR) data. The Temporarily Coherent Point (TCP) InSAR (TCP-InSAR) methodology developed by Zhang and Lu (2010a,b) was utilized. In brief, high precision maps of the land elevation at two different points in time were compared to determine the rate of vertical motion. USGS used Spaceborne SAR data from the European ERS-1/2 satellites[54] during 1992 and 1999 and the Japanese ALOS/PALSAR[55] during 2007 and 2010 for this purpose. USGS concluded that the ERS-1/2 deformation results were more reliable than those from the ALOS/PALSAR images due to the persistent orbital errors in the ALOS InSAR images, even after taking into account a correction procedure to reduce the orbit errors on the ALOS/PALSAR deformation results.

D.2.2. Benchmark Data

Benchmark data helped to augment the InSAR data outside the spatial domain of the InSAR data. The Mississippi Department of Transportation (MDOT), National Geodetic Survey (NGS), and contracted surveyors have established a network of precise elevations of stable benchmarks from the Florida panhandle, through Alabama and Mississippi, to Louisiana. The partners

[52] In the western-most areas of Mobile County and the western end of Dauphin Island, actual data values were extended outward into data voids to build the interpolation surface.
[53] LIDAR data provided by the City of Mobile, 2010
[54] ESA, 2012
[55] ERSDAC, 2006

include MDOT, Alabama Department of Transportation (ALDOT), Florida Department of Environmental Protection (FLDEP), and many others. The finalized elevations of this benchmark network are not yet available, but the 2009-10 field adjusted elevations were made available by NGS for use in this study. USGS compared vertical change at tide gages, benchmarks, and Continuously Operating Reference Stations (CORS) to vertical change contours by Holandahl and Morrison (1974) in Mobile and Baldwin Counties, Alabama. Vertical change rates reported by Shinkle and Dokka (2004) were considered. In all, vertical change rates for 75 benchmarks were provided by USGS based on surveys from 1969 compared to 2009 or 1984 compared to 2010, depending upon location. In addition to uncertainties associated with the benchmark survey measurements, the usefulness of both the benchmark and CORS data are somewhat limited due to their spatial incompleteness.

D.3. Vertical Land Surface Rates

This appendix provides the vertical land surface rates in millimeters per year for the benchmark surveys and corresponding InSAR Data in Mobile and Baldwin Counties.

Table 46: Vertical Land Surface Rates (mm/yr) for Benchmark (BM) Surveys and Corresponding InSAR Data in Mobile and Baldwin Counties

These are preliminary results from an analysis by K. Van Wilson, USGS, which were provided in draft reports to FHWA and the ICF project team.

ID Code	Latitude[56]	Longitude	BM Survey[57]	ERS [58]	PALSAR[59]
BG0094	30.522861	-87.493417	-0.8	1.0	-2.2
BG0098	30.517778	-87.480583	-0.7	0.7	-1.5
BG0099	30.518111	-87.463750	-0.4	0.6	-2.8
BG0100	30.521917	-87.453389	-0.4	1.1	ND
BG2485	30.527056	-87.512583	-0.4	1.7	-2.5
BG2487	30.531389	-87.519111	-0.3	-0.1	-1.8
BG2495	30.542167	-87.568583	-0.4	0.1	-2.8
BG2500	30.559528	-87.593417	0.0	0.2	-0.2
BG2506	30.567694	-87.633889	-0.6	0.7	-0.5
BG2508	30.567389	-87.661778	-0.7	0.7	-0.8
BG2512	30.563639	-87.682917	-0.6	0.2	-0.7
BG2513	30.564000	-87.698750	-0.6	1.1	-1.9
BG2516	30.562611	-87.713667	-0.6	1.5	1.1
BG2517	30.566944	-87.716389	-0.6	1.1	-0.4
BG2521	30.603611	-87.738194	-0.7	0.4	-0.2
BG2528	30.623444	-87.750750	-0.6	0.4	0.2
BG2532	30.632776	-87.759193	-0.9	1.3	-1.1
BG2534	30.632889	-87.790750	-0.9	1.4	1.3
BG2536	30.646389	-87.814167	-0.8	1.2	1.4
BG2537	30.647944	-87.828583	-0.8	1.4	2.5
BG2538	30.654944	-87.844583	-1.0	1.6	1.7
BG2540	30.673222	-87.852333	-1.2	1.3	1.5
BG2542	30.676667	-87.866944	-1.1	1.3	1.8
BG2544	30.671722	-87.883306	-1.3	1.0	-0.6
BG2546	30.670833	-87.897778	-1.0	1.8	1.1
BG2556	30.676750	-87.977444	-4.1	0.8	-1.6
BH0144	30.682667	-88.007000	-0.9	1.1	-1.0
BH0145	30.680750	-88.001028	-1.5	1.4	-1.8
BH0116	30.523333	-88.206667	-0.7	0.0	-4.0
BH0117	30.524417	-88.202722	-0.8	-0.4	-2.2
BH0120	30.546472	-88.174028	4.4	-0.6	0.1
BH0239	30.474528	-88.351167	-0.7	ND	ND
BH0240	30.476306	-88.342278	-0.8	ND	ND

[56] The horizontal datum is the WGS84.
[57] Interpolated from vertical change rate surface developed from vertical change rates of 1969-2009 and 1984-2010 benchmark surveys.
[58] Interpolated from vertical change rate surface developed from ERS vertical change rates from 25 satellite images between July 1992 and December 1999.
[59] Interpolated from vertical change rate surface developed from PALSAR vertical change rates from 13 satellite images between June 2007 and August 2010.

BH0243	30.486944	-88.310278	-0.9	ND	ND
BH0246	30.493803	-88.283297	-1.1	-0.1	ND
BH0250	30.498889	-88.266667	-0.8	0.1	ND
BH1465	30.666028	-88.049861	-0.8	-0.3	-2.5
BH1466	30.669389	-88.045000	-0.5	-0.2	0.4
BH1468	30.682028	-88.040889	-0.5	0.1	-1.2
BH1469[60]	30.690083	-88.041167	-0.8	0.2	0.2
BH1598[59]	30.692944	-88.031028	-1.9	0.0	-1.6
BH1599[59]	30.692833	-88.031917	-1.7	0.6	-1.5
BH1602	30.675750	-88.042222	-0.4	0.7	-1.2
BH1605	30.632056	-88.105194	-0.7	0.6	1.5
BH0117	30.524417	-88.202722	-0.8	-0.4	-2.2
BH0137	30.545000	-88.171111	-0.8	-0.2	-1.1
BH0138	30.531667	-88.170556	-0.8	-0.4	-2.4
BH0251	30.490556	-88.169722	-0.7	0.0	-2.3
BH0256	30.446389	-88.166389	0.5	0.2	-1.8
BH0259	30.403611	-88.148611	0.0	-0.6	-2.9
BH1722	30.546806	-88.173750	-0.8	-0.5	0.5
BH1723	30.501667	-88.169722	-0.6	0.1	-2.9
BH1724	30.485556	-88.169444	-0.6	0.0	-2.7
BH1725	30.485556	-88.169444	-0.7	0.0	-2.7
BH1726	30.462500	-88.168889	-0.6	-0.6	-4.5
BH1733	30.432500	-88.160833	-0.4	-0.2	-2.6
BH1734	30.377222	-88.159722	0.5	0.2	-0.3
BH1735	30.371111	-88.145833	0.0	0.3	-1.0
BH1736	30.350942	-88.121363	-0.4	0.1	-0.1
BH1737	30.338056	-88.128889	-0.3	-0.6	-0.1
BH1740	30.310278	-88.137778	-0.7	1.7	-1.7
BH1741	30.299167	-88.133889	-0.9	0.2	-2.5
BH1742	30.289135	-88.128657	-1.9	-0.8	-3.1
BH1743	30.290000	-88.128889	-1.9	-0.7	-3.0
BH1744	30.277778	-88.122500	-0.5	-1.7	-3.8
BH1745	30.265000	-88.115833	-0.9	ND	-4.4
BH1748	30.254167	-88.111667	-0.9	ND	-5.0
BH1749	30.253611	-88.112500	-0.8	ND	-4.4
BH1750	30.251111	-88.095000	-0.8	ND	-5.3
BH1751[61]	30.249722	-88.076389	-0.8	ND	-5.0
BH1752[60]	30.249444	-88.076667	-1.0	ND	-5.0
BH1755[60]	30.249672	-88.076022	-1.0	ND	-4.7
BH1756[60]	30.249582	-88.075489	-0.8	ND	-5.9
BH1757[60]	30.249167	-88.075556	-0.8	ND	-5.5
BH1758[60]	30.248806	-88.074944	-0.8	ND	-4.7
BH1760[60]	30.247900	-88.075283	-1.1	ND	-4.5
BH1761[60]	30.248028	-88.076278	-0.8	ND	-4.8

[60] BM about 1.2 miles (1.9 kilometers) south of Alabama State Docks tide gage at Mobile, which has an estimated vertical rate of 0.02 inches/year (0.5 millimeters/year).
[61] BM near Dauphin Island tide gage, which has an estimated vertical change rate of -0.5 inches/year (-1.2 millimeters/year).

D.4. Supplementary Sea level Rise Exposure Statistics

This appendix provides supplementary exposure statistics for the scenario-based analysis of future sea level rise.

Table 47: Supplementary Sea Level Rise Exposure Statistics

			Scenario		
Transportation Mode	**Asset**	**Criticality**	**2050 – 30 cm**	**2100 – 75 cm**	**2100 – 200 cm**
Highways	**Roads (miles)**	*Critical*	9 of 209 (4%)	11 of 209 (5%)	26 of 209 (13%)
		Not Critical	0 of 284 (0%)	0 of 284 (0%)	3 of 284 (1%)
	Evacuation Routes (miles)	*Not Critical*	5 of 367 (1%)	7 of 367 (2%)	21 of 367 (6%)
Rail	**Rail (miles)**	*Critical*	2 of 196 (1%)	2 of 196 (2%)	40 of 196 (20%)
		Not Critical	0 of 118 (0%)	0 of 118 (0%)	24 of 118 (21%)
	Rail Points (#)	*Critical*	0 of 5 (0%)	0 of 5 (0%)	2 of 5 (40%)
		Not Critical	4 of 12 (33%)	4 of 12 (33%)	6 of 12 (50%)
Pipelines	**Pipelines (miles)**	*Critical*	3 of 426 (1%)	7 of 426 (2%)	13 of 426 (3%)
		Not Critical	2 of 226 (1%)	4 of 226 (2%)	13 of 226 (6%)
Ports	**Ports (#)**	*Critical*	12 of 26 (46%)	18 of 26 (69%)	24 of 26 (92%)
		Not Critical	14 of 48 (29%)	18 of 48 (38%)	31 of 48 (65%)
Transit	**Facilities**	*Critical*	0 of 2 (0%)	0 of 2 (0%)	1 of 2 (50%)
	SDE Facilities (#)	*Not Critical*	0 of 193 (0%)	0 of 193 (0%)	10 of 193 (5%)
	Bus Stops (#)	*Not Critical*	0 of 907 (0%)	0 of 907 (0%)	15 of 907 (2%)
	Bus Routes (miles)	*Not Critical*	0 of 126 (0%)	0 of 126 (0%)	5 of 126 (4%)
	MODA Stops (#)	*Not Critical*	0 of 22 (0%)	0 of 22 (0%)	0 of 22 (0%)
	Bike Routes (miles)	*Not Critical*	1 of 132 (1%)	2 of 132 (2%)	13 of 132 (10%)
Airports	**Mobile Downtown Airport (mi^2)**	*Critical*	0 of 3 (1%)	0 of 3 (2%)	0 of 3 (3%)
	Mobile Regional Airport (mi^2)	*Critical*	0 of 4 (0%)	0 of 4 (0%)	0 of 4 (0%)
Other	**Medical Facilities (#)**	*Not Critical*	2 of 45 (4%)	3 of 45 (7%)	5 of 45 (11%)

*Exposure statistics reflect the percent of assets in the exposure zone. These statistics do not necessarily represent the assets that are actually overtopped by sea level rise.

D.5. Caveats, Gaps, and Replicability of Sea Level Rise Analysis

This appendix discusses the assumptions and simplifications used in this study's analysis of future sea level rise. These assumptions and simplifications should be taken into account when considering the results of the analysis or applying the methodology elsewhere.

First, this analysis assumes that future subsidence and uplift rates will remain constant over the next century. Since there are currently no robust predictions of changes in the soft sediment dynamics and tectonics that define the spatial heterogeneity of vertical change in the region, this assumption of constant vertical change is valid for this first-order analysis of potential inundation.

Second, the analysis does not take into account vertical addition or subtraction of sediment through coastal engineering, nor does it account for changes in the vertical accretion rate of wetlands.

The approach to sea level rise mapping used here is appropriate for initial exposure assessment. To more rigorously assess the exposure of the region's transportation to changes in land forms due to soft sediment dynamics, a sediment transport and erosion model (e.g., XBeach[62]) should be deployed. To more rigorously assess the impact of changes in wetland elevation and distribution, a model such as SLAMM (Sea Level Affecting Marshes Model[63]) could be used.

Third, the potential inundation analyses presented here do not account for small-scale protective barriers (e.g., sea walls and pumping systems) that are intended to prevent long-term flooding. These systems are generally only of very localized importance in the Mobile area. In areas where they are more prevalent and critical at the regional level as a whole (e.g., New Orleans), particularly where the land surface is at or below sea level, the SLAMM model can be used to account for them, provided that survey data or as-built information about these engineering structures is available.

Fourth, as noted previously, the LSLR scenarios used in this study do not account for changes in oceanic or atmospheric circulation or ocean density since these factors are likely to be of secondary importance in this region. In locations such as southern California, where changes in ocean circulation have had a strong influence on LSLR,[64] it would be more important to take these factors into account. Information about the regional net importance of these factors can be obtained from the periodic Intergovernmental Panel on Climate Change assessments[65] as well as the National Climate Assessment.[66]

[62] http://oss.deltares.nl/web/xbeach/
[63] http://warrenpinnacle.com/prof/SLAMM/index.html
[64] Bromirski et al., 2011
[65] See, for example, figure 5.15a and 5.16b from the IPCC Fourth Assessment Working Group 1 report, which show the regional distribution of decadal and longer-term sea level rise trends: http://www.ipcc.ch/pdf/assessment-report/ar4/wg1/ar4-wg1-chapter5.pdf
[66] Please see the U.S. Global Change Research Program's web page on the National Climate Assessment: http://www.globalchange.gov/what-we-do/assessment/nca-overview

Finally, due to the large uncertainties associated with future GSLR, it is not essential to use high resolution uplift and subsidence data (e.g., from InSAR) for initial exposure screening, as was done in this study. Coarse resolution analyses of local contributions to SLR can be obtained where tide gauge data are available for a few decades by subtracting out the estimated GSLR. This would be suitable for an initial assessment evaluating which assets are exposed to sea level rise. However, it would be useful for InSAR data to be available for the entire U.S. coastline to contribute to detailed vulnerability assessment and adaptation planning beyond the Mobile area.

D.6. Detailed Case Studies

This appendix provides more detailed summaries of the five case studies described in Section 2.8.1. These storms represent a sampling of the different types of storms that Mobile experiences, including a thunderstorm and tornado event, a hailstorm, a heavy rain event, a moderate hurricane (Georges), and an intense hurricane (Katrina).

The extra-tropical case studies include:

- a brief discussion of storm development identifying key meteorological conditions;
- storm event metrics including precipitation, discharge, temperature, wind, surface pressure, sea level, and storm surge; and
- a discussion of associated damages.

The hurricane case studies include:

- a brief discussion of storm track and intensification;
- storm event metrics including precipitation, discharge, wind, central storm pressure, sea level, and storm surge; and
- a discussion of associated damages.

D.6.1. Study 1: Severe Thunderstorms and Tornado Outbreak, November 15, 2006

Storm Development

Severe thunderstorms strong enough to produce six tornadoes struck the Mobile region on November 15, 2006.[67] These severe thunderstorms developed due to a strong southerly jet stream aloft that steered a low pressure system at the surface into Alabama. Figure 97, on the left, is a surface map of the southeastern United States for November 15, 2006 at 6:00 am (CST) showing the key features for the storm's development.[68]

As illustrated by the blue markers in Figure 97, the wind ahead of the cold front was from the south bringing warm moist air from the Gulf waters into Alabama. Warm moist surface air feeds thunderstorm development by encouraging convective activity.[69] Also noticeable in Figure 97 is the north-to-south gradient in the upper-level jet stream above Alabama, which is ideal for intensifying the surface low pressure system.

[67] NWS, 2009a. NWS Forecast office of Mobile/Pensacola analysis of this storm event.
[68] NWS, 2009a
[69] In these situations, convective activity may intensify if there is a layer of stable cold air above. However, the November 15 soundings of Birmingham, Alabama did not demonstrate the existence of a layer of stable cold air above (NOAA, 2011i). Soundings which demonstrate how temperature and humidity change from the surface to aloft are generated by NOAA website of archived meteorological data.

The key meteorological conditions for this storm development were: (1) a strong jet stream aloft, (2) a surface cold front associated with a low pressure system, and (3) warm moist surface air. As detailed earlier, this is a typical example of a severe storm event in Mobile, Alabama.

Figure 97: Surface Maps of the November 15, 2006 Storm at 6:00 am and 6:00 pm

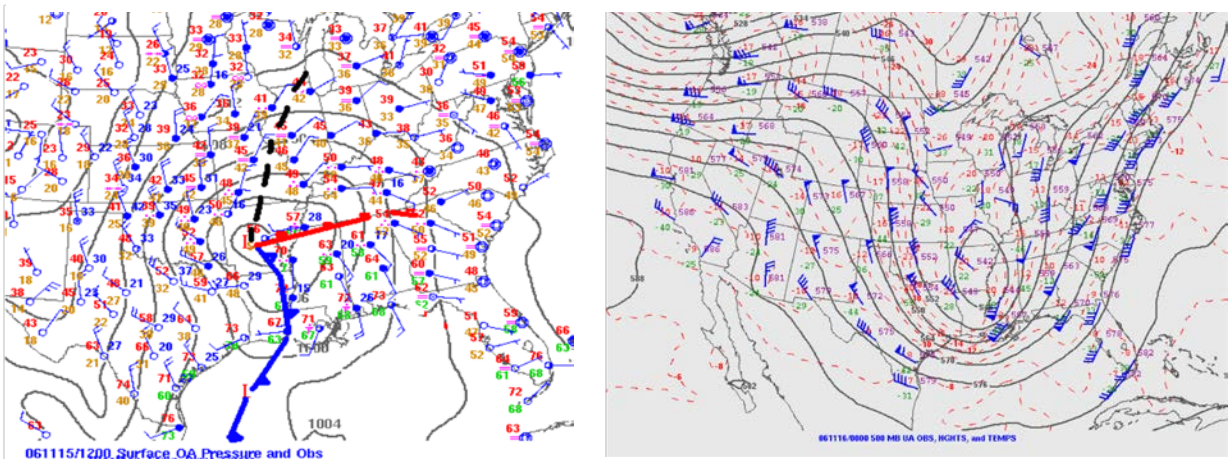

The surface low pressure system is marked with an "L" and the associated cold front is illustrated by the thick blue line with blue triangles. The black contour lines indicate the surface pressure in millibars (mb), and the blue lines attached to the blue circles illustrate wind direction and strength. The right figure is a 500 mb pressure map (500 millibars is about halfway up the lower atmosphere) also for November 15, 2006 at 6 pm (CST) illustrating the strong jet stream aloft, shown by the blue lines with triangles, the tightly spaced black atmospheric pressure lines, and the 'dip' in the black atmospheric pressure lines below Louisiana and Arkansas

Storm Event Data

Precipitation: 5.7 inches (14.3 centimeters) of rain fell at Mobile Regional Airport on November 15, 2006 occurring between 5:00 am and 3:00 pm (CDT).[70] Rainfall rates peaked at over 1.5 inches per hour (3.8 centimeters per hour) at 8:00 am and 11:00 am. The total rainfall from this storm event is equivalent to the total average November rainfall in Mobile, Alabama.

Radar-estimated precipitation amounts for the region are shown in Figure 98. This figure illustrates how precipitation varied across the region and shows the hotspots of heavy rainfall for southern Alabama and Mississippi. The precipitation estimates appear to be lower than the measured precipitation at Mobile Regional Airport, but radar-derived precipitation estimates may not be as accurate as the observation data.

[70] NCDC, 2011a. Meteorological storm data was collected from the National Climatic Data Center which archives the National Weather Service Cooperative Observer Program observational meteorological data and includes hourly precipitation.

Figure 98: Radar-Derived Precipitation Estimates for the Gulf Region, November 15, 2006, 12:00 pm

(Source: NWS, 2009a)

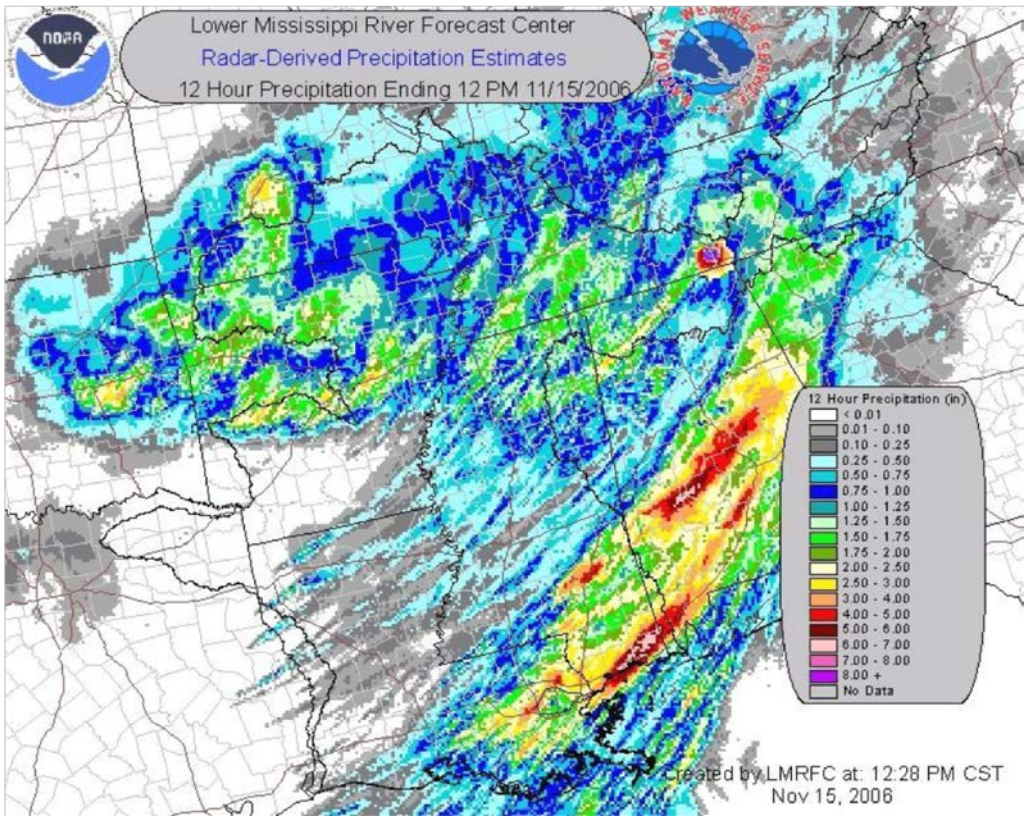

Streamflow: Three USGS streamflow gages in Mobile County showed a marked increase in stream discharge on November 15, 2006. The hourly measured discharge increased between 2- and 40-fold compared to the long-term average for that day.[71]

Temperature: The temperature on November 15, 2006 was considerably warmer than the days surrounding it, with a high of 73°F (23°C) and a low of 52°F (11°C) (compared to 66°F (19°C) and 40°F (4°C), respectively).[72] This is likely due to the warm moist Gulf air traveling into Alabama.

Wind: The highest observed wind gust recorded in Mobile during the storm was 52 miles per hour (83 kilometers per hour), recorded at 7:42 am on November 15, 2006. The fastest 2-minute sustained wind speed observed was 41 miles per hour (66 kilometers per hour). The average wind speed for the day was 13.6 miles per hour (21.8 kilometers per hour), compared to an average value for the surrounding week of 6.1 miles per hour (9.8 kilometers per hour). If the

[71] USGS, 2011a,b,c. United States Geological Survey (USGS) provides hourly discharge information by stream site within the United States.
[72] NCDC, 2011b. Meteorological storm data was collected from the National Climatic Data Center which archives the National Weather Service Cooperative Observer Program observational meteorological data and includes surface temperature, wind, and surface pressure.

day of the storm is not included in this average then the average wind speed for the week was 5.2 miles per hour (8.3 kilometers per hour).[73]

Table 48: Summary of Peak Storm Event Data for November 15, 2006 for the Mobile, Alabama Region (*11/16)

Variable	Value at Peak Storm Intensity	Value averaged across surrounding days
Maximum Surface Temperature	73°F	66°F
Minimum Surface Temperature	52°F	44°F
Precipitation Total	5.7 in (> 2 year event)	-
Peak Precipitation Rate	1.87 in/hr	-
Hourly Streamflow Discharge		
Crooked Creek	922 ft^3/s (> 2 year event)	10 ft^3/s
Chickasaw Creek*	5,660 ft^3/s (> 2 year event)	120 ft^3/s
Fowl River*	85 ft^3/s(< 2 year event)	25 ft^3/s
Wind Gust	52 mph	-
Sustained Wind	41 mph	-
Surface Pressure	992 mb	1008 mb
Tidal Datum		
Dauphin Island (MLLW)	2.07 ft (< 10 year event)	-
Dauphin Island (MHHW)	0.70 ft (< 10 year event)	-
Pensacola (MLLW)	1.99 ft (< 10 year event)	-
Pensacola (MHHW)	0.50 ft (< 10 year event)	-

Surface Pressure: The average surface pressure in Mobile on November 15 was observed at 992 millibars, representing a drop of about 16 millibars compared to the surrounding days.[74]

[73] NCDC, 2011b
[74] Ibid.

Water Level: Dauphin Island tidal station recorded peak water levels at 12:45 pm on November 15 of 2.07 feet (63.09 centimeters) above the mean lower-low level,[75] 1.5 feet (45.7 centimeters) higher than the expected water level of 0.57 feet (17.37 centimeters). At 3 pm on November 15, the Dauphin Island tidal station measured peak water levels of 0.70 feet (21.34 centimeters) above the mean higher-high level. [76]

Storm Highlights

- 6 thunderstorms produced F-0 to F-2 tornadoes
- Severe wind gusts at or above 57 mph (91 kph)
- The NWS Office in Mobile Alabama issued five flash warnings prompted by the extremely heavy rainfall of up to 4 to 8 inches (10 to 20 centimeters) across the Mobile region

The tidal station in Pensacola FL recorded similar water level disturbances, with 2 feet (61 centimeters) of water above the mean lower-low level at 3:30 pm, compared to the expected water height of 0.5 feet (15 centimeters).[77] The records also indicate 0.74 feet (22.56 centimeters) of water above the mean higher-high level at 3:30 pm, compared to the expected water height of -0.76 feet (-23.16 centimeters).

Storm Damage

Strong winds and tornadoes caused the majority of storm damage. This strong storm spawned six tornadoes near Mobile (see Figure 15).[78] In addition, the storm caused several extreme straight-line wind gusts. During the morning of November 15, four extreme wind gusts were reported in Mobile of 52, 43, 38, and 35 miles per hour (83, 69, 61, and 56 kilometers per hour).[79] The storm caused blocked roadways from debris and fallen trees and power lines. The NWS estimates that the storm's six tornadoes caused between $0.5 million and $1 million of damage.[80]

In addition to wind damage, transportation infrastructure was impacted by flooding caused by very heavy rain. Two heavy hour-long episodes accounted for over sixty percent of the rain. These heavy morning downpours caused flooding in many roads, streets, creeks, and streams in Mobile.

[75] NOAA, 2011a
[76] Ibid.
[77] NOAA, 2011c
[78] NWS, 2009a
[79] Ibid.
[80] Ibid.

Figure 99: November 15, 2006 Storm Reports

Source: NWS, 2009a

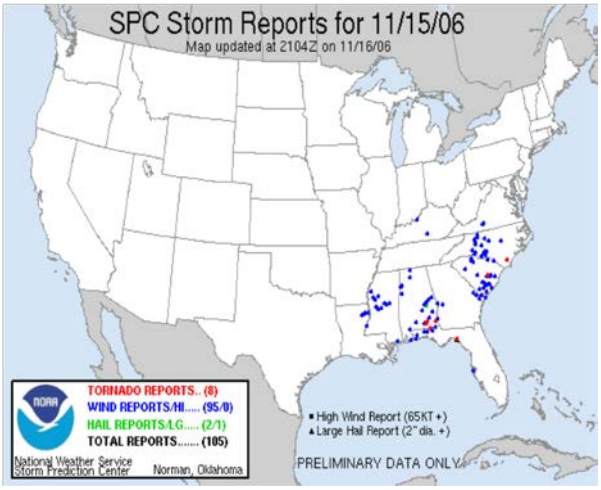

Figure 100: November 15, 2006 Tornado Tracks and Intensities

Source, NWS, 2009a. See Glossary for definition of tornado intensity scale (Fujita Scale, F1, F0)

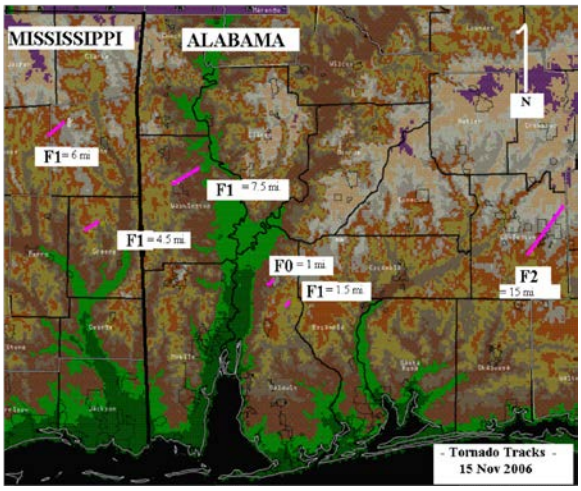

D.6.2. Study 2: Severe Hailstorm, March 5, 1998

Storm Development

Thirteen severe thunderstorms developed in the Mobile region on March 5, 1998. The storms brought hail to the Mississippi/Alabama region, with hailstones ranging between the size of a dime to the size of a baseball.[81] A number of key meteorological conditions led to the

[81]NWS, 2009b. Forecast office of Mobile/Pensacola analysis of this storm event.

development of this storm, including: a strong west-to-east jet stream aloft, the existence of cold, dry air in the middle layer of the atmosphere, vertical wind shear, and strong potential for convective thunderstorms.[82] In addition, a high pressure system over Florida brought warm moist air into Alabama, an important ingredient for severe thunderstorms in Alabama.

Figure 101: Surface Weather Map for March 5, 1998, 6:00 am

Source: NOAA, 1998

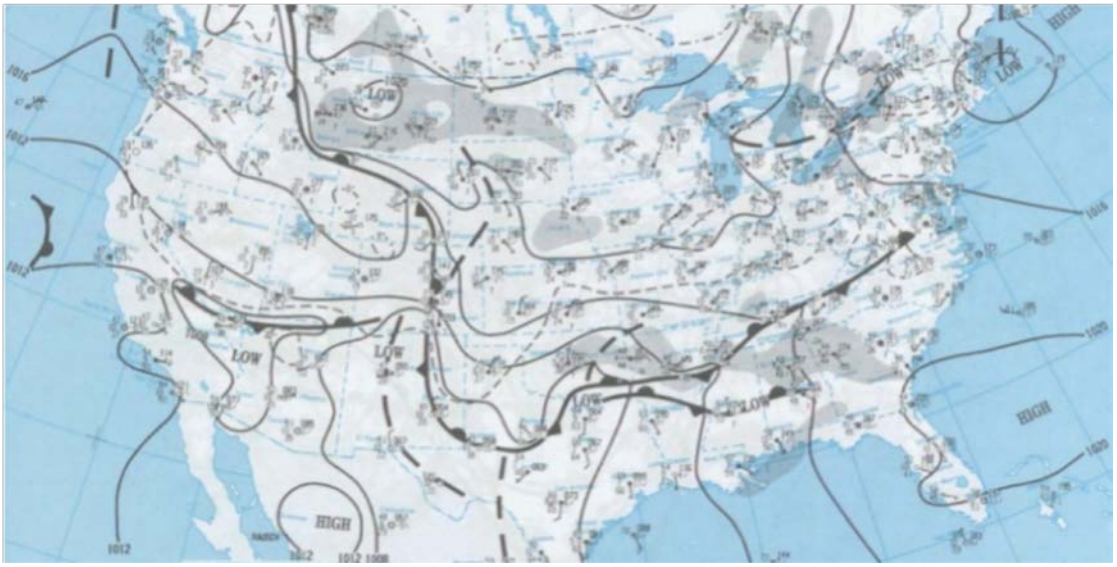

Figure 102: Zonal (West to East) Flow Diagram in Atmosphere

Source: NWS, 2009b

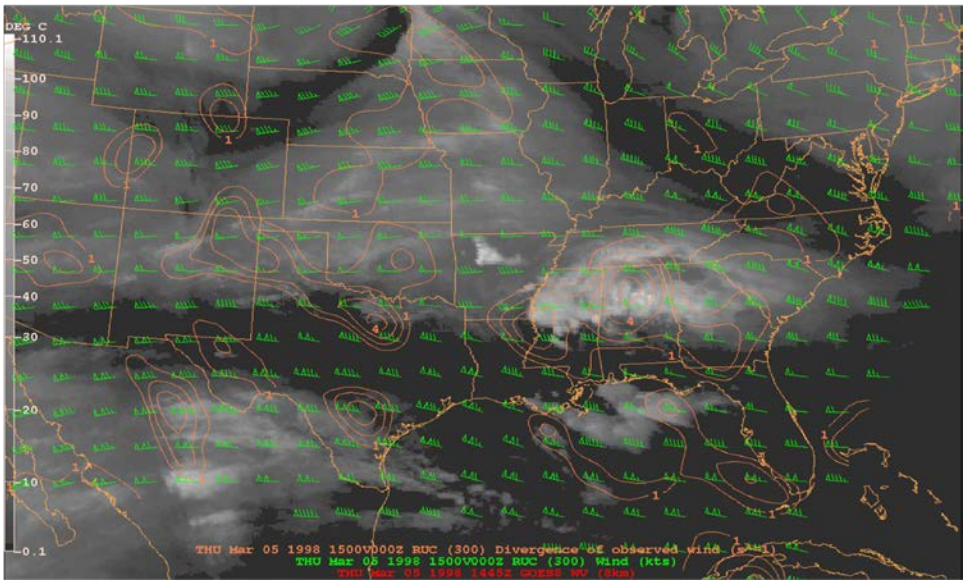

[82]NWS, 2009b. Also evident was a 'dip' in the zonal air flow over Arkansas and Louisiana at 700 mb (air situated at 700 mb is between the surface and 500 mb).

Storm Event Data

Precipitation: In total, 0.64 inches (1.63 centimeters) of rain were observed at Mobile Regional Airport on March 5, 1998.[83] The majority of rain fell between 12:00 pm and 8:00 pm, peaking at 12:00 pm at a rate of 0.29 inches per hour (0.74 centimeters per hour).[84] Though the precipitation amounts were minimal, hail stones ranging from 0.5 to 2 inches (1.3 to 5 centimeters) in diameter were reported in the area, with hail approaching 3 inches (8 centimeters) in diameter reported northwest of Leakesville, Mississippi.[85] Hail accumulation in Leakesville, where the most severe hail damage occurred, was about 6 to 12 inches (15 to 30 centimeters).[86]

Streamflow: Hourly discharge measurements at the stream gages in Mobile County were not abnormally high, which is expected given the low precipitation amounts in the storms, hourly discharge measurements at the stream gages in Mobile County were likewise not significant.[87] However, it is possible the precipitation from this event may have helped to saturate the soil and contribute to a much larger discharge event that was recorded in association with a precipitation event three days later.

Temperature: The temperature in Mobile on March 5, 1998 ranged from a low of 55°F (13°C) to a high of 75°F (24°C). These temperatures were warmer than previous days.[88] It is possible the warm moist Gulf air advecting into the region contributed to this increase in temperature.

Winds: The highest observed wind gust in Mobile during the storm was 18 miles per hour (29 kilometers per hour) at the Mobile Regional Airport. The Mobile National Weather Service (NWS) Cooperative Observer Program (COOP) station measured a high 2-minute sustained wind of 24 miles per hour (38 kilometers per hour).[89] The average wind speeds for the day were 6.4 and 7.5 miles per hour (10.2 and 12.0 kilometers per hour) at the two stations, respectively, compared to an average value for the surrounding week of 8.5 and 12.4 miles per hour (13.6 and 19.8 kilometers per hour).[90]

Table 49: Summary of Peak Storm Event Data for March 5, 1998 for the Mobile, Alabama region (including nearby Leakesville, Mississippi)

Variable	Value at Peak Storm Intensity	Value averaged across surrounding days
Surface Temperature – Max.	75°F	52°F
Surface Temperature – Min.	55°F	37°F
Precipitation Total	0.64 in (< 2 year storm)	-

[83] NCDC 2011a
[84] Ibid.
[85] NWS 2009b. Leakesville, Mississippi is about 60 miles northwest of Mobile, Alabama.
[86] Ibid.
[87] USGS, 2011a, b, c
[88] NCDC, 2011b
[89] Ibid.
[90] Ibid.

Variable	Value at Peak Storm Intensity	Value averaged across surrounding days
Precipitation Rate	0.29 in/hr	-
Hail Size (Diameter)	2 in	-
Hourly Streamflow Discharge		
Crooked Creek	51 ft^3/s (< 2 year event)	15 ft^3/s
Chickasaw Creek	308 ft^3/s (< 2 year event)	300 ft^3/s
Fowl River	40 ft^3/s (< 2 year event)	20 ft^3/s
Wind Gust (@ Airport)	18 mph	-
Sustained Wind		
Mobile	16 mph	-
Mobile Reg. Airport	24 mph	-
Surface Pressure	1007 mb	1007 mb
Tidal Datum		
Pensacola (MLLW)	1.62 ft (< 10 year event)	-

Surface Pressure: Surface pressure at both the Mobile Regional Airport and the Mobile weather stations averaged 1007 millibars on March 5, 1998, which was a typical value within that week.[91]

Storm Highlights

- Severe hail of 0.5 to 2 inches (1.3 to 5 centimeters) in diameter caused damage to houses and cars.

Water Level: The mean lower-low water level at the Pensacola tide station (the only tidal station with available data for March 1998) was unremarkable on March 5, 1998, peaking at 1.62 feet (49.38 centimeters) at high tide at 5:18 pm, close to the expected level of 1.08 feet (32.92 centimeters).[92] Similarly, the mean high-high water level did not demonstrate any significant difference from expected levels.[93]

[91] NCDC, 2011b
[92] NOAA, 2011c
[93] Mean high-high water level is the average of the higher high water height of each tidal day observed over the National Tidal Datum Epoch (tidesandcurrents.noaa.gov/datum-options.html)

Storm Damage

This storm caused approximately $60,000 of damage in the Leakesville area.[94] The severe hail chipped paint, dented house siding, stripped trees, and destroyed satellite dishes.[95] In addition, nearly every vehicle that encountered the hail experienced damage.[96]

Figure 103: Image from the March 5, 1998 Hailstorm

Source: NWS, 2009b

D.6.3. Study 3: Heavy Rain Event, April 4-5, 2008

Storm Development

On April 4, a line of intense storms moved east across central Alabama producing significant rainfall for the Mobile region. The storms developed in response to strong upper level north-to-south winds slowly steering a surface-level cold front into Mobile.[97] Additional contributors to the severity of the storm included the warm moist air from the Gulf that was pulled into Mobile ahead of the cold front and the presence of vertical wind shear.[98] Figure 104, on the left, shows a surface map of the United States for April 5, 1998 at 6 am (CST) demonstrating the cold front passing across Mobile, illustrated by the thick blue line with blue triangles.[99] The green shading indicates precipitation. The right image in Figure 104 is a 500 millibar pressure map for April 5, 1998 at 7 am (CST) illustrating the strong jet stream aloft, shown by the blue lines with triangles

[94] NWS, 2011b
[95] Ibid.
[96] Ibid.
[97] NWS, 2011c
[98] Ibid.
[99] NOAA, 2011e

moving in a northeast direction. A dip in the black atmospheric pressure lines below Louisiana and Arkansas is also evident.[100]

Figure 104: Surface Maps of the United States for April 5, 1998 at 6:00 am and 7:00 am (CST)

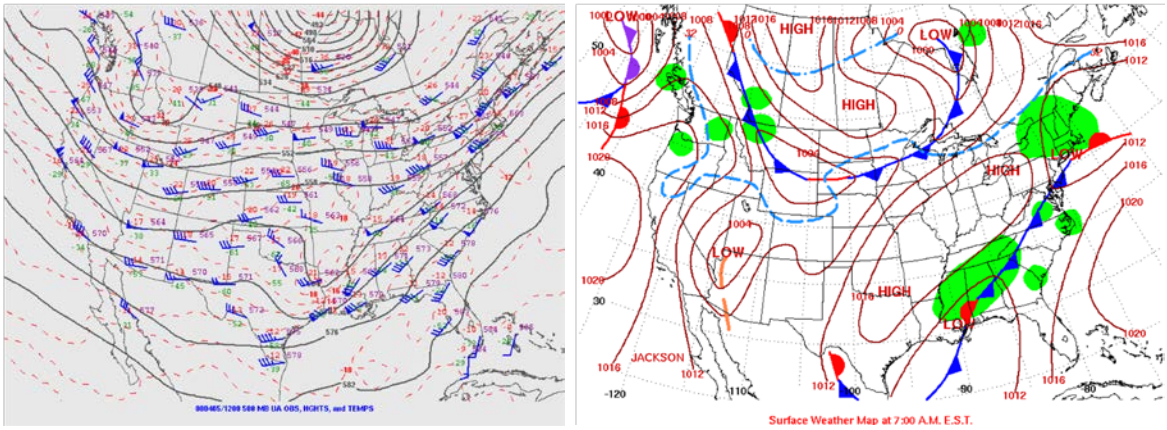

Storm Event Data

Precipitation: 8.32 inches (21.13 centimeters) of rain were observed at Mobile Regional Airport over a 15 hour period from 7:00 pm on April 4, 2008 to 10:00 am on April 5, 2008.[101] At its peak, the rate of rainfall was 1.71 inches per hour (4.34 centimeters per hour) (at around 10 am).[102]

Streamflow: Hourly stream discharge spiked in the afternoon and evening of April 5 at three USGS streamflow gages in Mobile County.[103] In that spike, discharge increased between 10- and 25-fold compared to the long-term average for that day.

Temperature: The high temperature on April 4-5, 2008 was 82°F (28°C), with a low of 60°F (16°C).[104] Overall Mobile temperatures cooled off after the storm, as would be expected with a frontal event.

Wind: The highest observed wind gust in Mobile during the storm was 31 miles per hour (50 kilometers per hour) at Mobile Regional Airport.[105] The fastest 2-minute sustained wind observed was 23 miles per hour (37 kilometers per hour).[106] The average wind speeds for April 4th and 5th were 13.2 miles per hour (21.1 kilometers per hour) and 7.8 miles per hour (12.5 kilometers per hour), respectively, compared to an average value for the surrounding week of 7.5

[100] NOAA, 2001f
[101] Ibid.
[102] Ibid.
[103] USGS, 2011a
[104] NCDC, 2011a
[105] Ibid.
[106] Ibid.

miles per hour (12.0 kilometers per hour).[107] If the day of the storm is not included, average wind speeds for the week were 6.4 miles per hour (10.2 kilometers per hour).

Table 50: Summary of Peak Storm Event Data for April 5, 2008 for the Mobile, Alabama Region

Variable	Value at Peak Storm Intensity	Value averaged across surrounding days
Surface Temperature – Max.	82°F	77°F
Surface Temperature – Min.	60°F	61°F
Precipitation Totals	8.32 in over 15 hr (~5 to 15 year storm)	-
Precipitation Rate	1.71 in/hr	-
Hourly Streamflow Discharge		
Crooked Creek	610 ft^3/s (< 2 year event)	12 ft^3/s
Chickasaw Creek	4,330 ft^3/s (< 2 year event)	275 ft^3/s
Fowl River	1,420 ft^3/s (< 2 year event)	40 ft^3/s
Wind Gusts	31 mph	-
Sustained Winds	23 mph	-
Surface Pressure	1003-1004 mb	1009 mb
Tidal Datum		
Dauphin Island	1.58 ft (< 2 year event)	0.71 ft
Mobile Docks	2.04 ft (< 2 year event)	0.97 ft
Pensacola	1.58 ft (< 2 year event)	0.95 ft

Surface Pressure: The average surface pressure in Mobile on April 4 and 5 was approximately 1004 millibars, representing a very minimal drop from average non-storm surface pressures of 1009 millibars.[108]

Water Level: At 7:05 am on April 5, the Dauphin Island tide station observed peak water levels of 1.58 feet (48.16 centimeters) above the mean lower-low level, more than twice the expected

[107] NCDC, 2011a
[108] Ibid.

water level of 0.71 feet (21.64 centimeters).[109] At 8 am, Dauphin Island tide station recorded peak water levels of 0.38 feet (11.58 centimeters) above mean higher-high level.[110]

Similar patterns were observed at the other Mobile tidal stations. At 7:48 am on April 5, the Mobile Docks tide station observed peak water levels of 2.04 feet (62.18 centimeters), compared to the expected water level of 0.97 feet (29.57 centimeters).[111] On April 5 at 1:24 am, Pensacola, Florida recorded 1.28 feet (39.01 centimeters) above the mean lower-low level compared to the expected water level of 0.70 feet (21.34 centimeters). Soon after noon time, Pensacola observed peak water level of 0.32 feet (9.75 centimeters) above mean higher-high levels, about 0.63 feet (19.20 centimeters) above expected levels.

Storm Damage

The April 4-5, 2008 storm moved slowly, inundating the region with varying amounts of rain. The majority of rain gauges in the area recorded around 8 inches (20 centimeters) of rain, but some reported close to 12 inches (30 centimeters) during the storm.[112] The rain caused flooding in the streets of downtown Mobile, submerging multiple vehicles.[113] The heavy rains also overwhelmed two wastewater pumping stations and caused over 13 million gallons (49 million liters) of sewage to spill into Mobile Bay.[114] The sewage spill tainted water in the area for several days. The storm, identified as a 25-year storm by the National Weather Service, also downed trees and power lines, causing 7,600 homes to lose power.[115] Throughout Alabama, the severe storm spawned tornadoes, damaging trees and buildings.

D.6.4. Study 4: Hurricane Georges, September 28, 1998

Storm Track and Intensification

Hurricane Georges began as a tropical depression on September 15, 1998, four hundred miles south-southwest of Cape Verde.[116] As the storm traveled westward, it steadily intensified, developing into a tropical storm on September 16 and reaching hurricane strength by September 17. On September 19, when it was just a few hundred miles east of the Caribbean, Hurricane Georges' strength peaked as a Category 4 storm with winds of 150 miles per hour (240 kilometers per hour).[117] Hurricane Georges caused damage in Puerto Rico, Dominican Republic, Haiti, and Cuba as it traveled towards the Gulf of Mexico, weakened at one point by the mountainous terrain of the Dominican Republic and Haiti.

[109] NOAA, 2011a
[110] Ibid.
[111] NOAA, 2011b
[112] NWS, 2011c
[113] CNN, 2008
[114] Smith, 2008
[115] Gordon, 2008
[116] U.S. Army Corps of Engineers, 1999
[117] Ibid.

Hurricane Georges entered the Gulf of Mexico on September 25, traveling north-northwest at an average speed of 11 miles per hour (18 kilometers per hour).[118] The storm began to strengthen as it moved into the warm waters of the Florida Straits moving in a west-northwest track. Sea surface temperatures in the Gulf near the track of Hurricane Georges were estimated to be 81.7°F (27.6°C).[119] Sea surface temperatures typically must be at least 82°F (28°C) for a storm to develop and maintain its strength.[120] Climatological monthly mean sea surface temperatures in the Gulf for the month of July range from about 77°F (25°C) to 86°F (30°C) with cooler temperatures towards the coastlines.

Figure 105: Storm Track of Hurricane Georges (left) and Infrared Image of Georges (right)

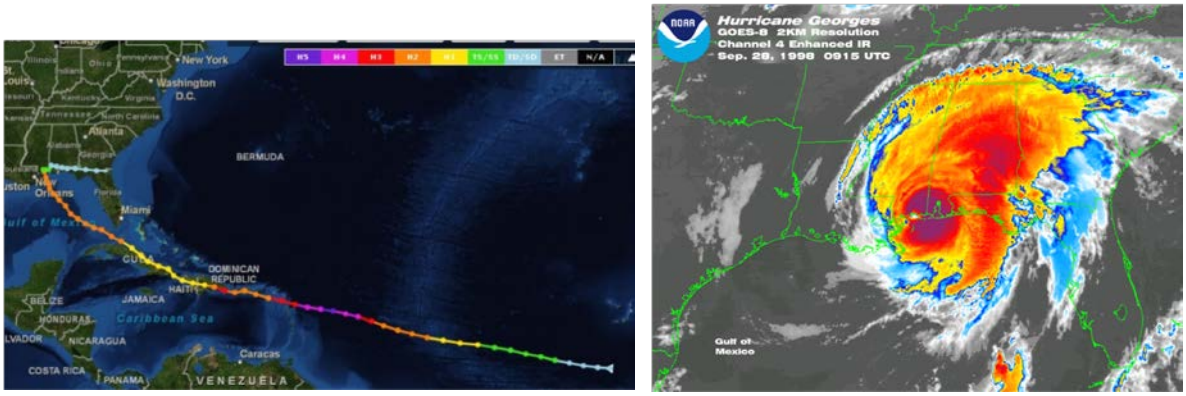

Georges made U.S. landfall near Biloxi, Mississippi around 6:30 am on September 28, 1998 as a Category 2 storm. The storm moved slowly over land and reached Mobile in the early morning of September 29.[121] Because the storm moved so slowly, Alabama experienced significant torrential rains and coastal storm inundation.[122] Figure 105 shows Georges' storm track approaching the Gulf Coast, where the color denotes the storm's Saffir-Simpson intensity rating.[123] The image at the right is an enhanced infrared image of Georges that shows the shape and activity of the storm soon after hitting land.[124]

[118] United States Department of the Interior, 2000
[119] Ibid. The sea surface temperatures were averaged from Sea-Viewing Wide field-of Sensor (seaWiFS) satellite data.
[120] NASA, 2003
[121] Though Biloxi is just 60 miles from Mobile, they have different shoreline characteristics. Biloxi sits directly on the Gulf of Mexico, while Mobile is inset on Mobile Bay, with some barrier islands between the Gulf and the inlet. The differences may affect storm surge and so the locations are considered separately in this analysis.
[122] U.S. Army Corps of Engineers, 1999
[123] NOAA, 2011g
[124] NOAA, 2011h

Figure 106: Total Rainfall from Hurricane Georges (Sept. 26-30, 1998)

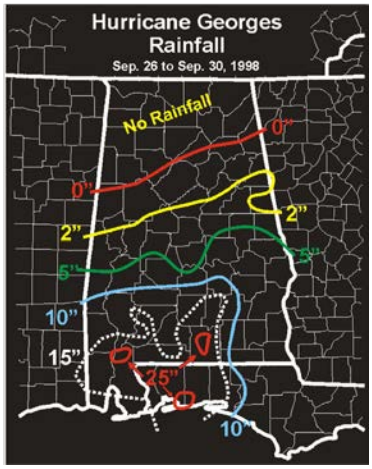

Source: NOAA, 2011j

Storm Event Data

Precipitation: Total precipitation at Keesler AFB in Biloxi, where Georges made landfall, was recorded at 9.18 inches (23.32 centimeters).[125] Total precipitation measured across much of southern Alabama ranged between 20 and 30 inches (51 and 76 centimeters) over the duration of the storm.[126] Mobile Regional Airport recorded 15.02 inches (38.15 centimeters) of total precipitation while downtown Mobile recorded 13.13 inches (33.35 centimeters).[127]

Streamflow: Hourly discharge at the three Mobile stream gages peaked on September 28 and 29 far above their typical levels. The stream gage at Chickasaw Creek experienced the most dramatic discharge increase to over 19,000 cubic feet per second (570 cubic meters per second), up to 180 times its typical levels.[128]

Wind: At landfall, maximum sustained surface winds were 105 miles per hour (168 kilometers per hour), which is a Category 2 storm on the Saffir-Simpson Scale.[129] Brief wind gusts up to 125 miles per hour (200 kilometers per hour) were observed at Keesler AFB in Biloxi.[130] Winds in Mobile the next day were sustained at 57.5 miles per hour (92.0 kilometers per hour), with gusts observed up to 80 miles per hour (128 kilometers per hour) at Dauphin Island.[131] Sustained winds at Mobile Regional Airport were 51 miles per hour (82 kilometers per hour), with peak gusts of 83 miles per hour (133 kilometers per hour), while measured winds at Mobile's

[125] U.S. Army Corps of Engineers, 1999
[126] Ibid.
[127] Ibid.
[128] USGS, 2011a, b, c
[129] U.S. Army Corps of Engineers, 1999
[130] Ibid.
[131] Ibid.

Brookley Field were sustained at 54 miles per hour (86 kilometers per hour) with peak gusts of 62 miles per hour (99 kilometers per hour).[132]

Surface Pressure: Central storm pressure was 964 millibars at landfall, and increased slowly as it approached Mobile to 986 millibars.[133]

Storm Surge and Water Level: At landfall in Biloxi, storm surge was as high as 8.8 feet (268.2 centimeters).[134] Figure 107 displays the storm surge measured at locations around the Mobile region. Storm surge ranged between 5 to 10 feet (152 to 305 centimeters) in Mobile County, with measured storm surge of 8.5 feet (259.1 centimeters) in Downtown Mobile.[135] The highest storm surge in Alabama was recorded in west Mobile Bay at 9.3 feet (283.5 centimeters).[136] Dauphin Island experienced storm surge of 5 feet (152 centimeters) on the bay side and 6.6 feet (201.2 centimeters) on the Gulf side, and the Mobile Bay Causeway experienced 8 to 9 feet (244 to 274 centimeters) of storm surge.[137] High water marks near landfall were between 7 and 10 feet (213 and 244 centimeters).[138] In Mobile, high water marks ranged between 7 and 8 feet (213 to 244 centimeters), while sites in Mobile County experienced high water marks up to 10.3 feet (313.9 centimeters).[139] Every coastal river and stream from Mississippi to the Florida panhandle experienced serious, life-threatening flooding.[140]

Table 51: Summary of Storm Event Data for Hurricane Georges

Variable	Value at Peak Storm Intensity	
	At Landfall (Biloxi, MS)	In Mobile
Precipitation Totals	9.18 in	10-20 in (for a given day, approximately a 10 year storm)
Hourly Streamflow Discharge		
Crooked Creek	-	1,070 ft^3/s (> 2 year event)
Chickasaw Creek	-	19,900 ft^3/s (~ 25 year event)
Fowl River	-	3,340 ft^3/s (< 5 year event)

[132] U.S. Army Corps of Engineers, 1999
[133] Guiney, 1999.
[134] U.S. Army Corps of Engineers, 1999. All storm surge data presented here is referenced to the National Geodetic Vertical Datum (NGVD) of 1929. FEMA requested COE use this datum which is the same used in the construction of the topographic charts published by USGS
[135] Ibid.
[136] Ibid.
[137] Ibid.
[138] Ibid.
[139] U.S. Army Corps of Engineers, 1999
[140] Ibid.

Variable	Value at Peak Storm Intensity	
	At Landfall (Biloxi, MS)	In Mobile
Wind Gusts	125.4 mph	83 mph
Sustained Winds	105 mph	57.5 mph
Central Storm Pressure	964 mb	986 mb
Highest observed water level	12.60 ft	10.33 ft
Storm Surge	8.8 ft	8.5 ft (> 10 year event)

Figure 107: Hurricane Georges representative storm surge above NGVD for Mobile, Baldwin, Jackson, and Escambia Counties

Adapted from U.S. Army Corps of Engineers, 1999

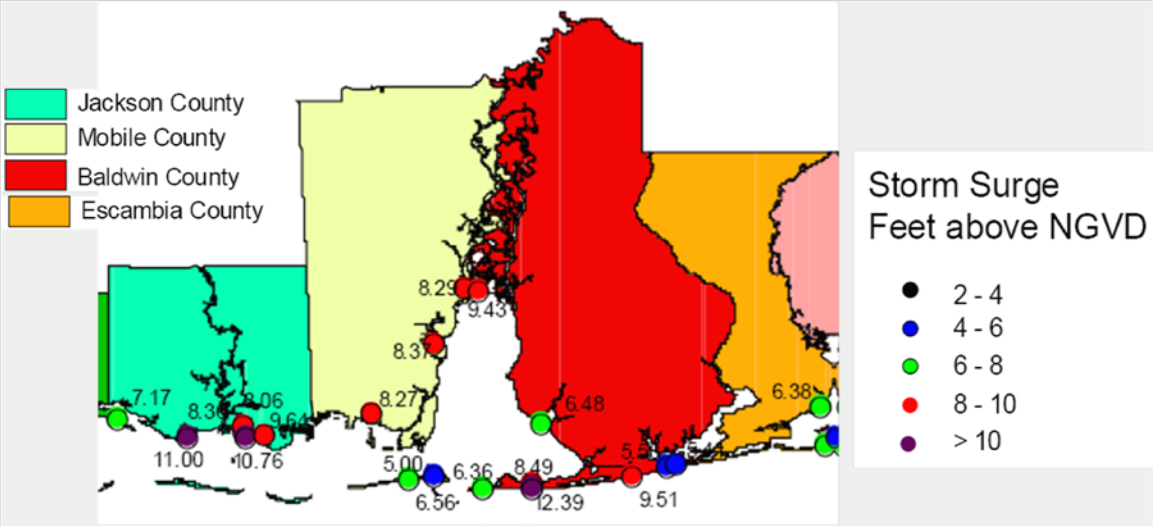

Storm Damage

Georges caused severe flooding along the Gulf Coast from Mississippi to Florida, including the Mobile region. Downtown Mobile was heavily flooded as a result of heavy precipitation and high storm surge (see Textbox below). This resulted in inundated and blocked roadways. The Mobile Bay Causeway was fully inundated, disabling transportation across the bay between Mobile and Baldwin Counties.

Damage Images from Hurricane Georges in Mobile, Alabama

Cars were flooded in a parking garage on Water Street in downtown Mobile and sailboats and debris piled on the lawn of a home on Dog River, a Mobile Bay tributary.

Photo credits: Associated Press. Used with permission.

D.6.5. Study 5: Hurricane Katrina, August 29, 2005

Storm Track and Intensification

Hurricane Katrina was one of the most destructive hurricanes to hit the United States.[141,142] The storm formed from the combination of a tropical wave, an upper-level trough, and the mid-level remnants of Tropical Depression Ten.[143] Hurricane Katrina began its early development on August 23 as a tropical depression about 175 miles (280 kilometers) southeast of Nassau, Bahamas.[144] On August 24, the tropical depression became a tropical storm as it headed towards the Bahamas. In the early evening of August 25, the storm strengthened to a Category 1 hurricane with sustained winds of 80 miles per hour (128 kilometers per hour) just before making landfall in Florida between Hallandale Beach and North Miami Beach. Hurricane Katrina crossed the southern tip of Florida through the night and then began to re-intensify once over the warm waters of the Gulf (sea surface temperatures were 2°F to 4°F (1°C to 2°C) above normal).[145]

From August 25 to August 31, Hurricane Katrina slowly turned to the northwest and north as a mid-level ridge that had been situated over Texas weakened. As Hurricane Katrina moved towards landfall, the upper atmosphere conditions and the above-normal sea surface temperatures aided in Katrina's continued intensification into a major hurricane. In addition, the vertical wind shear (i.e., caused by changes in the atmospheric wind direction and/or strength with altitude) was less than normal, which is conducive to hurricane intensification. On August

[141] NOAA, 2005a
[142] NOAA, 2005b
[143] Ibid.
[144] NOAA, 2005b. The remainder (?) of the "Storm track and Intensification" draws from this source.
[145] NOAA, 2005a

28, Hurricane Katrina became a Category 5 hurricane with peak winds speeds near 175 miles per hour (280 kilometers per hour) and a central pressure of 902 millibars. Katrina was a large storm extending out about 105 miles (168 kilometers) from its center with tropical storm force winds extending out another 100 miles (160 kilometers).

Figure 108: Storm Track and Infrared Image of Hurricane Katrina

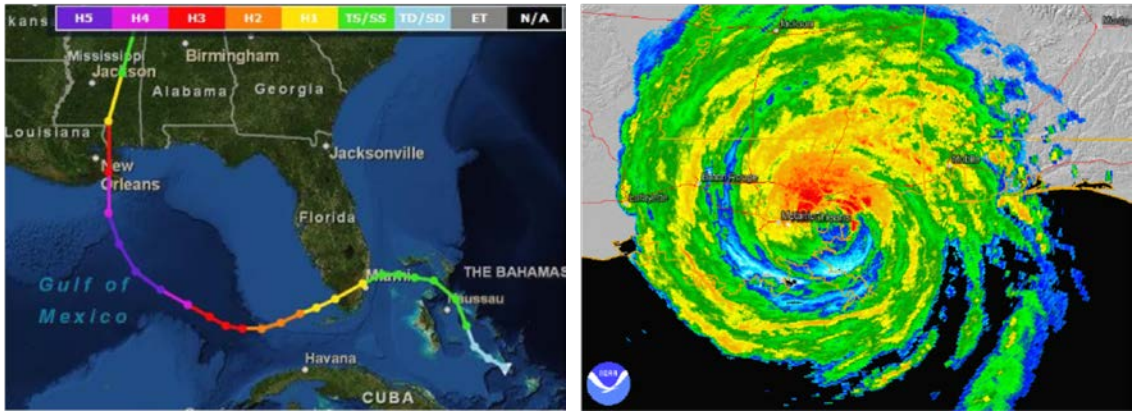

On the morning of August 29, Hurricane Katrina made landfall in Plaquemines Parish, Louisiana as a strong Category 3 hurricane with wind speeds of about 127 miles per hour (203 kilometers per hour) and a central pressure of 920 millibars. Hurricane Katrina made its final landfall near the Louisiana-Mississippi border at 9:45 am local time with winds reported at near 121 miles per hour (194 kilometers per hour).

Storm Event Data

Observations from Hurricane Katrina are provided below for both the site of landfall (near Slidell, LA and Gulfport, MS) and Mobile, AL.

Precipitation: Slidell, LA and Gulfport, MS, the two cities closest to Katrina's point of landfall, measured up to 11 to 12 inches (28 to 30 centimeters) of total precipitation on August 29.[146] Mobile reported a total of 3.8 inches (9.7 centimeters) of rainfall.[147]

Streamflow: At the three Mobile County stream gage sites, hourly discharge measurements demonstrate a drop a sharp increase on August 29-30.[148] These spikes were an increase of 4-, 16-, and 20-fold over typical discharge values at Crooked Creek, Chickasaw Creek, and Fowl River, respectively.

Wind: As Katrina made landfall at the Louisiana-Mississippi border, the hurricane had maximum sustained winds of 120.8 miles per hour (193.3 kilometers per hour), with gusts up to 123 miles per hour (197 kilometers per hour), which is within Category 3 wind speeds.[149] Mobile

[146] Knabb et al., 2006
[147] Ibid.
[148] USGS, 2011a
[149] Knabb et al., 2006

experienced maximum sustained winds of 66.7 miles per hour (106.7 kilometers per hour) and peak gusts of 84 miles per hour (134 kilometers per hour).[150]

Surface Pressure: Katrina's central pressure at landfall near Buras was 923 millibars.[151] The surface pressure in Mobile was measured at 984 millibars at 11:45 am, two hours after Katrina made landfall.[152]

Water Level: Hurricane Katrina caused a storm surge of 24 to 28 feet (7 to 9 meters) at the Slidell, LA / Gulfport, MS coastline.[153] Mobile County observed large storm surges of 10 to 15 feet (3 to 4.6 meters), and the storm caused flooding several miles inland from the Gulf coast along Mobile Bay, where there was a storm surge of 8 to 12 feet (2. to 3.7 meters. Dauphin Island recorded storm surge of 6.63 feet (2.02 meters) and Mobile State Docks recorded storm surge of 11.45 feet (3.49 meters).[154] High water marks surveyed in Mobile reached 11 to 12.5 feet (3.6 to 3.8 meters).[155] On the northeastern portion of Mobile Bay, flooding elevations reached over 13 feet (4 meters), north of Fairhope.[156]

Table 52: Summary of Storm Event Data for Hurricane Katrina

Variable	Value at Peak Storm Intensity	
	At Landfall (Slidell, LA / Gulfport, MS)	Mobile, Alabama
Precipitation Totals	11-12 in.	4 in (~ 2 year storm)
Hourly Streamflow Discharge		
Crooked Creek		330 ft^3/s (8/29) (< 2 year event)
Chickasaw Creek		3,140 ft^3/s (8/30) (< 2 year event)
Fowl River		677 ft^3/s (8/30) (< 2 year event)
Wind Gusts	123 mph	84 mph
Sustained Winds	121 mph	67 mph
Central Storm Pressure	928 mb	984 mb

[150] Ibid, Winds become dangerous to road maintenance, truck operations, and other road users at around 39 mph and are very dangerous at 74 mph (OFCM, 2002).
[151] Knabb et al., 2006
[152] Ibid.
[153] FEMA, 2006b. All observations discussed here are referenced to the North American Vertical Datum of 1988
[154] Ibid.
[155] Ibid.
[156] Ibid.

Variable	Value at Peak Storm Intensity	
	At Landfall (Slidell, LA / Gulfport, MS)	Mobile, Alabama
Highest observed water level	27.9	15 ft
Storm Surge	24-28 ft	10-15 ft (~ 25 year event)

Storm Damage

Mobile County experienced significant damage from Hurricane Katrina, primarily in the form of coastal flooding and storm surge. Storm surge on Dauphin Island destroyed or damaged dozens of homes. On Dauphin Island, flooding elevations were between 8.5 and 11.5 feet (2.6 and 3.5 meters).[157] In the city of Mobile, typical flood depths were on the order of 11 to 12.5 feet (33 to 3.8 meters), causing severe inundation and shut down of most major roadways.[158] These are close to the highest levels ever recorded in Mobile.[159] Downtown Mobile was entirely inundated, causing authorities to issue a dusk-to-dawn curfew for the area. The Mobile Bay Causeway was fully inundated, as it was during Georges, disabling transport across the bay.[160]

The Mobile area also experienced debris damage from oil rigs during Hurricane Katrina. Dauphin Island experienced damage from an offshore oil rig that washed up on the shore. In addition, an oil rig under construction along the Mobile River in Alabama was dislodged and carried 1.5 miles (2.4 kilometers) north where it struck the Cochrane Bridge just north of downtown Mobile.[161]

[157] FEMA, 2006a
[158] Ibid.
[159] Kieper, 2011. The highest value ever recorded was 11.60 feet on 5 July 1916.
[160] Ibid.
[161] Knabb et al., 2006

Damage Images from Hurricane Katrina in Mobile, Alabama

Severe flooding occurred in downtown Mobile.

Photos courtesy of wunderground.com; Used with permission.

D.7. Projected changes in U.S. and Global Storm Events

The United States experiences a wealth of storm activity including severe thunderstorms producing tornadoes, nor'easters producing intense winds and precipitation, and tropical storms and activities. The duration, frequency, location, and intensity of storm events in the United States will likely evolve in response to changes in climate. Studies suggest that storm events will increase in severity across the United States. This appendix discusses projected changes in storm events across the United States and world in the coming century, including extreme precipitation events, tropical storms and hurricanes.

D.7.1. Extreme Precipitation Events

By the end of the century, extreme precipitation events in the United States are projected to increase in both frequency and intensity. By the end of the century, heavy precipitation events that currently have a 5% chance of occurring in a given year are projected to have a 7 to 25% chance of occurring.[162] Extreme heavy downpours are also projected to produce more precipitation.[163] Meanwhile, light precipitation events are projected to become less frequent. Taken together, these projections suggest that total annual precipitation may not change significantly, but the way that precipitation is delivered might be different.[164]

Scientists do not entirely understand the physical mechanisms that contribute to storm intensification, particularly when characterizing the influence of natural variability such as El Niño events and other large-scale circulation patterns. However, some mechanisms in the development and/or steering of U.S. storms are well-understood, such as the location and strength of the jet stream.[165]

D.7.2. Tropical Storms and Hurricanes

The recent scientific consensus on tropical cyclonic activity suggests tropical cyclones may globally decrease in frequency but increase in intensity. This consensus suggests that the globally averaged intensity of tropical cyclones will increase by 2 to 11% by the end of the century but the globally averaged frequency will decrease by 6 to 34%.[166] This consensus is further supported by a recent study which estimates an increase in the number of more severe (Category 4 and 5) storms, but a decrease in the total number of tropical storms and hurricanes in the tropical Atlantic.[167]

There is observational evidence since about 1970 that the intensity of tropical cyclone activity has been increasing, correlated with increases in tropical sea-surface temperatures in the North Atlantic (a tropical cyclones refers to specific stages of hurricane development from tropical

[162] USGCRP, 2009
[163] USGCRP, 2009
[164] USGCRP, 2009
[165] USCCSP, 2008b
[166] Knutson et al., 2010
[167] Bender et al., 2010

depression to tropical storm whereupon the storm is named to hurricane).[168] There is also evidence of an increase in extreme wave height over the past two decades, associated with more frequent and intense hurricanes.[169] However, the World Meteorological Organization (WMO) Sixth International Workshop on Tropical Cyclones in 2006 agreed that "no firm conclusion can be made" about anthropogenic influence on tropical cyclone activity because "there is evidence both for and against the existence of a detectable anthropogenic signal in the tropical cyclone climate record."[170] Recently, there is growing confidence in the model projections that climate change may increase hurricane strength, but it is still unclear how the overall frequency of occurrence might change.[171]

D.8. Detailed Methodology for Scenario-based Storm Surge Analysis

This appendix describes in detail the methodology used to conduct a scenario- and model-based analysis of storm surge in the Mobile region.

The projected increase in hurricane intensity has the potential to increase flooding from coastal storms striking the Mobile area. As tropical storms and hurricanes approach Mobile, generally from a southerly direction, multiple physical properties promote flooding in the region:

- The storms' strong winds tend to push water toward the coast, causing the water level to rise and penetrate inland.
- The drop in surface pressure that is generally associated with the approach of a storm can locally raise the water level, thereby contributing to flooding.

A state-of-the-art storm surge model, the Advanced Circulation (ADCIRC) model, was used to represent these physical processes and to explore the implications of a range of hurricane scenarios that could strike the Mobile area. The exacerbating contribution from future sea-level rise was also examined.

The scenario- and model-based analysis included the following steps, which correspond to the sections of this appendix:

- Selection of storm surge scenarios
- Advanced circulation modeling
- Advanced circulation model testing
- Wave modeling
- Exposure mapping

[168] USCCSP, 2008b
[169] USCCSP, 2008b
[170] WMO, 2006
[171] NRC, 2010c

D.8.1. Selection of Storm Surge Scenarios

Although there is a strong theoretical basis underpinning the scientific assertion that the intensity of hurricanes will increase in the future, it is difficult to probabilistically estimate the number and intensity of hurricanes that will strike the Mobile region over the 21st Century. Therefore, as with the sea-level rise analysis, scenarios were selected to analyze the implications of a wide range of storms that could plausibly strike Mobile. For this analysis, records from historic storms were selected to use as the basis in developing these storm scenarios.

There were two main questions that the scenario-based analysis attempted to address:

1. *What are the implications of a moderate hurricane striking the region under a scenario of increased sea level?* According to the Gulf Coast Phase 1 report, planners in the Gulf Coast region can expect a Category 1 or 2 hurricane approximately once every five years.[172] A set of scenarios was developed to examine the extent of flooding from such storms when exacerbated by sea level rise.

2. *What are the implications of a strike by a larger hurricane than the region has experienced in recent history?* Although the odds of an intense hurricane strike are difficult to determine, those odds are increasing.[173] A set of scenarios was therefore developed to examine the implications of hurricanes in magnitude that have not yet been historically recorded for the region, but that will become more likely in the future. This was done by selecting a storm that occurred relatively recently, and intensifying it using different methods (described below) and including the effects of sea level rise.

In selecting the storms, historical storms were chosen that met the following criteria:

- Local tide gage data are available throughout most of the course of the storm, to assess the temporal character of the modeled evolution of the storm.
- Post-storm high water mark data are available in the Mobile area, to assess the model's representation of the spatial extent of flooding.
- The storm approached the coast relatively perpendicularly, thereby reducing the potential for prolonged and complex interactions between the storm and the coastline that could reduce the trustworthiness of the simulation.
- The strengths of the storms and their storm surges were appropriate to the two questions being addressed.

After reviewing records of all landfalling hurricanes in the Mobile area over the past few decades, the 1998 Hurricane Georges was selected to address Question #1, and the 2005 Hurricane Katrina was selected to address Question #2.

[172] CCSP, 2008
[173] Karl et al., 2008

Using Hurricanes Georges and Katrina as base storms, 11 storm scenarios (see Table 53) were developed by adjusting certain characteristics of the storm parameters to simulate what could happen under alternate conditions. For the Georges simulations, all four sea level rise scenarios (0 meters, 0.3 meters, 0.74 meters, and 2.0 meters (0, 1.0, 2.5, and 6.6 feet)) were examined. Results for ADCIRC are reported relative to Mean Sea Level.[174] For the Katrina simulations, the modeling considered different adjustments, including shifting the path of Katrina so that it hit Mobile directly, intensifying the storm, and adding in 0.75 meters (2.5 feet) of sea level rise. Two of the 11 scenarios were hindcasts of Georges and Katrina. They were used to validate the model and to serve as a basis from which to build the other 9 scenarios.

[174] Note that the mapping of potential inundation due to long-term sea level rise is conducted relative to Mean Higher High Water (MHHW) whereas the ADCIRC results are shown relative to Mean Sea Level (MSL). We show long-term inundation relative to MHHW so that the impacts above the tidal cycle are evident. We show the short-term flooding results relative to MSL since we do not know what the tidal stage of any particular future storm will be. MHHW is 0.77 feet above MSL at Mobile State Docks.

Anatomy of the "perfect storm"

A number of highly damaging storms have struck the Mobile area. However, none of them have had all of the characteristics that would maximize the impact. Below are features that would contribute to a "perfect storm."

- **High winds.** Although flooding is generally the greatest source of damage in a hurricane, winds are responsible for most of the storm surge that occurs. Damage to buildings increases exponentially in proportion to the wind speed. Hurricane Katrina was a Category 3 (winds of 111-30 mph) storm at landfall, whereas the strongest hurricanes reach Category 5 (winds greater than 156 mph).
- **Slow movement.** The slower the eye of the hurricane moves, the more time it has to pile up water against the coastline, thereby enhancing the storm surge. Although Hurricane Frederic was a Category 3 storm at landfall, its surge was similar to that of the weaker, Category 2 Hurricane Georges, due in part to Frederic's relatively rapid forward speed.
- **Large size and long travel distance (i.e., fetch).** The larger the wind field, the more water will be pushed against the coastline, thereby exacerbating the surge. The same is true for the fetch, in which the farther the storm travels across open water prior to landfall the greater its surge will tend to be.
- **High precipitation.** The precipitation from the storm can exacerbate the storm surge by creating inland flooding that meets the marine surge in the estuary or further up the rivers that feed into the estuary.

Table 53: Storm Scenarios

Name	Sea level rise	Track Shift	Amplification	Question Addressed[175]
Georges-Natural	None	No	None	Baseline
Katrina-Natural	None	No	None	Baseline
Georges-Natural-30cm	0.3 m	No	None	(1)
Georges-Natural-75cm	0.75 m	No	None	(1)
Georges-Natural-200cm	2.0 m	No	None	(1)
Katrina-Natural-75cm	0.75 m	No	None	(1), (2)
Katrina-Shift[176]	None	Yes	None	(2)
Katrina-Shift-75cm	0.75 m	Yes	None	(2)

[175] The two questions being address are: (1) What are the implications of a moderate hurricane striking the region with a higher sea level? (2) What are the implications of a strike by a larger hurricane than the region has experienced in recent history?

[176] The term "shift" indicates an eastward shift of the storm track. This is used to explore the potential for a direct hit of a major hurricane on the Mobile area.

Name	Sea level rise	Track Shift	Amplification	Question Addressed[175]
Katrina-Shift-ReducedPress-75cm	0.75 m	Yes	Central pressure reduced according to Knutson and Tuleya (2004)	(2)
Katrina-Shift-MaxWind	None	Yes	Max. wind speed sustained through landfall	(2)
Katrina-Shift-MaxWind-75cm	0.75 m	Yes	Max. wind speed sustained through landfall	(2)

Explanation of scenario names:

- The 0.3-, 0.75-, and 2.0-meter (1.0-, 2.5-, and 6.6-feet) identifiers indicate those scenarios that include an elevated stillwater level to represent an increase in global sea level. Uplift and subsidence (and other factors affecting LSLR) were not included since they are expected to be much less important than the magnitude of the surge itself.
- The term "natural" in the scenario names indicates that the *observed* storm track characteristics were used, as obtained from the National Oceanic and Atmospheric Administration (NOAA) (see next section below).
- The term "shift" in the scenario names indicates an eastward shift of the storm track from its actual landfalling location near the Mississippi-Louisiana border. Shifting was used to explore the potential for a direct hurricane hit on the Mobile area. The magnitude of the eastward shift was designed to maximize the intensity of the winds blowing northward up Mobile Bay. In a hurricane, the maximum winds are to the right of the forward direction of a storm (in the Northern Hemisphere) due to the combination of the storm's counter-clockwise rotation and its forward motion. Thus, landfall of the shifted storms was to the east of the Alabama-Mississippi border and to the west of Mobile Bay. Figure 109 and Figure 110 show the actual and shifted tracks.
- The term "ReducedPress"[177] indicates that the central pressure[178] of the storm along its entire track was reduced by 14% according to the findings of Knutson and Tuleya (2004). This study simulated increases in CO_2 levels of 1% per year[179] over the 21st century by a range of global climate models that included a nested, high-resolution regional model run using a range of convective parameterizations. Their aggregate results, averaged across all

[177] The ReducedPress, MaxWind, and shift scenarios were applied only to Katrina.
[178] The intensity of a hurricane is defined in part by its central pressure. The lower the central pressure, the more intense it is.
[179] A 1%/year increase in atmospheric CO_2 concentration corresponds roughly to the IPCC B1 scenario through approximately 2060 (Goose et al. 2010).

experiments, indicate a 14% greater central pressure fall of major hurricanes across the three major tropical storm basins. This is a measure of the anticipated intensification of storms.

- The term "MaxWind" indicates that the wind speeds were held constant at the values they had when the storm's maximum sustained wind speed (approximately 150 knots for Hurricane Katrina) was recorded (in the central Gulf of Mexico on August 28, 2005). It is plausible that a Category 5 storm such as this could strike the Mobile region.

Figure 109: Original Track of Hurricane Katrina

The image shows the observed track of Hurricane Katrina. Each dot represents the approximate location of the NOAA National Hurricane Center six-hour advisory bulletin used in the model simulations. kph = knots per hour. The times are UTC.

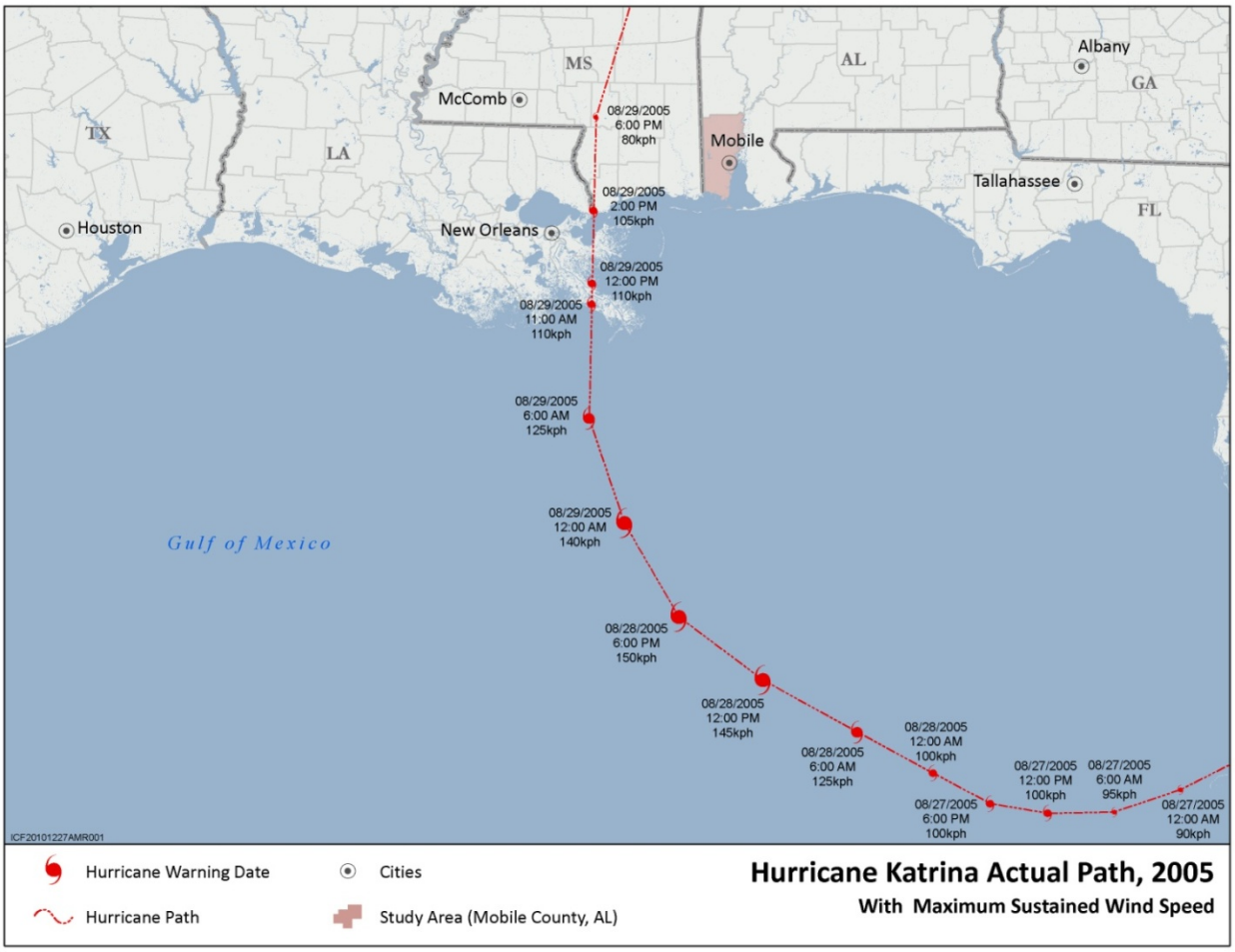

Figure 110: Shifted Track of Hurricane Katrina

This image shows the shifted track of Hurricane Katrina that corresponds to five of the scenarios that were explored in this study.

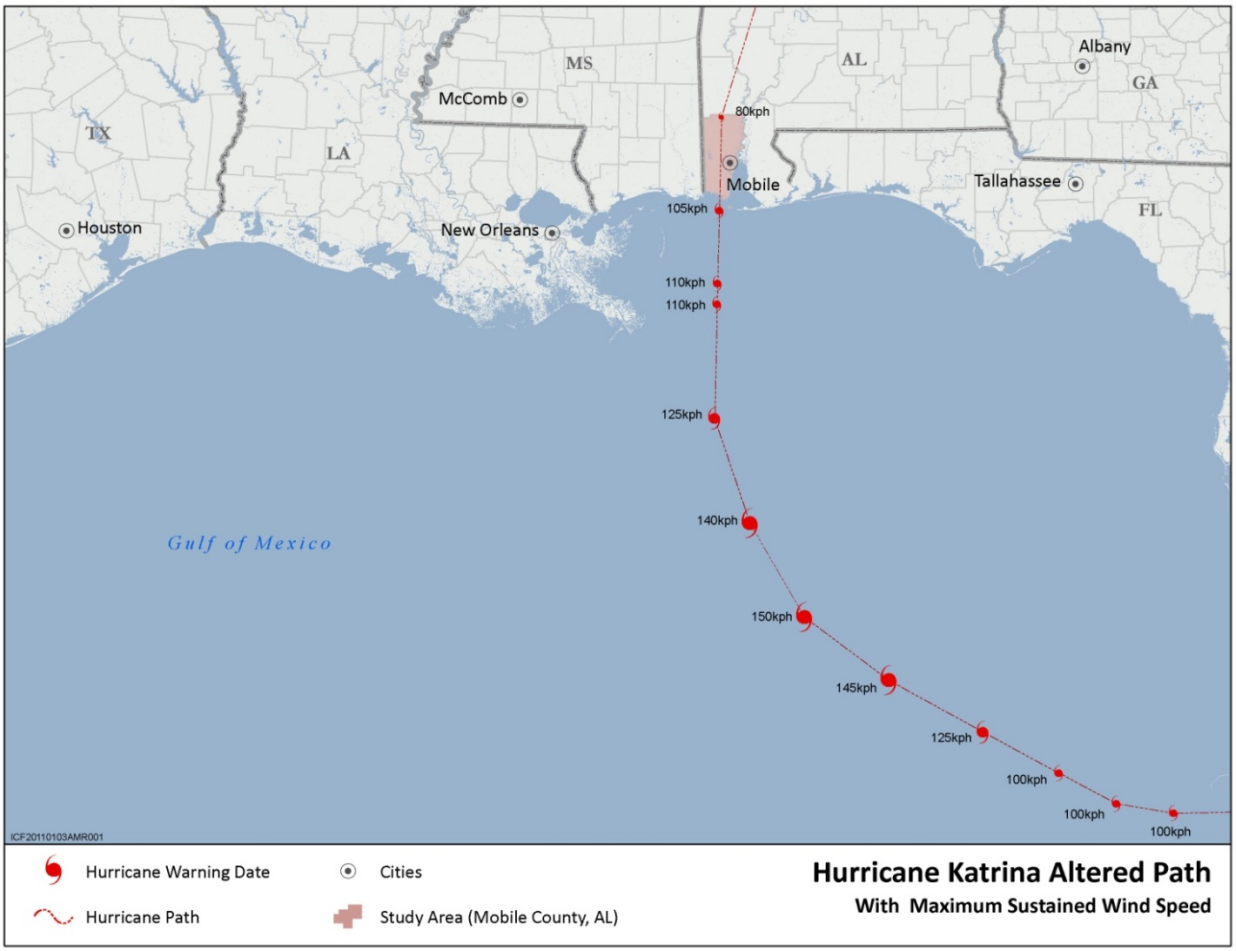

D.8.2. Advanced Circulation Modeling

Simulations of storm-induced water levels (i.e. storm surge) were performed using the ADvanced CIRCulation model, ADCIRC.[180] This finite-element hydrodynamic code is robust, well-developed, extensively-tested, and highly adaptable to a number of coastal-ocean processes. The storm simulations presented in this study were performed using the two-dimensional, depth integrated (2DDI) form of ADCIRC assuming barotropic forcing only (i.e. no density-driven flows). While the ADCIRC model is capable of applying a variety of internal and external forcings, including tidal forces and harmonics, inflow boundary conditions, density stratification, and wave radiation stresses, only the meteorological forcing input was used to drive the storm-induced flows and water levels.

The generalized wave continuity and momentum equations were discretized using finite-element techniques on an unstructured network of nodes and connective elements. These techniques allow for varying degrees of resolution throughout the computational domain, and provide great

[180] Luettich et al., 1992; Luettich and Westerink, 2004; Westerink et al., 1994

flexibility when modeling flows within complex or irregular boundaries. The organization of nodes and elements, and the information that the nodes contain (i.e., horizontal coordinates, elevation, roughness, etc.), is collectively referred to as the ADCIRC mesh. A diagram of the mesh used in this study is provided in Figure 111. A portion of this mesh (shown in red), extending from the Northwest Florida panhandle to the Mississippi-Alabama border, extends above mean sea level to accommodate storm surge inundation and flood modeling. Resolution in much of Mobile's metropolitan area ranges from 165 to 495 feet (50 to 150 meters). It is much coarser offshore in order to reduce the computational demand and computer run-time. Meshes such as these, which are quite time intensive to produce, are available for most of the U.S. coastline.[181]

Figure 111: Diagram of the ADCIRC Mesh (SSv31L) Used in this Model Study of Hurricanes Georges and Katrina

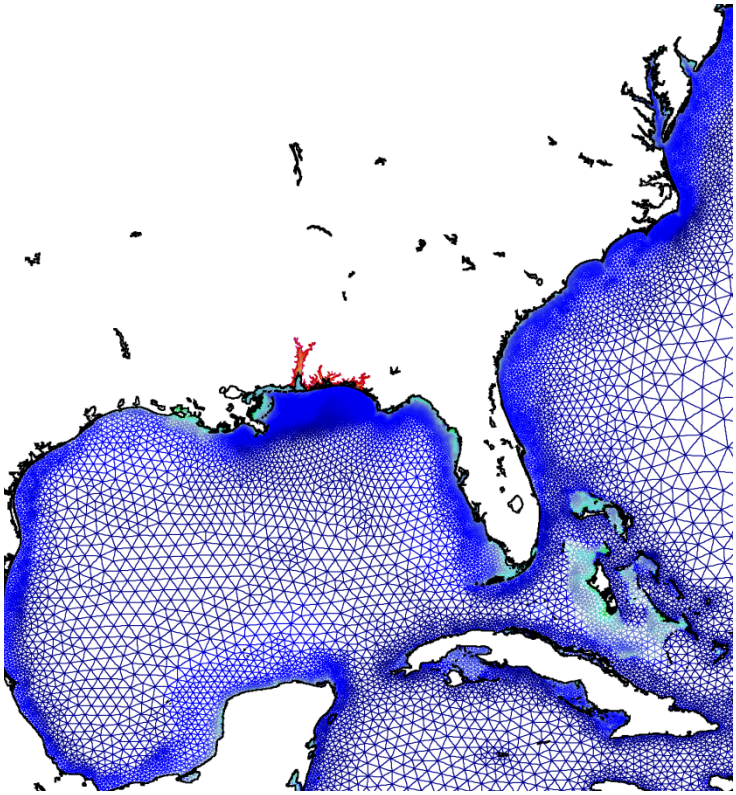

The ADCIRC mesh used in this study is composed of 446,459 discrete nodes with connective nodestrings creating 866,496 triangular mesh elements. Each node in the ADCIRC mesh contains at least two layers of information: the node's horizontal coordinate, which is given by latitude and longitude when performing simulations in spherical coordinates; and the node's elevation relative to mean sea level (MSL).

[181] ADCIRC, 2011

The model takes into account the slope of the land in its estimation of surge. However, since the surge model does not take into account wave breaking and wave run-up, it does not take into account the effect of the slope of the land on waves. The effect of the slope of the land is accounted for in the wave model (STWAVE, described below), but this does not feed back to the ADCIRC model since the two models are run asynchronously.

The ADCIRC storm simulations considered in this validation study were driven by meteorological forcing data extracted from six-hour advisory forecast and observation reports issued by the NOAA National Hurricane Center (NHC). The meteorological data required by the ADCIRC model includes a time code, the latitude and longitude of the eye, the maximum observed wind speed in knots, the minimum sea level pressure in millibars, and the radius, in nautical miles, from the center of the storm to a specified wind intensity (e.g., 34, 50, 64, or 100 knots) in each of the storm's four quadrants. These data must be assembled in a modified Automated Tropical Cyclone Forecast (ATCF) best track format as described in Luettich and Westerink (2004). An asymmetric hurricane vortex formulation[182] based on a Holland-type gradient wind model[183] was used to estimate the wind and pressure field of the storm. The Garratt (1977) formula was used to convert wind speed to an applied wind stress. These data are spatially interpolated onto the ADCIRC mesh, and a linear interpolation was used to map six-hour advisory data to each intermediate time that the model performs its calculations[184] falling between advisory information. A general schematic of this process is provided in Figure 111.

Figure 112: A Representative Model Schematic for Meteorological Coupling in ADCIRC Storm Simulations[185]

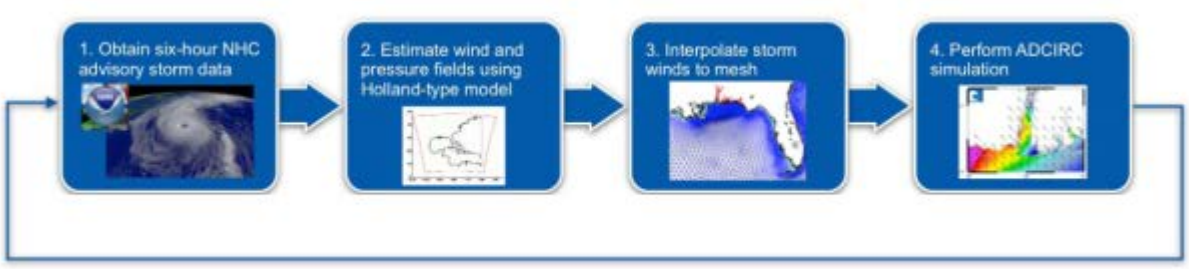

D.8.3. Advanced Circulation Model Testing

Hindcast simulations of storm-induced water levels using the ADCIRC hydrodynamic model were completed for Hurricanes Georges and Katrina. As noted above, these simulations were driven by historical parameters and tracks. They were used to evaluate the model's ability to accurately reproduce the spatial distribution and peak storm-induced water levels of historical events and to assign a quantitative measure of accuracy to model predictions. This evaluation is indicative of the veracity of simulations of the surge response to various future storm scenarios for which no equivalent comparators exist for model-data verification.

[182] Mattocks and Forbes, 2008; Mattocks et al., 2006
[183] Holland, 1980
[184] The model computes all parameters.
[185] After Blain et al., 2007

Hurricane Katrina

The hindcast ADCIRC simulation of Hurricane Katrina was initiated using data from August 27, 2005 at 1800 hrs UTC. By this time, Katrina had already made an initial landfall on the southeast coast of Florida, had weakened in intensity, and was beginning its first of two rapid intensification periods.[186] Hurricane Katrina made its final landfall at 1110 hrs UTC on August 29, 2005 near Grand Isle, Louisiana. At landfall, Katrina had maximum sustained winds ranging from 117 to 126 knots, as well as stronger gusts, and minimum central pressures ranging from 918 to 923 millibars.[187] An overview of Katrina's historical track is provided in Figure 109. In this figure, each dot represents the location of the eye of the storm when an NHC advisory bulletin was issued providing basic storm parameters such as location, maximum winds, minimum sea level pressure, and radius to specific wind speed intensities in each of the storm's four quadrants. The first dot denotes the beginning of the model simulation.

The total duration of the Katrina hindcast simulation is 2.75 days, including an initial 0.5-day ramp period to avoid instabilities associated with model spin-up. The initial starting time for the simulation was chosen to capture all relevant storm effects during its residence time in the Gulf of Mexico prior to landfall, including any setup along the Alabama shelf that may elevate pre-storm water levels above the astronomical tide. For evaluation purposes, a 3.75-day simulation was performed and no measurable differences were obtained over much of the simulated storm surge hydrograph.

Please see Appendix D.6.5 for more information on this storm.

Hurricane Georges

Hurricane Georges started as a tropical wave off the west coast of Africa. After a week of development, the storm reached its peak intensity of 135-knot winds at 0600 hrs UTC on September 20, 1998 in the Lesser Antilles. Shortly thereafter, the storm diminished in strength prior to making its first of several landfalls in the Lesser Antilles. A succession of weakening and re-intensification ensued while the storm passed through the Lesser Antilles and over Puerto Rico, until it was significantly weakened as it passed over the mountainous terrain of the island of Hispaniola and later Cuba. Upon entering the Gulf of Mexico, a modest re-intensification from 65 to 90 knot one-minute sustained wind speeds was accompanied by a gradual reduction in forward speed. Georges made landfall near Biloxi, Mississippi early on the morning of September 28, 1998. At landfall, Georges had maximum sustained winds of 90 knots and a minimum central pressure of 964 millibars. A more thorough report of Georges' history and characteristics can be found in Guiney (1999). The hindcast simulation of Georges began on September 26, 1998 at 0300 hrs UTC. An overview of Georges' historical track is provided in the Figure 113 below, where each dot represents the location of the eye of the storm when an NHC advisory bulletin was issued. The first dot denotes the beginning of the model simulation.

[186] Knabb et al., 2006
[187] USDOC, 2005

Figure 113: A General Overview of Hurricane Georges' Historical Track through the Caribbean Basin and Gulf of Mexico

The ADCIRC model simulation begins on 9/26/98 at 0300 UTC. Each dot represents the approximate location of the NHC six-hour advisory bulletin used in the baseline model simulation. The dates correspond to eye position at 0300 hrs UTC.

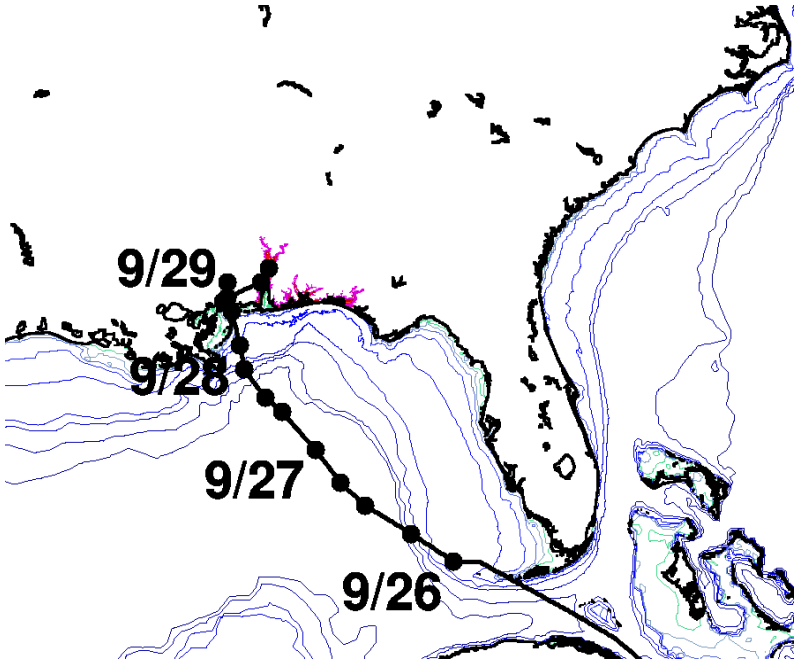

The total duration of the Georges hindcast simulation is 3.5 days, including an initial 0.5-day ramp period to avoid instabilities associated with model spin-up. The initial starting time for the simulation was chosen to capture all relevant storm effects during its residence time in the Gulf of Mexico prior to landfall, including any setup along the Alabama shelf that may elevate pre-storm water levels above the astronomical tide. For evaluation purposes, a 4-day simulation was performed and no measurable differences were obtained over much of the simulated storm surge hydrograph.

Please see Appendix D.6.4 for more information on this storm.

Evaluation Metrics

Two metrics were used to evaluate the ability of ADCIRC to accurately reproduce storm-induced water levels: time series of measured and simulated water levels at discrete spatial locations (i.e. storm surge hydrographs); and spatial distributions of measured high water marks (HWMs[188]) on land. Measured water levels were provided, where available, by a number of gages maintained by the NOAA's Center for Operational Oceanographic Products and Services (CO-OPS).[189] FEMA (2006a) provided measured HWMs for Katrina and USACE (1998) provided measured HWMs for Georges. The ADCIRC-simulated maximum water levels at each node in the mesh were interpolated to the geographic coordinates of the measured HWMs for comparison.

[188] The HWM for a particular storm is distinct from other regularly occurring tidal indices. For example, the Mean Higher High Water mark corresponds to the average of the higher high water height of each tidal day observed over the National Tidal Datum Epoch.
[189] NOAA, 2011

There are discrepancies associated with the comparison of measured and simulated HWMs, as HWMs are measured relative to a survey datum, while model output is provided relative to the MSL tidal datum. There are only two locations in Mobile County where the relationship between these two datum is known: Dauphin Island and Mobile State Docks. However, only the value at Dauphin Island is published by NOAA CO-OPS, because the values at Mobile State Docks, do not meet NOAA/NGS vertical accuracy requirements. The approximate error associated with this datum discrepancy may be +/- 0.59 feet (0.18 meters) for Katrina, where HWMs are provided in NAVD88. The approximate error may be closer to +/- 0.17 feet (0.05 meters) for Georges, where HWMs are provided in NGVD29[190]. Time-series water level comparisons were performed relative to a consistent survey datum (NAVD88). All tidal datum values correspond to the National Tidal Datum Epoch of 1983 – 2001. The comparison of high water marks for Georges and Katrina are presented here, but discussed in more detail in the following sections. The discussion focuses on Dauphin Island and Pensacola since those are the two nearby gages that had the most continuous records during the two storms.

Figure 114: Water Levels at Dauphin Island, Alabama during Hurricane Katrina

The predicted tide (red dash) is the level that would have been expected in the absence of the storm. The measured level (green circles) is what was actually observed. The simulated level (blue line) is the water elevation predicted by the model, driven by observed winds and atmospheric pressure, but without accounting for tides. The predicted and measured levels in feet relative to Mean Higher High Water were obtained from the NOAA Tides & Currents data repository using CO-OPS station 8735180. Note that the simulated water levels shown do not include values obtained during the initial 0.5-day model ramping period.

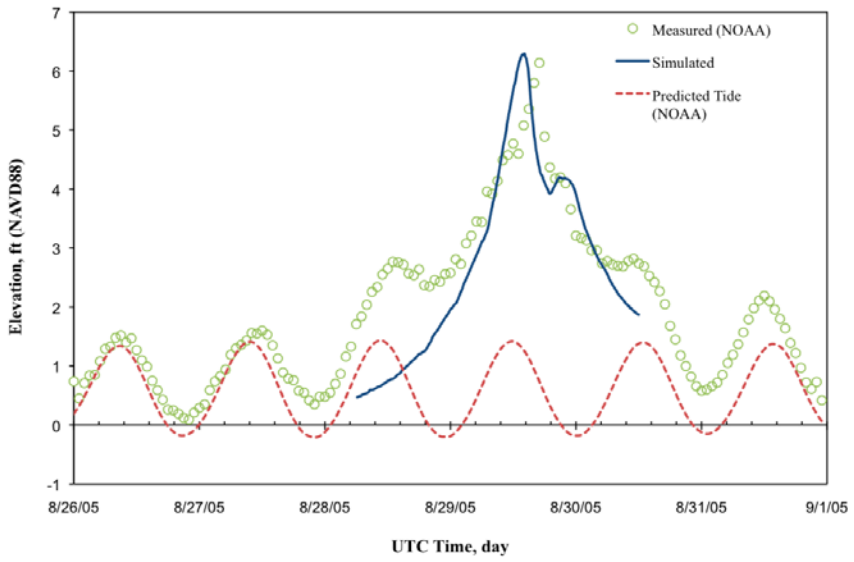

[190] The basis for this error analysis is provided in a report produced by South Coast Engineers for ICF titled: "Hydrodynamic Model Testing and Validation for Two Historical Storms: Hindcast Simulations of Hurricanes Katrina and Georges." It is available upon request from ICF.

Figure 115: Water Levels at Pensacola, Florida during Hurricane Katrina

The predicted tide (red dash) is the level that would have been expected in the absence of the storm. The measured level (green circles) is what was actually observed. The simulated level (blue line) is the water elevation predicted by the model, driven by observed winds and atmospheric pressure, but without accounting for tides. The predicted and measured levels in feet relative to Mean Higher High Water were obtained from the NOAA Tides & Currents data repository using CO-OPS station 8729840. Note that the simulated water levels shown do not include values obtained during the initial 0.5-day model ramping period.

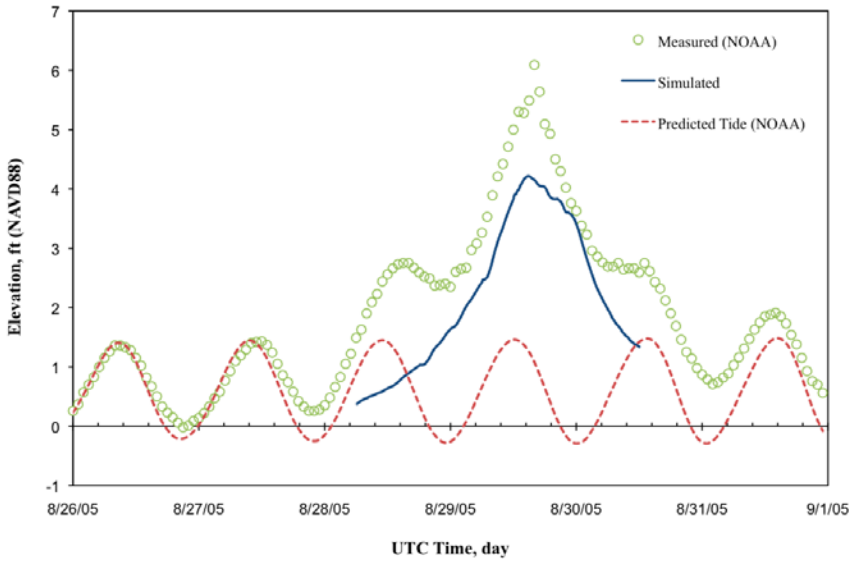

Figure 116: Water Levels at Dauphin Island, Alabama during Hurricane Georges

The predicted tide (red dash) is the level that would have been expected in the absence of the storm. The measured level (green circles) is what was actually observed. The simulated level (blue line) is the water elevation predicted by the model, driven by observed winds and atmospheric pressure, but without accounting for tides. The predicted and measured levels in feet relative to Mean Higher High Water were obtained from the NOAA Tides & Currents data repository using CO-OPS station 8735180. Note that the simulated water levels shown do not include values obtained during the initial 0.5-day model ramping period.

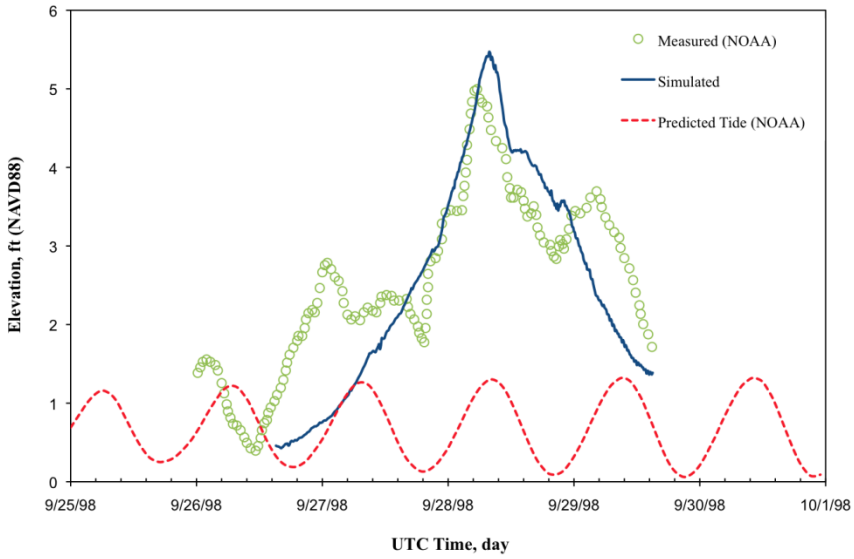

Figure 117: Water Levels at Pensacola, Florida during Hurricane Georges

The predicted tide (red dash) is the level that would have been expected in the absence of the storm. The measured level (green circles) is what was actually observed. The simulated level (blue line) is the water elevation predicted by the model, driven by observed winds and atmospheric pressure, but without accounting for tides. The predicted and measured levels in feet relative to Mean Higher High Water were obtained from the NOAA Tides & Currents data repository using CO-OPS station 8729840. Note that the simulated water levels shown do not include values obtained during the initial 0.5-day model ramping period.

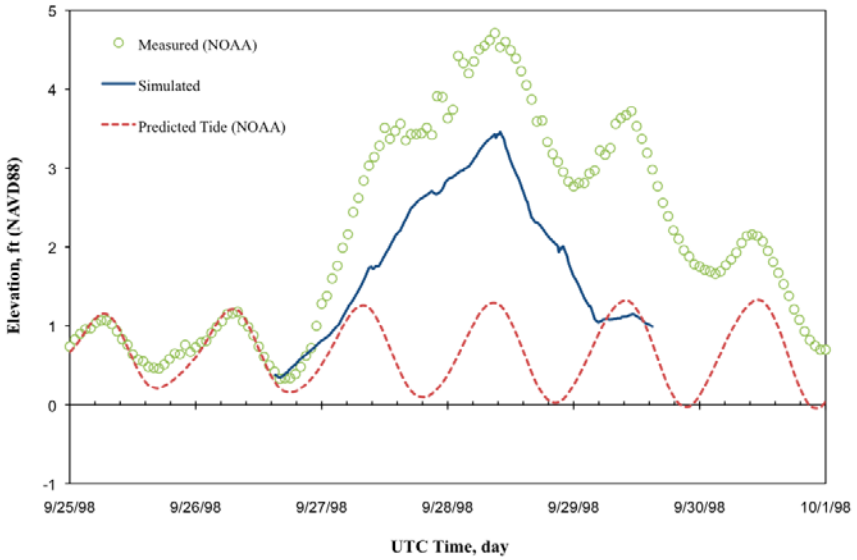

For Hurricane Katrina at Pensacola, the ADCIRC model reproduces the general shape and duration of the peak in the observed surge hydrograph, but underpredicts the observed peak water level by about 2 feet (0.6 meters). Note that this location is the most distant from the storm in the hindcast analysis. At Dauphin Island, the model appears to be in good agreement with measurements: the model reproduces the shape, duration, and elevation of the peak in the storm surge hydrograph.

For Georges, the performance of the model at Pensacola and Dauphin Island appears to be generally consistent with the hindcast simulation of Katrina. The model captures the general shape and duration of the peak in the storm surge hydrograph at Pensacola, but underpredicts the peak water level by about 1 foot (0.3 meters. At Dauphin Island, the model reproduces both the shape and elevation of the peak storm surge; however, the rising and receding limbs of the simulated hydrograph do not correspond precisely to the observations due to the absence of astronomical tidal oscillations in the model. The tidally-related error of the model simulations presented here is roughly ± 0.7 feet (0.2 meters), which is half the tidal amplitude in Mobile.

A quantitative error analysis covering the duration of both storm simulations was conducted. For Katrina, the root mean square (RMS) errors at Pensacola and Dauphin Island are 1.2 feet (0.4 meters) and 1.0 feet (0.3 meters), respectively. The Percent of Peak (POP), which is the RMS error divided by the maximum observed (measured) water level, was also computed. It is a more useful measure of model accuracy. The POP RMS errors for Katrina at Pensacola and Dauphin Island are roughly 20% and 16%, respectively. For Georges, the RMS errors between simulated

and measured water levels at Pensacola and Dauphin Island are 1.38 feet (0.42 meters) and 0.88 feet (0.27 meters), respectively. The corresponding POP RMS errors for Georges are 29.3% and 17.6%. Note that both the RMS and POP RMS errors have similar magnitudes for both hindcast simulations. Given the number of sources of uncertainty discussed below (e.g., lack of tides, wave breaking, and river runoff in the simulations), these uncertainties are quite low for this type of hindcast.

The spatial range of differences between simulated and observed high water marks for both storms is shown in Figure 118 and Figure 119 below.

Figure 118: A Comparison of Measured and Simulated High Water Mark Errors (in feet) in Mobile and Baldwin Counties during Hurricane Katrina

The comparison error is computed as (simulated) – (measured) such that positive and negative values suggest an over prediction and under prediction of water levels, respectively. A datum discrepancy between measurements (NAVD88) and simulated high water marks (MSL) may introduce differences on the order of +/- 0.7 feet.

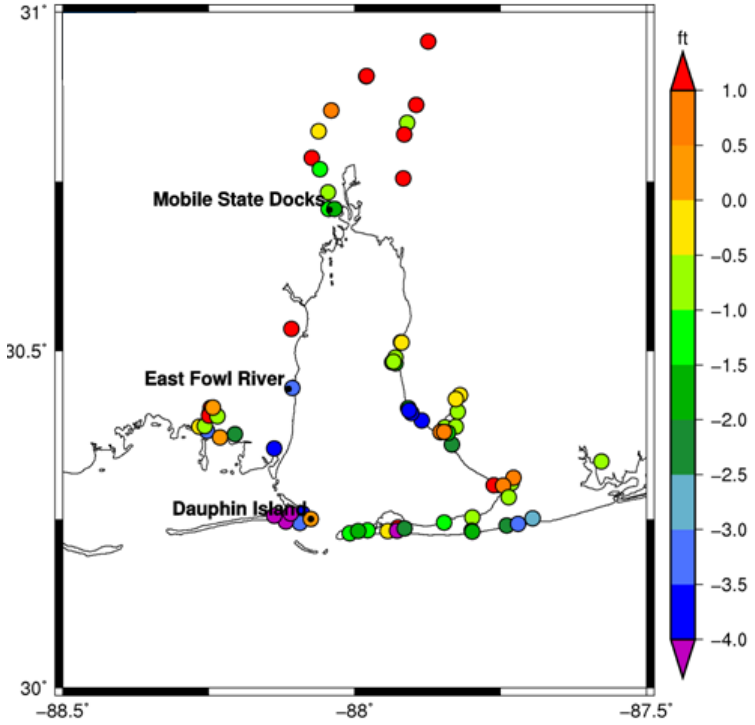

Figure 119: A Comparison of Measured and Simulated High Water Mark Errors (in feet) in Mobile and Baldwin Counties during Hurricane Georges

The comparison error is computed as (simulated) – (measured) such that positive and negative values suggest an over prediction and under prediction of water levels, respectively. A datum discrepancy between measurements (NAVD88) and simulated high water marks (MSL) may introduce differences on the order of +/- 0.7 feet.

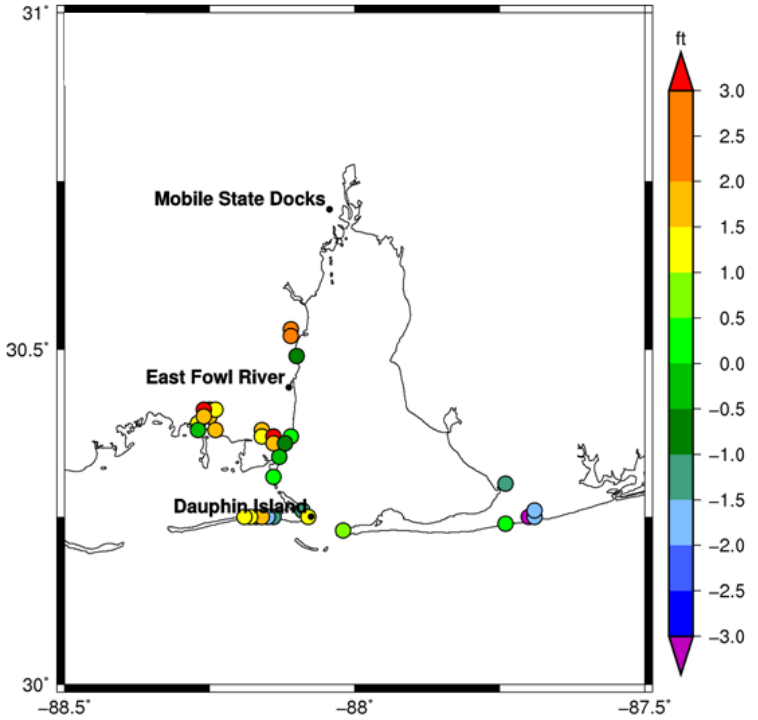

As noted in the discussion above, there are measureable differences in both the comparison of storm surge hydrographs and HWMs for Hurricanes Georges and Katrina. These differences may be attributed to a number of simplifications, or assumptions, applied to the model scenarios or to deficiencies in the hydrodynamic model itself. These possible causes are described below:

- *The hindcast simulations do not include the tide.* The tide ranges at Dauphin Island and Mobile State Docks are 1.19 feet (0.36 meters) and 1.52 feet (0.46 meters), respectively. As a result, the amplitude of the tide during a hindcast simulation may add or subtract approximately 0.59 to 0.76 feet (0.18 to 0.23 meters) to the simulated water levels in Mobile Bay if the peak of the storm surge hydrograph coincides with high or low tide, respectively. For Hurricanes Georges and Katrina, the absence of the tide may bias the simulated peak water levels by 5 to 10%. One of the purposes of the model validation sub-study was to assign a measure of accuracy to model predictions of water levels, so that a level of accuracy or error may be similarly assigned to the results of future climate change model scenarios. Therefore, a consistent methodology was applied to hindcasting and simulation of potential future events.
- *This implementation of ADCIRC does not implicitly include the effects of waves and wave breaking*[191] on simulated water levels. Wave breaking creates a gradient in wave momentum

[191] When a wave breaks against the shore it runs a distance horizontally up the beach slope.

across the breaking zone, which manifests itself as a superelevation of the water above the still water level. This is called wave setup. The contribution of wave setup can add roughly 18% of the breaking wave height to the flood elevation in a storm event.[192] Alternatively, FEMA suggests adding 1.52 to 2.51 feet (0.46 to 0.76 meters) to the 100-year stillwater flood elevation to account for the effects of wave breaking.[193]

- *The hindcast simulations do not consider watershed contributions* to the simulated storm surge hydrograph. The effects of excluding land-derived flows in storm surge hindcast simulations is much more difficult to quantify and would likely vary greatly as a function of storm (i.e. slow moving, fast moving, wet, dry, etc.) and watershed characteristics.
- *The meteorological forcing used to drive the hindcast scenarios is a gross simplification* of historical weather conditions during the simulation period and is certainly limited further by the estimations of storm characteristics provided by the NHC advisory bulletins. The model hindcasts consider only the asymmetric cyclonic wind field[194] generated by the storm instead of all observed meteorological conditions before, during, and after landfall. Moreover, the estimated wind field around the storm was interpolated to the entire ADCIRC mesh, which decays with distance from the storm; therefore, the accuracy of model predictions is assumed to degrade with distance from the storm. Furthermore, the meteorological forcing is applied in six-hour intervals, and is linearly interpolated between the six-hour observations to match the model time step, which in the case of these simulations is two seconds.

Note that increases in global sea level will not necessarily cause a corresponding one-to-one increase in peak storm surge elevations at all locations due to such factors as: non-linear variations in the forces increasing storm surge (such as wind setup) and forces resisting storm surge (such as bottom friction).

D.8.4. Wave Modeling

The wave characteristics accompanying each of the storm surge scenarios were simulated using a state-of-the-art model, STeady State spectral WAVE (STWAVE). It is a flexible, robust model for nearshore wind-wave growth and propagation. STWAVE is a steady-state, finite difference, spectral model based on the wave action balance equation. STWAVE simulates depth-induced wave refraction[195] and shoaling,[196] current-induced refraction and shoaling, depth- and steepness-induced wave breaking, diffraction,[197] wave growth based on wind input, and wave-wave interaction and white capping that redistribute and dissipate energy in a growing wave field. Recent upgrades to the model include wave-current interaction and steepness-induced wave breaking. STWAVE was written by the U.S. Army Corps of Engineers Waterways Experiment Station (USACE-WES). It is one of the most widely used models to compute waves

[192] Dean and Dalrymple, 1991
[193] FEMA, 2000
[194] Holland, 1980; Mattocks and Forbes, 2008; Mattocks et al., 2006. An asymmetric two-dimensional wind field formulation such as this one is more realistic than a circular one. The wind field does not account for the range of factors that can contribute to spatial inhomogeneities (e.g., squall lines; temporary lulls) that arise in typical storms. The aggregate effect of these factors is, however, relatively well represented.
[195] Refraction refers to the bending of a wave due to a change in speed along the length of the wave.
[196] Shoaling refers to the interaction between the seafloor and the wave.
[197] Diffraction refers to the bending of waves around obstacles in their path.

in coastal environments, based on wind and bottom topography. Model details can be found in Smith et al. (2001).

For each scenario, the STWAVE model was run following the ADCIRC model. The coupling between the models was asynchronous. The wind fields used to drive STWAVE were derived from the Holland-type model that was used to drive the ADCIRC model. Waves were simulated over both open water and the land simulated by ADCIRC to be inundated.

Note that Dauphin Island currently helps to protect the mainland by attenuating waves generated out in the open Gulf. Some of that attenuation may be diminished if the topography of the island is reduced through erosion from prior storm wave action. Changes in morphology of the island were not taken into account in the simulations performed in this study.

Ideally, validation simulations would have been performed, as was done for the ADCIRC model. Unfortunately, wave data sufficient to compare to the STWAVE model are not available for hurricanes in the Mobile region. However, the STWAVE model has been extensively tested against observations in other contexts. It has proven to give relatively good approximations of wave characteristics under a variety of conditions. Documentation on tests of STWAVE run under a range of conditions can be found at the USACE Coastal and Hydraulics Laboratory site.[198]

D.8.5. Exposure Mapping

Finally, a Geographic Information System was used to overlay inundation under each of the storm surge scenarios on top of the locations of the critical assets defined in Task 1 of the Gulf Coast Study. The analysis took into account the specific elevations of land on which each asset sits, although it did not consider the height of each asset. Thus, an asset is considered "inundated" if its location is inundated, but the asset itself is not necessarily overtopped.

[198] USACE, 2011. Results from Ponce de Leon Inlet, Florida, Willapa Bay, Washington, and Grays Harbor, Washington are available at: http://chl.erdc.usace.army.mil/chl.aspx?p=s&a=SOFTWARE;9

D.9. Supplementary Storm Surge Exposure Statistics

This appendix provides supplementary exposure statistics for the scenario-based analysis of future hurricane storm surge.

Table 54: Supplementary Storm Surge Exposure Statistics for Georges and Katrina Natural Simulations, and Georges Sea-Level Rise Simulations

			Scenario				
Mode	**Asset**	**Criticality**	**Georges-Natural**	**Katrina-Natural**	**Georges-Natural-30cm**	**Georges-Natural-75cm**	**Georges-Natural-200cm**
Highways	**Roads (mi)**	*Critical*	55 of 209 (27%)	58 of 209 (28%)	58 of 209 (28%)	63 of 209 (30%)	83 of 203 (40%)
		Not Critical	7 of 284 (2%)	8 of 284 (3%)	8 of 284 (3%)	11 of 284 (4%)	20 of 284 (7%)
	Evacuation Routes (mi)	*Not Critical*	35 of 367 (10%)	38 of 367 (10%)	38 of 367 (10%)	46 of 367 (12%)	71 of 367 (19%)
Rail	**Rail (mi)**	*Critical*	111 of 196 (57%)	116 of 196 (60%)	114 of 196 (59%)	119 of 196 (61%)	132 of 196 (68%)
		Not Critical	31 of 118 (26%)	31 of 118 (26%)	31 of 118 (26%)	32 of 118 (27%)	41 of 118 (35%)
	Rail Points (#)	*Critical*	4 of 5 (80%)	4 of 5 (80%)	4 of 5 (80%)	4 of 5 (80%)	5 of 5 (100
		Not Critical	10 of 12 (83%)	10 of 12 (83%)	10 of 12 (83%)	10 of 12 (83%)	10 of 12 (83%)
Pipelines	**Pipelines (mi)**	*Critical*	14 of 426 (3%)	15 of 426 (3%)	15 of 426 (3%)	24 of 426 (6%)	50 of 426 (12%)
		Not Critical	10 of 207 (5%)	10 of 207 (5%)	10 of 207 (5%)	13 of 207 (6%)	33 of 207 (16%)
Ports	**Ports (#)**	*Critical*	24 of 26 (92%)	24 of 26 (92%)	24 of 26 (92%)	24 of 26 (92%)	24 of 26 (92%)
		Not Critical	43 of 48 (90%)	44 of 48 (92%)	44 of 48 (92%)	44 of 48 (92%)	44 of 48 (92%)
Transit	**Facilities**	*Critical*	1 of 2 (50%)	1 of 2 (50%)	1 of 2 (50%)	1 of 2 (50%)	1 of 2 (50%)
	SDE Facilities (#)	*Not Critical*	29 of 193 (15%)	32 of 193 (17%)	32 of 193 (17%)	56 of 193 (29%)	73 of 193 (38%)
	Bus Stops (#)	*Not Critical*	64 of 907 (7%)	81 of 907 (9%)	69 of 907 (8%)	147 of 907 (16%)	209 of 907 (23%)
	Bus Routes (mi)	*Not Critical*	10 of 126 (8%)	11 of 126 (8%)	10 of 126 (8%)	15 of 126 (12%)	23 of 126 (18%)
	MODA Stops (#)	*Not Critical*	2 of 22 (9%)	6 of 22 (27%)	4 of 22 (18%)	20 of 22 (91%)	22 of 22 (100
	Bike Routes (mi)	*Not Critical*	15 of 132 (11%)	16 of 132 (12%)	16 of 132 (12%)	20 of 132 (15%)	31 of 132 (24%)
Airports	**Mobile Downtown Airport (mi^2)**	*Critical*	0 of 3 (4%)	0 of 3 (5%)	0 of 3 (5%)	0 of 3 (7%)	0 of 3 (15%)
	Mobile Regional Airport (mi^2)	*Critical*	0 of 4 (0%)	0 of 4 (0%)	0 of 4 (0%)	0 of 4 (0%)	0 of 4 (0%)
Other	**Medical Facilities (#)**	*Not Critical*	0 of 45 (0%)	0 of 45 (0%)	0 of 45 (0%)	0 of 45 (0%)	4 of 45 (9%)

*Exposure statistics reflect the percent of the assets in the exposure zone. These statistics do not necessarily represent the assets that are actually overtopped by storm surge.

Table 55: Supplementary Storm Surge Exposure Statistics for Katrina Sea-Level Rise and Shifted Simulations

			Scenario					
Mode	**Asset**	**Criticality**	**Katrina-Natural-75cm**	**Katrina-Shift**	**Katrina-Shift-75cm**	**Katrina-Shift-MaxWind**	**Katrina-Shift-MaxWind-75cm**	**Katrina-Shift-ReducedPress-75cm**
Highways	**Roads (mi)**	*Critical*	69 of 209 (33%)	95 of 209 (46%)	114 of 209 (55%)	140 of 209 (67%)	149 of 209 (75%)	124 of 209 (60%)
		Not Critical	15 of 284 (5%)	23 of 284 (8%)	29 of 284 (10%)	39 of 284 (14%)	41 of 284 (15%)	33 of 284 (12%)
	Evacuation Routes	*Not Critical*	52 of 367 (14%)	87 of 367 (24%)	107 of 367 (29%)	144 of 367 (39%)	157 of 367 (43%)	123 of 367 (33%)
Rail	**Rail (mi)**	*Critical*	127 of (65%)	140 of 196 (71%)	144 of 196 (73%)	150 of 196 (77%)	154 of 196 (79%)	146 of 196 (74%)
		Not Critical	33 of 118 (28%)	44 of 118 (37%)	56 of 118 (47%)	78 of 118 (66%)	83 of 118 (70%)	65 of 118 (55%)
	Rail Points (#)	*Critical*	5 of 5 (100%)	5 of 5 (100%	5 of 5 (100%	5 of 5 (100%)	5 of 5 (100%)	5 of 5 (100%)
		Not Critical	10 of 12 (83%)	11 of 12 (92%)	11 of 12 (92%)	12 of 12 (100%)	12 of 12 (100%)	11 of 12 (92%)
Pipelines	**Pipelines (mi)**	*Critical*	44 of 426 (10%)	51 of 426 (12%)	54 of 426 (13%)	62 of 426 (15%)	67 of 426 (16%)	56 of 426 (13%)
		Not Critical	25 of 207 (12%)	36 of 207 (17%)	38 of 207 (18%)	47 of 207 (23%)	49 of 207 (24%)	39 of 207 (19%)
Ports	**Ports (#)**	*High*	24 of 26 (92%)	24 of 26 (92%)	25 of 26 (96%)	26of 26 (100%)	26 of 26 (100%)	25 of 26 (96%)
		Not Critical	44 of 48 (92%)	48 of 48 (100%	48 of 48 (100%	48 of 48 (100%)	48 of 48 (100%)	48 of 48 (100%)
Transit	**Facilities**	*Critical*	1 of 2 (50%)	1 of 2 (50%)	1 of 2 (50%)	1 of 2 (50%)	1 of 2 (50%)	1 of 2 (50%)
	SDE Facilities (#)	*Not Critical*	66 of 193 (34%)	86 of 193 (45%)	105 of 193 (54%)	131 of 193 (68%)	140 of 193 (73%)	115 of 193 (60%)
	Bus Stops (#)	*Not Critical*	171 of (19%)	286 of 907 (32%)	374 of 907 (41%)	622 of 907 (69%)	653 of 907 (72%)	483 of 907 (53%)
	Bus Routes (mi)	*Not Critical*	18 of 126 (14%)	32 of 126 (26%)	46 of 126 (36%)	78 of 126 (62%)	83 of 126 (65%)	60 of 126 (47%)
	MODA Stops (#)	*Not Critical*	20 of 22 (100%)	22 of 22 (100%	22 of 22 (100%	22 of 22 (100%)	22 of 22 (100%)	22 of 22 (100%)
	Bike Routes (mi)	*Not Critical*	23 of 132 (18%)	40 of 132 (30%)	53 of 132 (40%)	67 of 132 (51%)	69 of 132 (53%)	59 of 132 (45%)
Airports	**Mobile Downtown Airport (mi^2)**	*Critical*	0 of 3 (9%)	2 of 3 (65%)	2 of 3 (90%)	3 of 3 (100%)	3 of 3 (100%)	3 of 3 (98%)
	Mobile Regional Airport (mi^2)	*Critical*	0 of 4 (0%)	0 of 4 (0%)	0 of 4 (0%)	0 of 4 (0%)	0 of 4 (0%)	0 of 4 (0%)
Other	**Medical Facilities**	*Not Critical*	2 of 45 (4%)	7 of 45 (16%)	14 of 45 (31%)	17 of 45 (38%)	18 of 45 (40%)	14 of 45 (31%)

*Exposure statistics reflect the percent of the assets in the exposure zone. These statistics do not necessarily represent the assets that are actually overtopped by storm surge.

D.10. Caveats, Gaps, and Replicability of Storm Surge Analysis

This appendix discusses the assumptions and simplifications used in this study's analysis of future storm surge, as well as lessons learned that could be useful in extending the results to other locations.

D.10.1. Assumptions and Simplifications

Not all factors affecting storm surge were taken into account in this study. For example, the study did not account for river flooding that often accompanies strong storms and tends to contribute to storm surge. Nor did it account for changes in beach profiles.

River Flooding

In an estuary such as Mobile Bay, river flooding that often accompanies strong storms will tend to contribute to storm surge. Riverine inputs to the northern head of the Bay can increase significantly during heavy precipitation events. To help minimize computational complexity, river flooding was not directly accounted for in this study's numerical simulations. As a result, the results presented in this study will tend to be lower bounds for surge levels near rivers.

Changes in Beach Profiles

If any of the surges associated with the shifted Katrina scenarios were to strike the Mobile area, they would lead to significant changes in beach profiles. For example, the larger surges would batter Dauphin Island, perhaps opening new cross-island channels, or even removing significant parts of the island. The simulations presented here are most robust for the present state of the shoreline. In a subsequent study, it would be useful to simulate the erosional and depositional effects of major storms and long-term sea level rise on the morphology of the barrier island using a model such as XBeach. The surge and wave modeling used in this study could then be repeated to assess the impacts of the changes in coastal morphology on storm surge and waves on both the island and the mainland.

D.10.2. Lessons Learned

In the process of conducting this series of storm surge and wave modeling simulations, several lessons were learned that may be useful in extending the results from this study to other locations while minimizing resource requirements.

- For this analysis, separate ADCIRC model runs were done for each increment of sea level rise. However, the model runs showed that the storm surge dynamics did not significantly change with these increments of sea-level rise. These results indicate that increments of sea level rise can simply be mapped onto a base surge simulation in other regions with similar topography to simulate moderate-sized hurricanes and the effect of sea level rise. This

approach is much less computationally demanding than running separate surge simulations for each increment of sea level rise.

- If resources are limited and the objective is to simply identify the general magnitude of the storm surge, there are other less computationally intensive approaches that could be used (e.g., the SLOSH model). However, a dynamically realistic model such as ADCIRC should be utilized where the results will be applied to the design and engineering of specific adaptation approaches.
- Most of the waves associated with a hurricane that directly affect urban infrastructure will be limited by the depth of the water. Since the winds associated with hurricane storm surge are generally quite high and the depth of dryland inundation is often relatively low, one could use a simplifying assumption that the waves will be depth-limited. Depth-limited maximum wave heights are generally approximately 0.8 times the water depth. However, in situations in which adaptation options are being designed, a dynamic wave model such as STWAVE or SWAN should be used.
- Finally, the results presented here are of significant potential interest to other sectors beyond transportation in the Mobile region and elsewhere. These sectors include health, water supply, water sanitation, agriculture, commerce, industry, recreation, energy, communications, and disaster risk management. A still more comprehensive assessment of the impacts of storm surge and sea level rise on the transportation system would benefit if sectors such as energy and disaster risk management, including their cascading impacts on transportation, could be incorporated. This would promote a fuller understanding of the ways in which impacts on other sectors could have cascading implications for the transportation sector. For example, impacts on the electric grid during a storm could significantly impair transportation response due to effects on traffic signaling, rail switching, communications, storm water pumping, and other transportation-related activities.